STUDIECENTRUM VOOR KERNENERGIE
CENTRE D'ÉTUDE DE L'ÉNERGIE NUCLÉAIRE

EXTERNAL REPORT
SCK•CEN-ER-76

Fracture Toughness Measurements at Elevated Loading Rates - SCK·CEN activities 2008 within ISO, ASTM and IAEA CRP-8 (topic area #2)

Electrabel/Tractebel-Suez - SCK·CEN Convention 2008
Sub-task 2.2

E. Lucon

CO-90.03.17.00

December, 2008

SCK•CEN
Boeretang 200
2400 Mol
Belgium

EXTERNAL REPORT OF THE BELGIAN NUCLEAR RESEARCH CENTRE
SCK•CEN-ER-76

Fracture Toughness Measurements at Elevated Loading Rates - SCK·CEN activities 2008 within ISO, ASTM and IAEA CRP-8 (topic area #2)

Electrabel/Tractebel-Suez - SCK·CEN Convention
2008
Sub-task 2.2

E. Lucon

CO-90.03.17.00

December, 2008
Status: Unclassified
ISSN 1782-2335

SCK•CEN
Boeretang 200
2400 Mol
Belgium

Belgian Nuclear Research Centre
Boeretang 200
2400 Mol
Belgium

Phone +32 14 33 21 11
Fax +32 14 31 50 21

http://www.sckcen.be

Contact:
Knowledge Centre
library@sckcen.be

Abstract

This report summarizes the activities performed in 2008 by SCK•CEN for the standardization of fracture toughness tests performed at loading rates higher than the quasi-static range presently envisaged by the ASTM E1921-08 standard (i.e. $\dot{K}$ > 2 MPa√m/s). More specifically, efforts have been focused on impact toughness tests performed on precracked Charpy (PCC) specimens using instrumented pendulums at loading rates in the order of 10^5 MPa√m/s.

An account is given of SCK•CEN contributions to the relevant standardization activities currently in progress within both ASTM (subcommittee E08.08, revision of E1921 and E1820) and ISO (committee TC164/SC4F, preparation of a new test standard). Furthermore, a final update is provided on the Coordinated Research Project Phase 8 (CRP-8) of IAEA, topic area #2 (*loading rate effects*). The project is now completed (the final meeting was held in Vienna in April 2008) and the Final Report (IAEA TECDOC) is currently in preparation.

Keywords

Master Curve, elevated loading rates, instrumented impact tests on precracked Charpy specimens, ASTM E1921, ASTM E1820, ISO, IAEA CRP-8, loading rate effects.

Table of contents

1 Introduction

The application of experimental and analytical procedures for fracture toughness tests at elevated loading rates is presently the focus of several coordinated activities in the framework of standardization committees (ISO TC164/SC4F, ASTM E08.08) and international collaborations (IAEA CRP-8). In particular, emphasis is placed on impact toughness measurements performed on precracked Charpy (PCC) specimens tested using an instrumented pendulum.

SCK•CEN has a longstanding experience on such tests, and is obviously interested in both following and contributing to the worldwide activities in the field.

This report summarizes SCK•CEN contributions during the year 2008 within the following umbrellas:

- ASTM: subcommittee E08.08 is working on a revision of the E1921-08 standard on Master Curve testing, which will extend the methodology to tests performed at elevated loading rates (higher than the current quasi-static limit, $\dot{K}$ > 2 MPa√m/s). SCK•CEN is responsible for the drafting, proposal and implementation of the relevant additional sections. In parallel, a new annex to E1820-08 (A17) prepared by SCK•CEN, containing the experimental procedure for testing precracked Charpy specimens at impact loading rates, has been balloted at sub-committee level in the course of summer 2008.
- ISO: within committee TC 164 (*Mechanical Testing*) and subcommittee SC4/F (*Fracture*), a new working item was initiated in 2005 for the standardization of fracture toughness tests performed at impact loading rates on PCCv specimens using an instrumented pendulum. E. Lucon is the convenor of the corresponding working group and is responsible for drafting, editing and updating the document through the various balloting stages. During 2008, the document moved from the CD (Committee Draft) to the DIS (Draft International Standard) stage, which corresponds to the next to last step before official publication.
- IAEA CRP-8: in 2004, the International Atomic Energy Agency launched a Coordinated Research Project (CRP-8) on "*Master Curve Approach to Monitor Fracture Toughness of Reactor Pressure Vessels in Nuclear Power Plants*". SCK•CEN is significantly involved in all three topic areas, but most significantly in topic area #1 (bias and constraint effect, with M. Scibetta as co-leader) and topic area #2 (loading rate effects, with E. Lucon as co-leader). The most relevant activities within topic area #2 were the execution of a Round-Robin Exercise on impact toughness tests using PCC specimens and the investigation of loading rate effects on the Master Curve reference temperature. The project has been completed with a final meeting held in Vienna (April 2008) and the final report is currently in preparation under the supervision of B. Server.

2 ASTM E08.08: extension of E1921 to elevated loading rates and inclusion in E1820 of impact toughness tests on PCC specimens

2.1 Revision of E1921

The current version of ASTM E1921 (2008) only allows testing at quasi-static loading rates, by requiring the stress intensity rate $\dot{K}$ in the linear elastic regime to be in the range 0.1 – 2 MPa√m/s. Within this range, the reference temperature is expected to be insensitive to the loading rate within 10 °C [1]. Below 0.1 MPa√m/s, testing is allowed provided environmental effects are negligible. No provisions are made for $\dot{K}$ > 2 MPa√m/s.

A proposal formulated in 2006 by SCK•CEN to the responsible ASTM committee (E08.08) envisaged the extension of the method to higher loading rates, including instrumented impact tests performed on precracked Charpy (PCC) specimens. Indeed, the applicability of the Master Curve approach to impact toughness tests on PCC specimens has been fully demonstrated [2-5] and is now widely accepted.

The most relevant points of the original SCK•CEN proposal have been already detailed in [6,7].

This original proposal was balloted twice during 2006 and 2007, first at sub-committee level and then at main committee level. In both cases, several negatives and comments were received and responses were provided through the sub-committee chairmen (R. Tregoning and M. Sokolov). In particular, it was felt that the experimental methodology was not mature enough from a standardization point of view to allow analyzing these tests with the Master Curve approach in accordance with E1921.

A related issue was the need to control the difference between absorbed energy measured by the machine encoder or dial (KV) and calculated from the area under the force/displacement curve (W_t), which might highlight possible calibration problems of the instrumented striker.

During the subcommittee meeting in Denver, Colorado (May 2008), it was decided to completely reformulate the proposal of revision along the following lines:

- allow testing at $\dot{K}$ > 2 MPa√m/s, on condition that the prescriptions of Test Method E1820-08 Annex 14 (*Special Requirements for Rapid-Load J-Integral Fracture Toughness Testing*) are followed and the corresponding validity requirements fulfilled (in particular, the minimum test time t_w);
- tests performed at impact loading rates on PCC specimens will not be specifically mentioned (nor specifically excluded) until the new E1820 annex (A17) has been approved.

The new proposal, which was balloted at sub-committee level during summer 2008, also suggested the following relationship for estimating the tensile strain rate which corresponds to the loading rate of a fracture toughness test [8,9]:

$$\dot{\varepsilon} = \frac{\sigma_{YS}}{t_f \cdot E} \tag{1}$$

where σ_{YS} and E are the quasi-static yield strength and Young's modulus at the test temperature, and t_f is the time to fracture in the case of small scale yielding, or the time interval of the initial linear part of the force-time record in the case of distinct elastic-plastic material behavior. Other relevant features of the proposed revision were:

- the reference temperature $T_{0,X}$ has to be reported along with an index (X) denoting the order of magnitude (decade) of the average loading rate;
- an empirical relationship proposed by K. Wallin [10] is provided as a mean to estimate the optimum testing temperature range for tests performed at elevated loading rates.

The ballot received one negative from Rob Tregoning, concerning the need of providing more theoretical background for eq.(1). After discussing this issue during the subcommittee meeting in St. Louis (November 2008) and a presentation from SCK•CEN outlining some practical applications of eq.(1), Tregoning decided to withdraw his negative and the item will proceed to concurrent sub/main committee ballot in early 2009.

The text of the E1921 ballot item, concerning testing at elevated loading rates, is reproduced in Annex 1.

2.2 New Annex (A17) for E1820

As previously mentioned, during the May meeting in Denver it was decided to implement the experimental procedure for testing PCC specimens at impact loading rates in a new Annex (A17) of Test Method E1820.

The annex, titled "*Fracture Toughness Tests at Impact Loading Rates Using Precracked Charpy Specimens*", was first drafted in June 2008 and circulated for comments to a restricted working group (Scibetta, Joyce, Tregoning). It closely mirrored the draft ISO standard (see Section 3).

A revised and abridged version of Annex A17 was then balloted at sub-committee level during July-August 2008, receiving four negatives and several comments. Some of them were directly handled via e-mail communication between myself and the voters, which led to the withdrawal of one negative (S. Graham). The outstanding issues were discussed during the November meeting in St. Louis, namely:

(a) the possibility of indicating the test loading rate using only the decade (magnitude);
(b) the theoretical background of the two relationships used for estimating dynamic tensile properties from an instrumented (precracked or notched) Charpy test [11];
(c) the applicability of the minimum testing time t_w requirement (E1820 Annex A14) to PCC impact tests;
(d) the distinction between instrumented curves of Type I (essentially linear-elastic) and II (unstable fracture without significant stable crack extension, i.e. $\Delta a < 0.2$ mm);

(e) removal of alternative methods not detailed in the annex but just provided as literature references (i.e. Impact Response Curve, Crack Tip Strain Gage method, Basic Key Curve, Analytical 3 Parameter approach);
(f) excessive number of technical/scientific references, which are generally discouraged in the "Blue Book" of ASTM.

Agreement was reached on all the issues under discussion. In particular, as far as item (c) above is concerned, recent work by Joyce [12] has shown that the t_w requirement is equivalent to the 3τ requirement[1] given in the ISO draft and in the balloted E1820 annex.

A revised annex A17 was produced after the St. Louis meeting and circulated via e-mail to all sub-committee members who have returned negatives or comments. Once feedback has been received and further modifications made, the annex will be submitted to concurrent sub/main committee ballot in early 2009.

The current version of Annex A17 (as modified after the discussion in St. Louis) is reproduced in Annex 2.

3 ISO TC164/SC4F: new standard on "Measurement of fracture toughness at impact loading rates using precracked Charpy V-notch test pieces"

During the ISO TC164/SC4F meeting which took place at NPL, Teddington (UK) in October 2005, I proposed to initiate a new work item for the standardization of impact fracture toughness tests on PCC specimens.

The work item went through the stages of WD (Working Document) and CD (Committee Draft). It was circulated for voting among the different national delegations in 2006, 2007, 2008 and discussed at the SC4/F meetings held in Pretoria, South Africa (September 2007) and Hannover, Germany (September 2008).

At the time of writing, the document (which bears the number ISO 26843) has been moved to the DIS (Draft International Standard) stage and will be circulated for voting in 2009. After the discussion at the next ISO TC164 meeting in Sapporo, Japan (September 2009), and provided no significant unresolved technical issues remain, the document will move to the last stage before publication, i.e. FDIS (Final Draft International Standard). At that stage, no more technical changes will be allowed, but only editorial revisions. According to this time schedule, ISO 26843 could be officially issued as an ISO standard in 2010.

The current version of the document (ISO/DIS 26843) is reproduced in Annex 3.

4 IAEA CRP-8: topic area #2 - "Loading Rate effects on fracture toughness"

In October 2004, the International Atomic Energy Agency (IAEA) launched a new Coordinated Research Project (Phase 8) under the title "*Master Curve Approach to Monitor Fracture Toughness of Reactor Pressure Vessels in Nuclear Power Plants*".

One of the primary issues is the evaluation and use of Master Curve data generated under dynamic loading conditions, including the development of standardized test methods for measuring dynamic toughness from small specimens; this issue is addressed by topic area #2 (*Application of the Master Curve for dynamic testing*) under the co-leadership of Hans-Werner Viehrig (Forschungszentrum Dresden, FZD – Germany) and myself.

The main activities within topic area #2 are:

- a Round-Robin Exercise (RRE) consisting of impact toughness tests on PCC specimens of JRQ steel in the ductile-to-brittle transition region, to be analyzed using the Master Curve approach;

[1] In order to calculate fracture toughness using the same analytical formulas as for quasi-static testing, fracture must occur after at least 3 oscillations, i.e. $t_f > 3\tau$, where τ is the period of force oscillation.

- an investigation of the loading rate sensitivity of RPV steels, using data from JRQ and various national steels.

The results of the RRE have been given in [6,7] and presented at the PVP 2007 conference which took place in San Antonio, Texas (July 2007) [13]. With respect to the results presented in [7], an additional data set from KFKI (Budapest, Hungary) has been included in the final RRE analyses.

In April 2008, the final meeting of CRP-8 was held at the IAEA headquarters in Vienna. The contents of the final report, to be published as an IAEA TECDOC, were defined and drafting was initiated.

At the time of writing, the document is in the final polishing stages c/o Bill Server (CRP-8 scientific coordinator). It should be published by the end of 2008.

The final contribution to the TECDOC report corresponding to topic area #2 (Loading Rate Effects, RRE Results and Additional Items) is reproduced in Annex 4.

References

[1] J. A. Joyce, R.L. Tregoning and C. Roe, "On Setting Testing Rate Limitations for the Master Curve Reference Temperature, T_o, of ASTM E 1921," *Journal of Testing and Evaluation* 34/No. 2 (March 2006).

[2] K. Wallin, "Summary of the IAEA/CRP3 Fracture Mechanical Results," Proceedings of a Specialists Meeting Organized by the International Atomic Energy Agency (IWG-LMNPP-95/5; Espoo, Finland: IAEA, Vienna, Austria, 1995).

[3] J. A. Joyce, "On the Utilization of High Rate Pre-Cracked Charpy Test Results and the Master Curve to Obtain Accurate Lower Bound Toughness Predictions in the Ductile-To-Brittle Transition," ASTM STP 1329 (ed. W.R. Corwin, S.T. Rosinski and E. van Walle; West Conshohocken, PA: American Society for Testing Materials, 1998), 253-73.

[4] R. L. Tregoning and J. A. Joyce, "Investigation of Censoring Limits for Cleavage Fracture Determination," ASTM STP 1405 (ed. M. A. Sokolov, J. D. Landes and G. E. Lucas; West Conshohocken, PA: American Society for Testing Materials, 2002).

[5] H.-W Viehrig and J. Böhmert, "Use of Instrumented Charpy Impact Tests for the Determination of Dynamic Fracture Toughness Values," Proceedings of Charpy Centenary Conference - CCC 2001, Poitiers, France, 3-5 October, 2001.

[6] E. Lucon and M. Scibetta, "Fracture Toughness Measurements at Elevated Loading Rates - SCK•CEN activities 2006 within ISO, ASTM and IAEA CRP-8 (topic area #2)", External Report SCK•CEN-ER-22, December 2006.

[7] E. Lucon and M. Scibetta, "Fracture Toughness Measurements at Elevated Loading Rates - SCK•CEN activities 2007 within ISO, ASTM and IAEA CRP-8 (topic area #2)", External Report SCK•CEN-ER-44, December 2007.

[8] G. R. Irwin, "Crack-Toughness Testing of Strain-Rate Sensitive Materials", Journal of Engineering for Power, Trans. ASME, Oct 1964, pp.444-450.

[9] A. K. Shoemaker, "Factors Influencing the Plane-Strain Crack Toughness Values of a Structural Steel", Journal of Basic Engineering, Trans. ASME, Sep 1969, pp.506-511.

[10] K. Wallin, "Effect of Strain Rate on the Fracture Toughness Reference Temperature T_0 for Ferritic Steels", in *Recent Advances on Fracture*, R.K. Mahidhara, A.B. Geltmacher and K. Sadananda, eds., The Mineral, Metals & Materials Society, 1997.

[11] W. L. Server, "General Yielding of Charpy V-Notch and Precracked Charpy Specimens," Journal of Engineering Materials and Technology, Vol.100, Apr 1978, pp. 183-188.

[12] J. A. Joyce, "Review of the Rate Limitations Prescribed by ASTM E1820", presented at the ASTM E28/E08 Workshop on Instrumented Charpy Testing Using Notched, Precracked and Miniature Specimens, St. Louis MO, 16 November 2008.

[13] E. Lucon and H.-W. Viehrig, "Round-Robin Exercise on Instrumented Impact Testing of Precracked Charpy Specimens (IAEA Coordinated Research Program Phase 8)", Proceedings of PVP2007, 2007 ASME Pressure Vessels and Piping Division Conference, July 22-26, 2007, San Antonio, Texas, Paper PVP2007-26088.

ANNEX 1

E1921 ballot item
concerning testing at elevated loading rates
(summer 2008)

Ballot Item 2: Allow Testing at Higher Loading Rates

Rationale for allowing tests at higher loading rates

The standard is being revised in order to allow testing at higher loading rates than previously permitted ($\dot{K}$ < 2 MPa√m/s), provided that the tests are performed according to the requirements of Annex A14 of Test Method E 1820 and the corresponding validity requirements are met. This ballot allows test results which are currently valid under E1820 to be analyzed using the E1921 method, presuming that all requirements associated with this standard are met. However, it has been previously demonstrated that tests with $\dot{K}$ > 2 MPa√m/s can change the T_o value that is determined using the E1921 method. These changes are primarily related to the yield strength elevation that often occurs at these elevated testing rates. Therefore, this ballot requires that the corresponding reference temperature has to be reported as $T_{o,X}$ where X specifies the average order of magnitude (decade) of the average loading rate. Additionally, an empirical relationship is provided so that the user can determine a trial testing temperature range for elevated loading rate tests. There are also requirements for using the material's dynamic yield strength to satisfy the validity criteria in E1921 instead of conservative, quasistatic properties. These requirements ensure that the yield strength values measured in a tensile test are representative of those that govern cleavage fracture in one of the E1921 test specimens.

Several other changes are needed to E1921 to support this ballot. These include adding appropriate definitions, incorporating new references to support the proposed method and requirements, and delineating between quasistatic and dynamic testing requirements. All necessary changes are summarized below.

A. Add following statement to end of current Section 1.5 to allow higher loading rate testing

1.5 "… Provision is also made for higher loading rates (dK/dt > 2 MPa√m/s)."

B. Rename $\dot{K}$ and add discussion delineating measurement requirements (new text in red below)

3.3.21 *test loading rate,* $\dot{K}$ $[FL^{-3/2}T^{-1}]$— rate of increase of applied stress intensity factor.

3.3.21.1 *Discussion*— It is generally evaluated as the ratio between K_{Jc} and the corresponding time to cleavage. For tests where partial unloading compliance is used and provided the unloading and re-loading rates are constant during the linear elastic portion of the test, the ratio between stress intensity factor and time within this linear elastic portion shall be used.

C. Add new definition for estimated value of $T_{o,X}$, $T_{o,X}^{est}$, used to determine high loading rate test temperature

3.3.23 *temperature,* $T_{o,X}^{est}$ *[°C]*— estimated value of the reference temperature corresponding to an elevated loading rate X, to be used only for test temperature selection in accordance with 8.4.2.

D. Clarify that 8.4.1 only pertains to Quasi-static loading rate tests (new text in red below)

"8.4.1 *Quasi-static loading rates*—If the loading rate complies with the limits stated in Section 8.7.1, Charpy V-notch data can be used as an aid for predicting a viable test temperature…"

E. Add new section and supporting references for selecting testing temperatures for elevated loading rate tests using quasi-static properties

8.4.2 *Elevated loading rates* —If tests at elevated loading rates (Section 8.7.2) are performed and if the value of T_o under quasi-static loading rate conditions is known, the following relationship can be used to derive an estimated value of $T_{o,X}$ ($T_{o,X}^{est}$) to facilitate test temperature selection **(21):**

$$T_{o,X}^{est} = \frac{(T_o + 273.15)\cdot\Gamma}{\Gamma - \ln(X)} - 273.15 \qquad (3)$$

with $X = \dot{K}$ in MPa√m/s and temperatures in °C. The function Γ is given by:

$$\Gamma = 9.9\cdot\exp\left[\left[\frac{(T_o + 273.15)}{190}\right]^{1.66} + \left(\frac{\sigma_{ys}^{T_o}}{722}\right)^{1.09}\right] \qquad (4)$$

with $\sigma_{ys}^{T_o}$ = yield strength measured or estimated at T_o and at quasi-static strain rates (~ 10^{-6} to 10^{-4} s^{-1}). See E 8 (or E 8M) for additional guidance. Eqs.(3) and (4) shall not be used for calculating and reporting values of reference temperatures corresponding to elevated loading rates.

Reference: (21) Wallin, K., "Effect of Strain Rate on the Fracture Toughness Reference Temperature T_o for Ferritic Steels", in *Recent Advances on Fracture*, R.K. Mahidhara, A.B. Geltmacher and K. Sadananda, eds., The Mineral, Metals & Materials Society, 1997.

F. Renumber existing 8.4.2 and include clarification that 8.4.1 and 8.4.2 are only used to determine test temperature (new text highlighted in red below)

8.4.3 The procedures outlined in 8.4.1 and 8.4.2 are only appropriate for determining an initial test temperature. The iterative scheme described in 10.4.3 may be necessary to refine this test temperature in order to increase T_o accuracy. Testing below the temperature specified in Eq. 2 or Eq. 3 may be appropriate for low upper-shelf toughness materials to avoid ductile crack growth before cleavage onset, and for low yield strength materials to avoid specimen size invalidity (Eq. 1)

G. Clarify that 8.7.1 requirements are for quasi-static loading rates only (new text highlighted in red below)

8.7.1 *Quasi-static Loading*—Load specimens at a rate such that $\dot{K}$ during the initial elastic portion is between 0.1 and 2 MPa√m/s.

H. Add new section 8.7.2 with high loading rate requirements validity requirement pertaining to E1820 and requirements for using dynamic yield strength to satisfy E1921 validity requirements

8.7.2 *Elevated Loading Rates*—For loading rates that exceed 2 MPa√m/s, tests shall be performed and results shall be calculated according to Annex A14 of Test Method E 1820. The corresponding requirements of this test method, including transition time and data smoothness requirements, shall be fulfilled in order for the test result to be considered valid.

8.7.2.1 The use of quasi-static tensile properties to fulfill the requirements of this test method will lead to a conservative estimate of the dynamic yield strength. Alternatively, dynamic tensile test results can be used, provided that it can be demonstrated that the corresponding strain rate is representative of the rate in the fracture toughness tests. An approximate equivalent strain rate for the fracture mechanics test may be calculated from (**23, 24**):

$$\dot{\varepsilon} = \frac{\sigma_{YS}}{t_f \cdot E} \qquad (6)$$

where σ_{YS} and E are the quasistatic yield strength and Young's modulus at the temperature of the fracture toughness test, and t_f is the time to fracture in the case of small scale yielding, or the time interval of the initial linear part of the force-time record in the case of distinct elastic-plastic material behavior. Eq 6 provides an estimate of strain rate values at the edge of the plastic zone ahead of the crack tip. The tensile test shall then be conducted at this strain rate to obtain the dynamic yield strength.

8.7.2.2 Calculate K_{Jc} according to Annex A14 of Test Method E1820. The number of specimens shall meet the requirements of Table 2. Only tests having $\dot{K}$ values within the same order of magnitude shall be used in the calculation of T_o corresponding to the average $\dot{K}$.

8.7.2.3 Calculate $T_{o,X}$ according to Section 10 with X = the order of magnitude of the average loading rate $\dot{K}$ for all tests performed (in MPa√m/s). For example, if the average calculated loading rate is 3×10^4 MPa√m/s, the corresponding reference temperature shall be designated $T_{o,4}$.

References:

(**23**) Irwin, G. R., "Crack-Toughness Testing of Strain-Rate Sensitive Materials", *Transactions of the ASME, Journal of Engineering for Power*, Oct 1964, pp. 444-450.

(**24**) Shoemaker, A. K., "Factors Influencing the Plane-Strain Crack Toughness Values of a Structural Steel," *Transactions of the ASME, Journal of Basic Engineering*, Sep 1969, pp. 506-511.

I. Add new Section 11 reporting requirements for high rate loading and modify other requirements to address high rate loading (new text highlighted in red below)

11.1.11 For testing rates outside the range defined in 8.7.1, load-line displacement rate $\dot{\Delta}_{LL}$ and test loading rate $\dot{K}$,

11.1.12 Reference temperature of master curve, T_o (°C), and/or T_{oX} (°C), and method used for calculation (single temperature or multi-temperature).

11.2.4 Force-displacement or, for elevated loading rate tests, force-time and force-displacement records.

ANNEX 2

Proposed Annex A17 for Test Method E1820 (modified after ASTM November 2008 meeting)

2. Referenced Documents

Add the following standards:

2.1 *ASTM Standards:*
E 23 Standard Test Methods for Notched Bar Impact Testing of Metallic Materials
2.2 *Other Standards:*
ISO 14556 Steel — Charpy V-notch pendulum impact test — Instrumented test method

3. Terminology

Add the following definitions (in the correct alphabetical order):

3.2.X $\delta_{cd,X}$ *[L], n* – dynamic equivalent of δ_c, with X = $\dot{\delta}$ (see 3.2.X).

3.2.X $\delta_{ud,X}$ *[L], n* – dynamic equivalent of δ_u, with X = $\dot{\delta}$ (see 3.2.X).

3.2.X $\delta_{Qd,X}$ *[L], n* – dynamic equivalent of δ_Q, the fracture toughness near the onset of stable crack extension from a preexisting fatigue crack, with X = $\dot{\delta}$ (see 3.2.X).

3.2.X $\dot{\delta}$ *[LT^{-1}], n* – rate of change of crack-tip opening displacement.

3.2.X $\dot{\varepsilon}$ *[T^{-1}], n* – dynamic strain rate.

3.2.X F_{cd} *[F], n* – applied force corresponding to the onset of unstable crack extension during an instrumented impact test having force/displacement record of Type I (Fig. A17.1).

3.2.X *general yield force,* F_{gy} *[F], n* – applied force corresponding to general yielding of the specimen ligament during an instrumented impact test.

3.2.X *maximum force,* F_m *[F], n* – maximum value of applied force during an instrumented impact test.

3.2.X $J_{cd,X}$ *[FL^{-1}], n* – dynamic equivalent of J_c, with X = $\dot{J}$ (see 3.2.X).

3.2.X $J_{ud,X}$ *[FL^{-1}], n* – dynamic equivalent of J_u, with X = $\dot{J}$ (see 3.2.X).

3.2.X $J_{Qd,X}$ *[FL^{-1}], n* – dynamic equivalent of J_Q, the fracture toughness near the onset of stable crack extension from a preexisting fatigue crack, with X = $\dot{J}$ (see 3.2.X).

3.2.X $\dot{J}$ *[$FL^{-1}T^{-1}$], n* – rate of change of J-integral.

3.2.X K_{Id} *[$FL^{-3/2}$], n* – dynamic plane strain fracture toughness.

3.2.X $\dot{K}$ *[$FL^{-3/2}T^{-1}$], n* - rate of change of stress intensity factor.

3.2.X *dial energy, KV [FL], n* – absorbed energy as indicated by the impact machine encoder or dial indicator, as applicable.

3.2.X *dynamic effective yield strength,* σ_{Yd} *[FL^{-2}], n* – average of dynamic yield strength and dynamic ultimate tensile strength.

3.2.X σ_{TSd} *[FL^{-2}], n* – dynamic ultimate tensile strength, measured at the equivalent strain rate of the fracture toughness test.

3.2.X σ_{YSd} *[FL^{-2}], n* – dynamic yield strength, measured at the equivalent strain rate of the fracture toughness test.

3.2.X t_f *[T], n* – time to fracture (or fracture time).

3.2.X t_i *[T], n* – time at the onset of crack propagation.

3.2.X v_o *[LT^{-1}], n* – striker velocity at impact.

3.2.X W_m *[FL], n* – absorbed energy at maximum force.

3.2.X W_t *[FL], n* – total absorbed energy, calculated under the complete force/displacement test record.

3.2.X W_0 *[FL], n* – available impact energy.

A17. FRACTURE TOUGHNESS TESTS AT IMPACT LOADING RATES USING PRECRACKED CHARPY SPECIMENS

A17.1 Scope

A17.1.1 This Annex specifies requirements for performing and evaluating instrumented impact tests on precracked Charpy specimens using a fracture mechanics approach. Minimum requirements are given for measurement and recording equipment such that similar sensitivity and comparable measurements are achieved. Dynamic fracture mechanics properties determined are comparable to conventional large-scale fracture mechanics results when the validity criteria of Annexes A8-A11 and Annex A14 are met. Because of the small absolute size of the Charpy specimen, this is often not the case. Nevertheless, the values obtained can be used in research and development of materials, in quality control and service evaluation and to establish the variation of properties with test temperature and loading rate under impact loading rates.

A17.2 Principle

This Annex prescribes impact bend tests which may be performed on fatigue precracked Charpy notch specimens to obtain dynamic fracture mechanics properties of materials. This Annex extends the procedure for V-notch impact bend tests in accordance with Test Method E 23, and may be used for evaluation of the Master Curve in accordance with Test Method E 1921. Instrumented testing machines are required, together with ancillary instrumentation and recording equipment in accordance with ISO 14556. Fracture toughness properties depend on material response reflected in the force/time diagrams described in Table A17.1 and Fig. A17.1. Note that only Type I diagrams can be linearly fitted up to fracture.

Table A17.1 Fracture toughness properties to be determined

Material response/fracture behavior	**Corresponding diagram type** [see Figure A17.1]	**R-curve**	**Characteristic parameters**
Essentially linear-elastic	I	-	$K_{Id}\ (\dot{K}_I)$
Elastic-plastic, unstable fracture without significant stable crack extension [$\Delta a < 0.2$ mm]	II	-	$J_{cd}\ (B,\ \dot{J})$
Elastic-plastic, unstable fracture after significant stable crack extension [$0.2\text{ mm} \le \Delta a \le 0.15\ (W\text{-}a_0)$]	II	-	$J_{ud}\ (B, \Delta a,\ \dot{J})$
Elastic-plastic, unstable fracture after substantial stable crack extension [$\Delta a > 0.15\ (W\text{-}a_0)$]	III	$J_d\text{-}\Delta a$ $\delta_d\text{-}\Delta a$	$J_{Qd}\ (\dot{J})$ $\delta_{Qd}\ (\dot{\delta})$
Elastic-plastic; no unstable fracture	IV	$J_d\text{-}\Delta a$ $\delta_d\text{-}\Delta a$	$J_{Qd}\ (\dot{J})$ $\delta_{Qd}\ (\dot{\delta})$

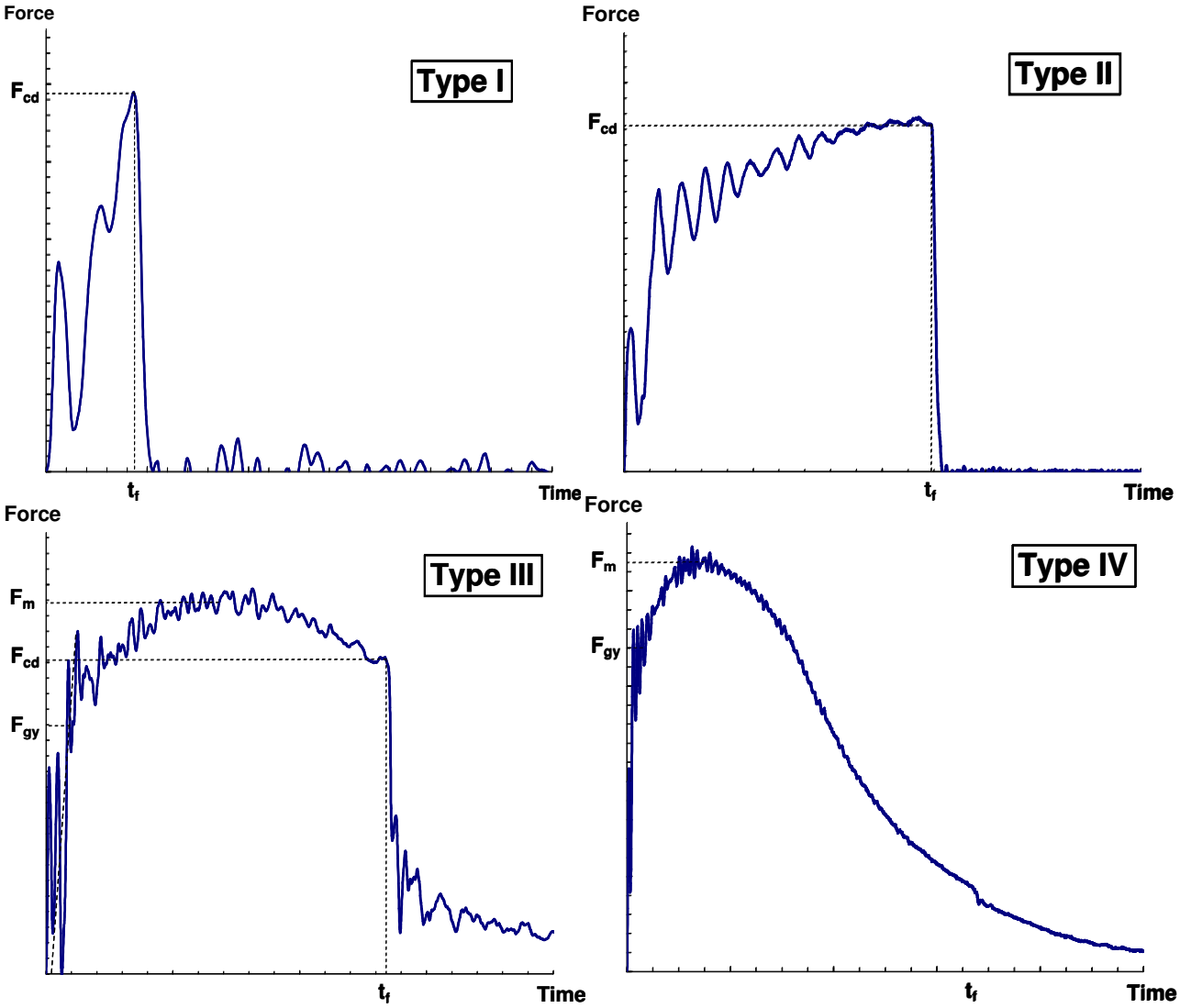

FIG. A17.1 — Typical force-time diagrams [schematic]

A17.3 Specimen Size, Configuration, and Preparation

A17.3.1 Specimens shall be prepared in accordance with the dimensions of the type A Charpy impact specimens of Test Method E 23, with or without the 2.0 mm V-notch, followed by fatigue precracking.

A17.3.2 Fatigue precracking shall be conducted in accordance with 7.4.

A17.3.3 Specimens are fatigue precracked to produce an initial crack size a_o normally in the range $0.30 < a_o/W < 0.70$. If the results in terms of J or δ are to be directly comparable to full-size standard fracture toughness values determined in accordance with Annexes A8-A12, a_o/W shall be in the range $0.45 < a_o/W < 0.70$. Otherwise, shorter crack lengths ($0.30 < a_o/W < 0.45$) may be more advantageous.

A17.3.4 Specimens may be side-grooved in accordance with 7.5.

A17.4 Apparatus

A17.4.1 The preferred testing apparatus is the instrumented Charpy pendulum impact testing machine according to ISO 14556, modified to have a variable pendulum release position. The machine shall have a variable striking velocity up to 5.5 m/s.

A17.4.2 Other pendulum machines may be used, with either fixed anvil/moving striker or fixed striker/moving anvil, and fixed or moving test specimen. The pendulum release position for such machines is normally variable, and the striker or anvils are normally instrumented to provide force/time or force/displacement records. The machine should have a variable striking velocity up to 5.5 m/s.

A17.4.3 Falling weight testing machines, which may be spring assisted and have no restrictions on impact velocity or mass of falling weight, are allowed. The striker is normally instrumented to provide force/time or force/displacement records.

A17.4.4 Other testing machines which comply with the calibration and other requirements of ISO 14556 are not excluded.

A17.4.5 *Requirements on Absorbed Energy* – The reliability of instrumented force values on which these tests are based depends on the quality of the acquisition system and the calibration of the instrumented striker. The calibration of the striker shall be performed in accordance with ISO 14556. Additionally, for each test in which the entire force signal has been recorded (i.e. until the force returns to the baseline), the difference between KV and W_t shall be within ±15% of KV or ±1 J, whichever is larger. If this requirement is not met but the difference does not exceed ±25% or ±2 J, whichever is larger, force values may be adjusted using an iterative procedure until the equivalence $KV = W_t$ is achieved (**28**,**29**). If the difference exceeds ±25% of KV or ±2 J, whichever is larger, the test shall be discarded and the user shall check and if necessary repeat the instrumented striker calibration. If recording of the entire force signal is not possible (for example due to the specimen being ejected from the machine without being fully broken), the user shall demonstrate conformance of the testing system to the requirements above by testing at least five standard (non-precracked) Charpy specimens of any equivalent material, and showing that in all cases the difference between KV and W_t is within ±15% of KV or ±1 J, whichever is larger. If this requirement is not met but the difference does not exceed ±25% of KV or ±2 J, the force adjustment described above shall be applied.

NOTE—From a theoretical point of view, KV is expected to be slightly higher than W_t, the difference being due to vibrational energy losses and other smaller contributions such as secondary impacts between striker and specimen. For more insight on the difference between KV and W_t, see reference (**30**).

A17.5 Test Procedures and Measurements

A17.5.1 Tests are performed in a manner similar to the standard Charpy impact test of Test Method E 23, especially with regard to the pendulum hammer and the handling of pre-cooled or pre-heated specimens.

A17.5.2 *Key Data* - The force/displacement diagram is recorded according to ISO 14556, from which the key data values F_m, F_{cd}, W_m and W_t are determined. In addition to the procedures of ISO 14556, procedures are provided concerning striking velocity, available energy and measurement of crack size. These data form the basis for evaluation of toughness parameters according to A17.6-A17.9.

A17.5.3 *Impact velocity* - This standard applies to any impact velocity v_0, typically in the range from 1 to 5.5 m/s. Impact velocities for pendulum or falling weight testing machines can be varied by adjusting the striker release height. The impact velocity v_0 for a pendulum machine can be determined as follows: release the pendulum from the appropriately reduced height, with no specimen in place. Read the energy KV_0 (in J) indicated by the pointer on the analogue scale. From this, the corresponding impact velocity is calculated as:

$$v_o = v_{os}\sqrt{\frac{W_o - KV_o}{W_o}} \tag{A17.1}$$

where v_{os} is the maximum pendulum velocity corresponding to W_o, the pendulum capacity. A reduced velocity (1 to 2 m/s) can be advantageous, especially for brittle materials, since it reduces the effect of oscillations by lowering their relative amplitude and by increasing their number within the fracture time t_f (see A17.6.2).

A17.5.4 *Time to fracture* - When the time t_f to initiate unstable fracture is less than the minimum test time t_w of A14.3.1.4, the instant of crack initiation is not detectable in the force signal with adequate accuracy because of oscillations (see Fig. A17.1 - Type I), and fracture toughness cannot be evaluated using this test method.

A17.5.5 *Multiple Specimen Tests* - To determine dynamic R-curves by multi-specimen techniques, the fracture process is interrupted at a certain stable crack extension Δa. This procedure is described in A17.7.

A17.5.6 *Single Specimen Tests* - It is possible to estimate dynamic R-curves by single specimen techniques, as described in A17.8.

A17.5.7 *Crack Size Measurements* - Original crack size and final physical crack size shall be measured in accordance with 8.5.

A17.6 Analysis of Results

A17.6.1 *Fracture Behavior* - The adequacy of fracture toughness parameters depends on the fracture behavior of the test specimen as reflected in the force-displacement diagrams described in Table A17.1. Therefore the measured force-displacement or force-time diagram shall be assigned to one of the diagram types shown in Fig. A17.1.

A17.6.2 *Unstable Fracture* – In the case of unstable fracture as in Fig. A17.1 - Types I or II, the applicable evaluation method depends on the oscillations superimposed on the force signal. If time to fracture is more than the minimum test time of A14.3.1.4, fracture toughness shall be evaluated according to the quasistatic approach of A6 and A7. Impact velocity may be reduced in order to obtain a force signal with more oscillations preceding fracture.

A17.6.3 *Stable Crack Extension* – In the case of stable crack extension as in Fig. A17.1 - Types III or IV, either multi-specimen or single-specimen techniques described in A17.7 and A17.8, respectively, are to be used to determine the R-curve. The determination of characteristic fracture toughness values from dynamic R-curves is described in A17.9.

A17.6.4 *Loading Rate* – As indicated in Table A17.1, fracture toughness values shall be stated with the corresponding loading rate added in parentheses. The latter may be estimated as follows:

Type I:
$$\dot{K}_I = \frac{K_{Id}}{t_f} \tag{A17.2}$$

Type II:
$$\dot{J} = \frac{J_{cd}}{t_f} \quad \text{or} \quad \dot{J} = \frac{J_{ud}}{t_f} \tag{A17.3}$$

Type III and IV:
$$\dot{J} = \frac{F_m \cdot v_o}{B_N \cdot (W - a_o)} \cdot \eta_{pl} \left(\frac{a_o}{W} \right) \tag{A17.4}$$

$$\dot{\delta} = \frac{0.4 \cdot (W - a_o) \cdot v_o}{S} \tag{A17.5}$$

For practical purposes, the loading rate shall be indicated using its order of magnitude (for example, 4×10^5 MPa$\sqrt{m}$ shall be indicated as 5).

A17.6.5 *Dynamic Yield Stress* – The dynamic yield and ultimate tensile stresses at the relevant strain rate may be required for certain evaluation procedures and validity checks. An approximate equivalent strain rate for the fracture mechanics test, which can be used for dynamic tensile testing, may be calculated from (**31**,**32**):

$$\dot{\varepsilon} = \frac{\sigma_{YS}}{\bar{t} \cdot E} \tag{A17.6}$$

where: σ_{YS} and E are values corresponding to quasistatic strain rates (10^{-6} to 10^{-4} s^{-1}) and evaluated at the temperature of the fracture mechanics test; $\bar{t}$ is the time to fracture in the case of small scale yielding (type I in Fig A17.1), or the time interval of the initial linear part of the force-time record in the case of distinct elastic-plastic material behavior (types II-IV in Fig. A17.1). Eq A17.6 provides an estimate of strain rate values at the edge of the plastic zone ahead of the crack tip.

A17.7 Determination of R-curves at Impact Loading Rates by Multiple Specimen Methods

A17.7.1 The following methods make it possible to determine fracture toughness parameters in those cases where stable crack extension occurs, Fig. A17.1 – Types III and IV. The multi-specimen procedure involves loading a series of nominally identical specimens to selected displacement levels, resulting in corresponding amounts of stable crack extension. Each specimen tested provides one point on the resistance curve. The requirements and procedures of Annexes A8-A11 concerning number and spacing of data points shall be fulfilled.

A17.7.2 *Low-blow Test* - This test procedure is intended to limit the available impact energy W_0 of a pendulum hammer or a drop weight so that it is sufficient to produce a certain stable crack extension, but not sufficient to fully break the specimen. By selecting different energy levels in a series of tests on nominally identical specimens, a series of different crack extensions Δa_i are produced. From the corresponding J-values or δ-values, J-Δa or δ-Δa R-curves are constructed.

A17.7.2.1 The following procedure is recommended.

(a) Prepare 7 – 10 specimens to nominally the same initial crack length a_0.

(b) Perform a full blow instrumented impact bending test on one of the specimens. Evaluate the energy at maximum force and the total fracture energy, W_m and W_t, in accordance with ISO 14556.

(c) Determine the energy spacing as $\Delta W_0 = 2W_m/N$, where N is the number of available specimens.

(d) Perform an impact test by setting the release position of the pendulum hammer, or the height of the drop weight, such that $W_0 = 2W_m/N$. Avoid a second impact of the hammer.

(e) Repeat the test on the remaining specimens, increasing the available fracture energy W_0 by the amount $\Delta W_0 = 2W_m/N$ at each test.

(f) In order to mark the crack extension, fatigue cycling or heat tinting may be used.

(g) Break all specimens open after testing. Care is to be taken to minimize post-test specimen deformation. Cooling ferritic steels may help to ensure brittle behavior during specimen opening.

(h) Measure a_0 and $\Delta a_p = \Delta a_i$ (where 'i' is the test index, with $1 \le i \le N$-1) in accordance with 8.5.

(i) Calculate J_i according to A1.4.2.1.

(j) Plot the resulting N-1 pairs of values (J_i, Δa_i) in a J-Δa diagram or (δ_i, Δa_i) in a δ-Δa diagram and determine the J-R or δ-R curve according to A8 or A10 respectively and J_{Ic} or δ_{Ic} according to A9 or A11.

A17.7.2.2 The differences in impact velocity and loading rate between the various tests are small enough to have a negligible influence on the results and can be ignored, provided velocity and loading rate do not vary by more than a factor 3.

A17.7.3 *Cleavage R-curve Method* - This test method can only be used for steels that exhibit a brittle-ductile transition. The test temperature is varied within the ductile-to-brittle transition zone so that stable crack extensions of varying lengths Δa_p are obtained from tests terminated by cleavage fracture. J_{ud} calculated according to A1.4.2 with the corresponding Δa_p represent points on the cleavage J-Δa curve which can be analyzed in accordance with A8 and A9. Differences between the temperatures of the various resistance points can be neglected, provided they don't exceed 50°C. The requirements and the validity criteria of Annexes A8-A11 remain valid. Details of this method are given in (**33**).

A17.8 *J*-R Curve Determination by Single-Specimen Methods

A17.8.1 Since, at the present time, there is no generally accepted way to measure and record crack growth during the impact fracture test, determination of the J-R curve from a single specimen requires that the crack growth be estimated either theoretically or numerically. Often, a key curve or normalization technique has to be used to theoretically estimate crack growth as a function of time during the dynamic test.

A17.8.2 The Normalization Data Reduction technique in accordance with A15 can be applied, including the additional requirements of A15.3.

A17.8.3 Presently, no single-specimen method is available for estimating the δ-Δa R-curve.

A17.9 Determination of Fracture Toughness Near the Onset of Stable Crack Extension

A17.9.1 From J-Δa R-curves determined according to A17.7 or A17.8, or from δ–Δa R-curves determined according to A17.7, fracture toughness values near the onset of stable crack extension can be determined in conformance to A9 or A11. Test validity as per A9 and A11 requirements will be difficult to achieve if the specimen undergoes significant plasticity during crack extension because of the relatively small size of the specimen. In this case, values of J_{Qd} and δ_{Qd} cannot be regarded as material properties independent of specimen size and their use in safety assessments may result in non-conservative results. Nevertheless, these values can be used for research and development of materials, in quality control and service evaluation and to establish the variation of properties with test temperature.

A17.9.2 The construction line for J_Q calculation shall have the following expression, see also Eq (A9.4):

$$J = M \sigma_{Yd} \Delta a \tag{A17.7}$$

where σ_{Yd}, the effective dynamic yield strength, is the average of the dynamic yield strength and the dynamic ultimate tensile strength:

$$\sigma_{Yd} = \frac{\left(\sigma_{YSd} + \sigma_{TSd}\right)}{2} \tag{A17.8}$$

σ_{YSd} and σ_{TSd} shall preferably be obtained from dynamic tensile tests, provided that it can be demonstrated that the corresponding strain rate is equivalent to that of the fracture toughness tests (see A17.6.7). Alternatively, estimated values can be obtained from the force/displacement test record of the impact test as (**34**):

$$\sigma_{YSd} = \frac{2.732 F_{gy} W}{(W - a_0)^2 B_N} \quad \text{(A17.9)}$$

and

$$\sigma_{TSd} = \frac{2.732 F_m W}{(W - a_0)^2 B_N} \quad \text{(A17.10)}$$

NOTE—For plane-sided specimens, $B_N = B$.

A17.10 Report

In addition to the information listed in 10, the test report shall include the following.

A17.10.1 Identification and type of testing apparatus.

A17.10.2 Striker impact velocity v_o (A17.5.3).

A17.10.3 Nominal energy of the striker at velocity v_o.

A17.10.4 Absorbed energy *KV* according to Test Method E 23.

A17.10.5 Fracture parameters determined as:

(a) value of K_{Id} obtained, if applicable;

(b) value of $\dot{K}$ obtained, if applicable (only order of magnitude);

(c) value of J and/or δ obtained, if applicable;

(d) value of $\dot{J}$ and/or $\dot{\delta}$ obtained, if applicable (only order of magnitude);

(e) type of force-time diagram, with reference to Fig. A17.1, Types I – IV;

(f) a copy of the test record.

REFERENCES

Add the following references:

(**28**) S. Winkler, A. Michael, and G. B. Lenkey, "Analysis of the Low Blow Charpy Test", *Evaluating Properties by Dynamic Testing*, ESIS 20, E. van Walle, ed., 1996, Mechanical Engineering Publications, London, pp. 207-233.

(**29**) Lucon, E., Chaouadi, R., and van Walle, E., "Different Approaches for the Verification of Force Values Measured with Instrumented Charpy Strikers," *Pendulum Impact Machines: Procedures and Specimens, ASTM STP 1476*, T. A. Siewert, M. P. Manahan, Sr., and C. N. McCowan, eds., ASTM, 2006, pp. 95-103.

(**30**) Manahan, M. P., and Stonesifer, R. B., "The Difference Between Total Absorbed Energy Measured Using an Instrumented Striker and that Obtained Using an Optical Encoder," *Pendulum Impact Testing: A Century of Progress*, *ASTM STP 1380*, T. A. Siewert, ed., ASTM, 2000, pp. 181-197.

(**31**) Irwin, G. R., "Crack-Toughness Testing of Strain-Rate Sensitive Materials", *Journal of Engineering for Power*, *Trans. ASME*, Oct 1964, pp. 444-450.

(**32**) Shoemaker, A. K., "Factors Influencing the Plane-Strain Crack Toughness Values of a Structural Steel," *Transactions of the ASME, Journal of Basic Engineering*, Sep 1969, pp. 506-511.

(**33**) Böhme, W., "Experience with Instrumented Charpy Tests obtained by a DVM Round Robin and Further Developments," ESIS 20, E. van Valle, ed., MEP Publications, London, 1996, pp. 1-23.

(**34**) Server, W.L., "General Yielding of Charpy V-Notch and Precracked Charpy Specimens," *Journal of Engineering Materials and Technology*, Vol.100, Apr 1978, pp. 183-188.

ANNEX 3

ISO/DIS 26843

ISO TC 164/SC4 N465.6

Date: 2008-09-16

ISO/DIS 26843

ISO TC 164/SC 4F/WG

Secretariat: ANSI

Metallic materials - Measurement of fracture toughness of steels at impact loading rates using precracked Charpy specimens

Matériaux métalliques - Mesure de la ténacité d'éprouvettes Charpy préfissurés en acier soumises à un chargement d'impact

Warning

This document is not an ISO International Standard. It is distributed for review and comment. It is subject to change without notice and may not be referred to as an International Standard.

Recipients of this draft are invited to submit, with their comments, notification of any relevant patent rights of which they are aware and to provide supporting documentation.

Document type: International Standard
Document subtype:
Document stage: (20) Preparatory
Document language: E

C:\ISO TC164\SC4F (Fracture)\Dynamic toughness PCCv specimens\DIS stage\ISO_N465_6 (E) DIS (revised after CS comments).doc STD Version 2.1c2

Contents

Page

Foreword

ISO (the International Organization for Standardization) is a worldwide federation of national standards bodies (ISO member bodies). The work of preparing International Standards is normally carried out through ISO technical committees. Each member body interested in a subject for which a technical committee has been established has the right to be represented on that committee. International organizations, governmental and non-governmental, in liaison with ISO, also take part in the work. ISO collaborates closely with the International Electrotechnical Commission (IEC) on all matters of electrotechnical standardization.

International Standards are drafted in accordance with the rules given in the ISO/IEC Directives, Part 2.

The main task of technical committees is to prepare International Standards. Draft International Standards adopted by the technical committees are circulated to the member bodies for voting. Publication as an International Standard requires approval by at least 75 % of the member bodies casting a vote.

Attention is drawn to the possibility that some of the elements of this document may be the subject of patent rights. ISO shall not be held responsible for identifying any or all such patent rights.

ISO/DIS 26843 was prepared by Technical Committee ISO/TC 164, *Mechanical Testing*, Subcommittee SC 4F, *Fracture*.

This second/third/... edition cancels and replaces the first/second/... edition (), [clause(s) / subclause(s) / table(s) / figure(s) / annex(es)] of which [has / have] been technically revised.

Introduction

This International Standard is closely related to ISO 14556, *Steel – Charpy-V pendulum impact test – Instrumented test method*, and was derived from a draft procedure prepared by the Working Party 'European Standards on Instrumented Precracked Charpy Testing' of the European Structural Integrity Society [ESIS] Technical Subcommittee on Dynamic Testing at Intermediate Strain Rates (TC5).

Steel - Measurement of fracture toughness at impact loading rates using precracked Charpy V-notch test pieces

1 Scope

This International Standard specifies requirements for performing and evaluating instrumented precracked Charpy impact tests on steels using a fracture mechanics approach. Minimum requirements are given for measurement and recording equipment such that similar sensitivity and comparable measurements are achieved.

This International Standard may be applied to other metallic materials by agreement. Dynamic fracture mechanics properties determined using this International Standard are comparable to conventional large-scale fracture mechanics results when the corresponding validity criteria are met. Because of the small absolute size of the Charpy specimen, this is often not the case. Nevertheless the values obtained can be used in research and development of materials, in quality control and service evaluation and to establish the variation of properties with test temperature under impact loading rates.

Fracture toughness properties determined through the use of this International Standard may differ from values measured at quasistatic loading rates. Indeed, an increase in loading rate causes a decrease in fracture toughness when tests are performed in the brittle or ductile-to-brittle regimes; the opposite is observed (i.e., increase in fracture toughness) in the fully ductile regime. More information on the dependence of fracture toughness on loading (or strain) rate is given in ref. [1]. In addition, it is generally acknowledged that fracture toughness also depends on test temperature. For these reason, the user is required to report the actual test temperature and loading rate for each test performed.

2 Normative references

The following referenced documents are indispensable for the application of this document. For dated references, only the edition cited applies. For undated references, the latest edition of the referenced document (including any amendments) applies.

ISO 148-1 Metallic materials - Charpy pendulum impact test - Part 1: Test method

ISO 148-2 Metallic materials - Charpy pendulum impact test - Part 2: Verification of the testing machine

ISO 3785 Metallic materials - Designation of test specimen axes in relation to product texture

ISO 12135 Metallic materials - Unified method of test for the determination of quasi-static fracture toughness

ISO 14556 Steel - Charpy-V pendulum impact test - Instrumented test method

3 Symbols and definitions

For the purposes of this document, the symbols and definitions given in Table 1 apply.

Table 1 — Symbols and definitions used in this International Standard

Symbol	Definition	Unit
a	crack length	mm
a_0	initial crack length	mm
Δa	crack extension [$a - a_0$]	mm
Δa_s	crack extension corresponding to displacement s	mm
a_n	length of machined notch	mm
a_f	fatigue crack length	mm
B	specimen thickness	mm
B_e	specimen effective thickness as defined in Equation (E.7)	mm
B_N	specimen net thickness after side-grooving	mm
C_m	compliance of the test machine	m/N
δ	crack-tip opening displacement (CTOD)	mm
$\delta_{0,2Bd}$	dynamic equivalent of $\delta_{0,2BL}$ in ISO 12135	mm
$\mathrm{d}\delta/\mathrm{d}t$	rate of crack-tip opening displacement	mm s^{-1}
E	Young's modulus of elasticity	GPa
$\mathrm{d}\varepsilon/\mathrm{d}t$	strain rate	s^{-1}
f_g	output frequency limit	Hz
F	force	N
F_{cd}	applied force at onset of unstable crack extension in Fig. 1 – Type I	N
F_f	maximum fatigue precracking force during the final precracking stage	N
F_{gy}	applied force at onset of yielding as defined in ISO 14556	N
F_m	maximum applied force as defined in ISO 14556	N
J	experimental equivalent of the J-integral	MJ/m²
J_{cd}	dynamic equivalent of J_c in ISO 12135	MJ/m²
J_{ud}	dynamic equivalent of J_u in ISO 12135	MJ/m²
$J_{0,2Bd}$	dynamic equivalent of $J_{0,2BL}$ in ISO 12135	MJ/m²
$\mathrm{d}J/\mathrm{d}t$	rate of change of J-integral	MJ/m² s^{-1}
K_I^{dyn}	dynamic stress intensity factor	MPa $m^{0,5}$
K_{Id}	dynamic plane strain fracture toughness	MPa $m^{0,5}$
$\mathrm{d}K/\mathrm{d}t$	rate of change of stress intensity factor	MPa $m^{0,5}$ s^{-1}
KV	absorbed energy as defined in ISO 148 Part 2	J
M	total mass of moving striker	kg
n	strain hardening exponent of the Ramberg-Osgood material law	-
N	number of available test specimens	-
R_{fd}	dynamic flow stress, defined as the average of dynamic yield strength and dynamic tensile strength	MPa

Symbol	Definition	Unit
R_{md}	dynamic tensile strength determined at the strain rate of the fracture toughness test	MPa
R_{pd}	dynamic yield (proof) strength determined at the strain rate of the fracture toughness test	MPa
R_p	yield (proof) strength measured at quasistatic strain rate	MPa
s	displacement (calculated according to ISO 14556)	mm
s_{pl}	plastic component of displacement	mm
S	span between outer loading points	mm
T	temperature	°C
t	time	s
t_f	time to fracture	s
t_i	time at the onset of crack propagation	s
t_r	signal rise time	s
t_o	time of striker impact	s
τ	period of force oscillation	s
v_0	striker impact velocity	m s^{-1}
W	specimen effective width	mm
W_m	energy at maximum force defined in ISO 14556	J
W_s	actual total fracture energy (area under the force-displacement diagram up to displacement s)	J
W_{sp}	non-recoverable fracture energy corresponding to force F_s and displacement s	J
W_t	calculated energy from area under complete force-displacement curve to F = 0,02 F_m as defined in ISO 14556	J
W_o	available impact energy	J
z	initial distance of the notch opening gauge measurement position from the notched edge of the specimen (see ISO 12135 – Figure 8b)	mm
ν	Poisson's ratio	-

4 Principle

This International Standard prescribes impact bend tests which may be performed on fatigue precracked Charpy notch specimens to obtain dynamic fracture mechanics properties of materials. This International Standard extends the procedure for V-notch impact bend tests in accordance with ISO 148, and may be used for evaluation of the Master Curve in accordance with ASTM E 1921 [2]. Instrumented testing machines are required together with ancillary instrumentation and recording equipment in accordance with ISO 14556.

Fracture toughness properties depend on material response reflected in the force-time diagrams described in Table 2 and Figure 1. The logical structure for fracture property determination is shown in the flow chart of Figure 2.

Table 2 — Fracture toughness properties to be determined

Material response/fracture behaviour	Corresponding diagram type [see Figure 1]	R-curve	Characteristic parameters
Essentially linear-elastic	I	-	K_{Id} (dK_I/dt)
Elastic-plastic, unstable fracture without significant stable crack extension [Δa < 0,2 mm]	II	-	J_{cd} (B,dJ/dt)
Elastic-plastic, unstable fracture after significant stable crack extension [0,2 mm ≤ Δa ≤ 0,15 (W-a_0)]	II	-	J_{ud} (B,Δa,dJ/dt)
Elastic-plastic, unstable fracture after substantial stable crack extension [Δa > 0,15 (W-a_0)]	III	J_d-Δa δ_d-Δa	$J_{0,2Bd}$ (dJ/dt) $\delta_{0,2Bd}$ ($d\delta/dt$)
Elastic-plastic; no unstable fracture	IV	J_d-Δa δ_d-Δa	$J_{0,2Bd}$ (dJ/dt) $\delta_{0,2Bd}$ ($d\delta/dt$)

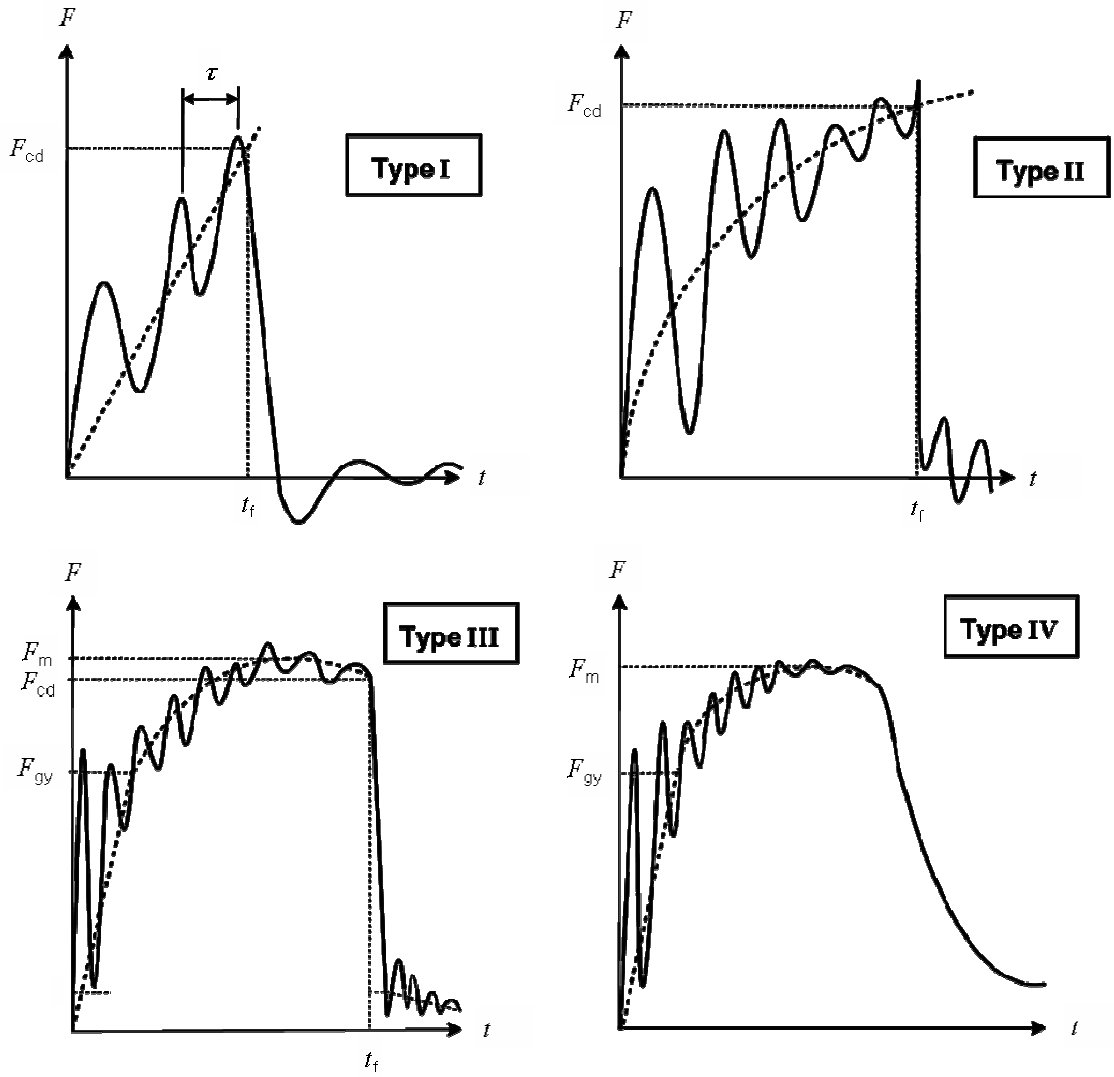

Figure 1 — Typical force-time diagrams [schematic]

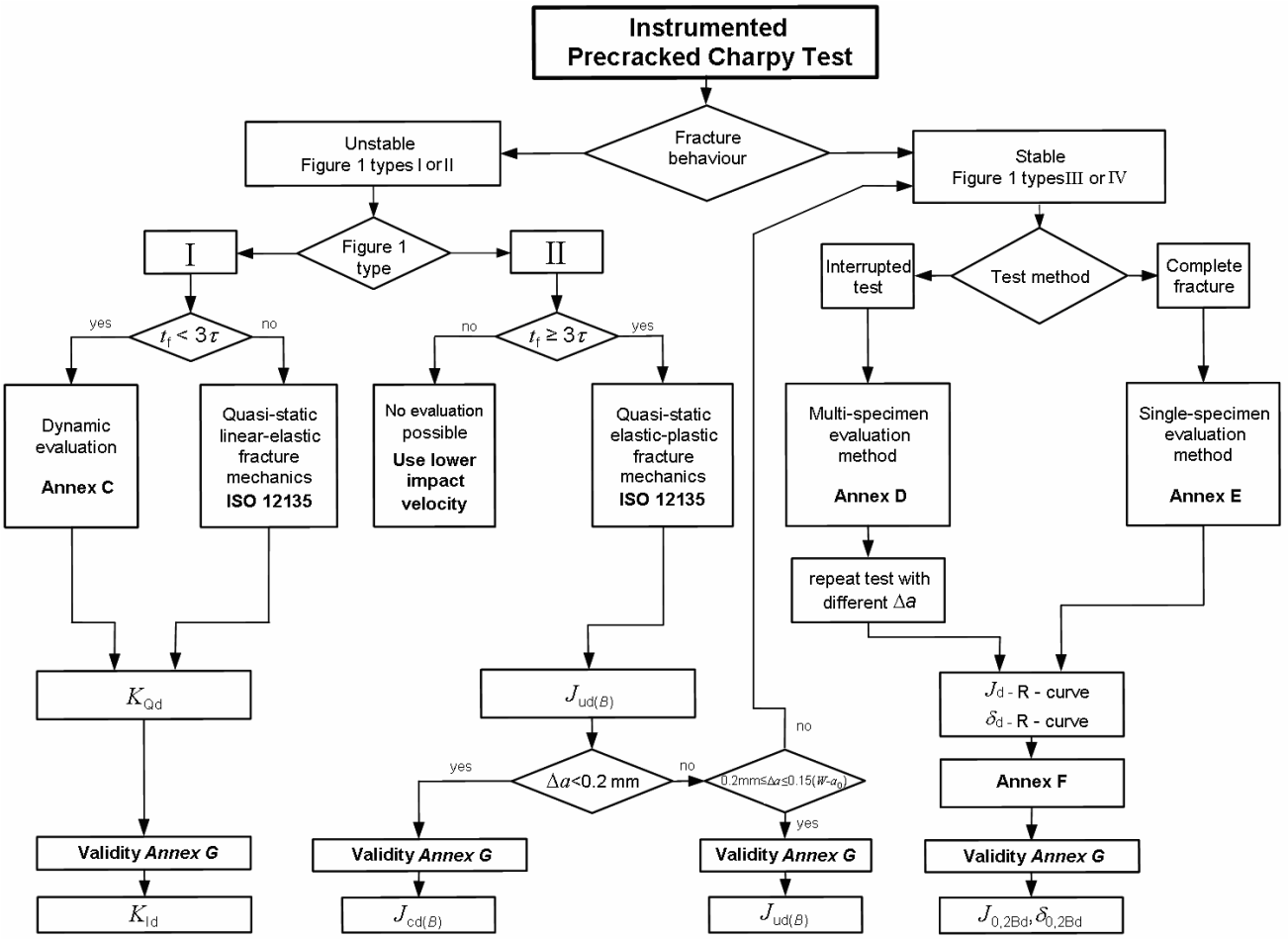

Figure 2 — Flow chart for selecting the test method

5 Test specimens

5.1 Specimens shall be prepared in accordance with the standard specimens of ISO 148 Part 1, with or without the 2,0 mm V-notch, followed by fatigue precracking. By agreement, alternative specimen dimensions may be used.

5.2 To initiate fatigue precracking, machine or spark erode a slot into the specimen to a depth of at least 1,0 mm less than the desired initial crack length a_o. For specimens with an existing V-notch, fatigue precracking may initiate at the bottom of the notch.

5.3 During the final 1,3 mm or 50 % of precrack extension, whichever is less, the maximum fatigue precracking force shall be the lower of:

$$F_f = \frac{0{,}8B(W-a_0)^2}{S} \tag{1}$$

or

$$F_f = \xi E \left[\frac{\sqrt{WBB_N}}{f\left(\frac{a_0}{W}\right)} \right] \left(\frac{W}{S}\right) \quad (2)$$

where ξ = 1,6 × 10^{-4} $m^{1/2}$ and the function $f\left(\frac{a_0}{W}\right)$ is given in Annex H, Equation (H.6).

The ratio of minimum to maximum fatigue pre-cracking force shall be in the range 0 to 0,1 except that to expedite crack initiation one or more cycles of -1,0 may be first applied.

NOTE For plain-sided specimens, $B_N = B$.

5.4 When fatigue precracking is performed at temperature T_1 and testing is done at temperature T_2, F_f in Equation (2) shall be factored by the ratio R_p [T_1] / R_p [T_2], where R_p [T_1] is the yield strength at temperature T_1 and R_p is the yield strength at temperature T_2. In addition, F_f determined from Equation (1) shall be evaluated using the lowest value between R_p [T_1] and R_p [T_2].

NOTE Experience has shown for a wide variety of steels that a fatigue precrack can be initiated in a Charpy specimen with an initial mean force of 2 kN and a range of ±1 kN at a/W of 0,3 which are then both progressively reduced by equal amounts to a level of 0,7 kN over the final 0,5 mm of crack extension. To avoid retardation effects during crack extension, small 10 % progressive reductions in the force levels as crack extension progresses are desirable.

5.5 Specimens are fatigue precracked in 3-point or pure bending to produce an initial crack length a_o normally in the range 0,3 < a_o/W < 0,55.

NOTE 1 If the results in terms of J or δ are to be directly comparable to full-size standard fracture toughness values such as $J_{0,2BL}$ or $\delta_{0,2BL}$ (as defined in ISO 12135), then a_0/W shall be in the range 0,45 < a_0/W < 0,55. Otherwise shorter crack lengths may be more advantageous.

NOTE 2 An Impact Response Curve for 0,28 < a_0/W < 0,32 may be established, see [3-5].

5.6 Specimens may be side grooved using a V-notch cutter in accordance with ISO 148 Part 1 to a depth of 1,0 mm on each side. Side grooving is recommended for all J-Δa R-curve tests. For details of crack length measurement see clause 7.7.

6 Testing machines

6.1 The tests may be carried out using testing machines of the general types specified in Annex A. Other machines which comply with the calibration and other requirements are not excluded. Not all machines can perform all types of test - see Annex A. In all cases the striker and anvil dimensions shall conform to ISO 148 Part 2.

6.2 Details of machine instrumentation and calibration procedures are specified in ISO 14556.

6.3 For every test in which the entire force signal has been recorded (i.e. until the force returns to the baseline), the difference between *KV* and W_t shall be within ±15 % of *KV* or ±1 J, whichever is larger. If this requirement is not met but the difference does not exceed ±25 % of *KV* or ±2 J, whichever is larger, force values may be adjusted until *KV* = W_t [6]. If the difference exceeds ±25 % of *KV* or ±2 J, whichever is larger, the test shall be discarded and the calibration of the instrumented striker user shall be checked and if necessary repeated. If recording of the entire force signal is not possible (for example due to the specimen being ejected from the machine without being fully broken), conformance to the requirements stated above shall be demonstrated by testing at least five non precracked Charpy specimens of similar absorbed energy level.

7 Test procedures and measurements

7.1 General

Tests are performed in a manner similar to the standard Charpy impact test of ISO 148-1, especially with regard to the pendulum hammer and the handling of pre-cooled or pre-heated specimens.

7.2 Key data

The force-displacement diagram is recorded according to ISO 14556, from which the key data values F_m, F_{cd}, W_m and W_t are determined. Additional to the procedures of ISO 14556 are the present procedures for striking velocity, available energy and measurement of crack lengths, which are specified below. These data form the basis for evaluation of toughness parameters according to Annexes C to G.

7.3 Impact velocity

This International Standard applies to any impact velocity v_0, typically in the range from 1 to 5,5 ms^{-1}.

NOTE 1 Impact velocities for pendulum or falling weight testing machines can be varied by adjusting striker release height.

NOTE 2 The reduced impact velocity v_0 can be determined as follows: release the pendulum from the appropriately reduced height, without a specimen on specimens supports. Read the energy KV_0 (in J) indicated by the pointer on the analogue scale. From this the reduced impact velocity is calculated for a 300 J pendulum as:

$$v_0 = v_{0s}\sqrt{\frac{300 - KV_0}{300}} \tag{3}$$

If the pendulum capacity is different than 300 J, replace 300 in Equation (3) with the actual pendulum capacity. A reduced velocity (1 to 2 m/s) can be advantageous, especially for brittle materials, since it reduces the effect of oscillations by lowering their relative amplitude and by increasing their number within the fracture time t_f (see clause 8.2).

7.4 Time to fracture

When the time t_f to initiate unstable fracture is less than 3τ [7-9], the instant of crack initiation is not detectable in the force signal with adequate accuracy because of oscillations, see Figure 1 - Type I, and an independent measurement of t_f is required as described in Annex C.

7.5 Multiple specimen tests

To determine dynamic R-curves by multi-specimen techniques, the fracture process is interrupted at a certain stable crack extension Δa. This procedure described in Annex D.

7.6 Single specimen tests

It is possible to estimate dynamic R-curves by single specimen techniques, as described in Annex E.

7.7 Crack length measurements after testing

7.7.1 General

After a test has been performed, the fracture surfaces of the specimens are examined to determine the initial crack length a_0 and the amount of stable crack extension Δa (if applicable). The procedure is based on measurements of average crack length. Although an area average method might provide a more reliable estimate, the 5-point average method produces acceptable results.

Difficulties may arise in measuring highly irregular crack fronts with spikes or regions of disconnected crack extension. For such situations, it may only be practicable to estimate the crack length by ignoring the spikes or subjectively averaging the crack extension regions. Care shall be exercised when the results derived from highly irregular crack fronts are used to assess structural integrity. For ductile steels it is recommended that such assessments should be based solely on crack initiation parameters and no advantage be taken of the crack extension fracture resistance behaviour.

The method used to measure crack length and the occurrence of irregular crack fronts shall in all cases be reported.

7.7.2 Five-point average method

7.7.2.1 Initial crack length is to be measured to an accuracy of 0,25 % or 0,05 mm, whichever is the greater, between two reference lines defined at the minimum thickness positions as shown in Figure 3. The measurements are to be made at 5 equally spaced points for all tests.

7.7.2.2 For K tests, the initial crack length a_0 shall be obtained as a simple average. For J and $CTOD$ tests, measurements are made at 5 equally spaced points, where the outer points are located at $0{,}01B$ inward from the reference lines. The value of a_0 is obtained by first averaging the two measurements at $0{,}01B$ inward from the surfaces, and then averaging this value with the 3 inner points. If the difference between a_0 and any of the individual measurement points contributing to a_0 exceeds ±10 %, then report non-uniform crack extension as required in the test report (clause 9).

7.7.2.3 Measure to an accuracy of 0,25 % or 0,01 mm, whichever is the greater, the minimum difference between the end of the machined notch and the end of the fatigue precracked zone. If the difference does not exceed 0,05 a_0, report insufficient fatigue precrack. The plane of the fatigue precrack shall be within 10° of the central plane of the machined notch.

7.7.2.4 Measure the total crack extension Δa between the initial and final crack fronts to an accuracy of 0,05 mm using the appropriate averaging procedure described in clauses 7.7.2.1 and 7.7.2.2.

7.7.2.5 Measure the maximum and minimum crack extension between measurement positions 2 to 4 in Figure 3. If the difference is greater than 20 % of the average crack extension Δa or 0,15 mm, whichever is the greater, then report non-uniform crack extension as required.

7.7.2.6 Examine the fracture surfaces for evidence of arrested unstable crack extension regions ahead of the fatigue precrack and/or any other unusual features. Record the number of regions and associated fracture appearance as required.

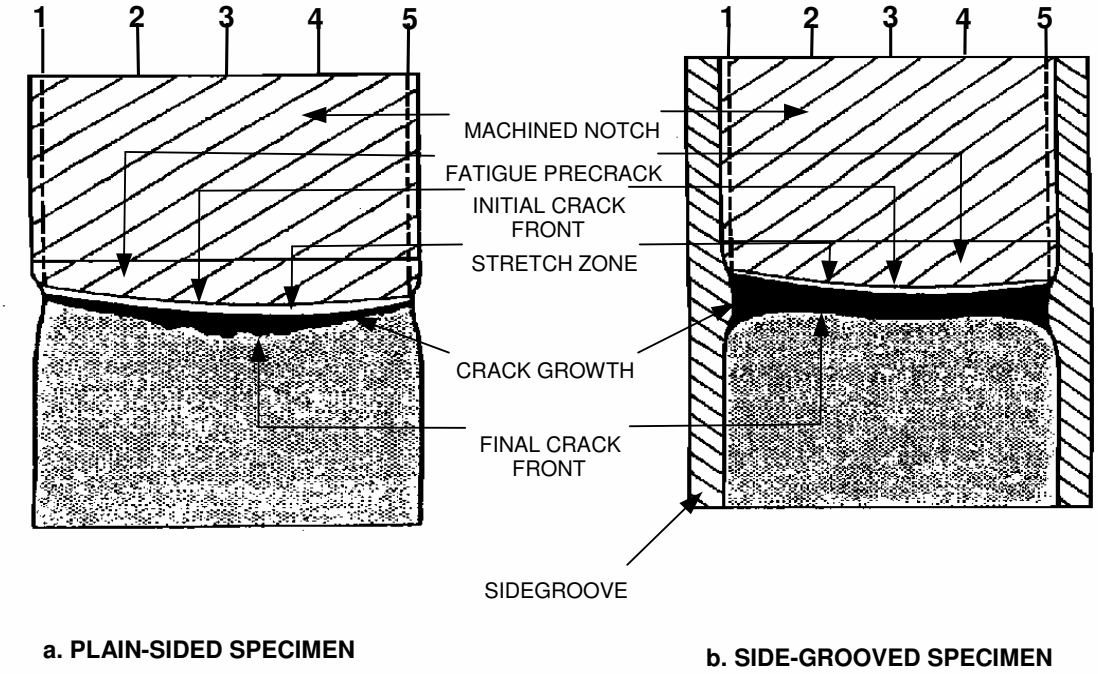

Figure 3 — Measurement of crack length on precracked Charpy specimens

7.7.3 Area average method

7.7.2.1 This method provides the most reliable result for crack length measurement. Both the accuracy and precision of measurement of initial crack length a_0 and stable crack extension Δa by this method is superior to the 5-point average method, especially in the case of highly irregular crack fronts.

7.7.2.2 The area average method is intended to determine the crack length based on the real contour of the crack front. This is done by use of a measuring microscope (reflected light microscope) mounted on an X-Y translation stage with position sensors and a computer interface.

NOTE The displacement measurement chain shall be calibrated. For measurement microscopes with a X-Y translation stage and a position sensor, an overall sensitivity of the displacement measurement chain of 0,02 mm can easily be achieved for both axes and is considered sufficient.

7.7.2.3 As shown in Figure 4, the contour of the relevant area of the fracture surface is defined step by step, first positioning the X-Y translation stage, then manually marking each step and storing the data in a computer. The edge of the specimen is always taken as the reference line, so the machined notch area is included in the measurement area. For efficiency, markings are only required when there are significant changes in the direction of the contour.

NOTE For materials with inhomogeneous microstructure, resulting in fracture surfaces with high roughness, or in the case of poor contrast among fatigue crack, stable crack and brittle crack after heat tinting, the use of dark field illumination and/or filters may be beneficial. Care shall always be taken that the specimen is properly aligned with respect to the axes of the X-Y translation stage.

7.7.2.4 After digitising a contour, the corresponding area value is calculated using the trapezium formula. The average value of initial crack length a_0 may then be calculated by dividing the fatigue crack area value by the specimen thickness B. For determining the average value of stable crack extension Δa, the value of stable

crack area reduced by the fatigue crack area is divided by the thickness B of the specimen. For side-grooved specimens, B is replaced by the net section thickness B_N.

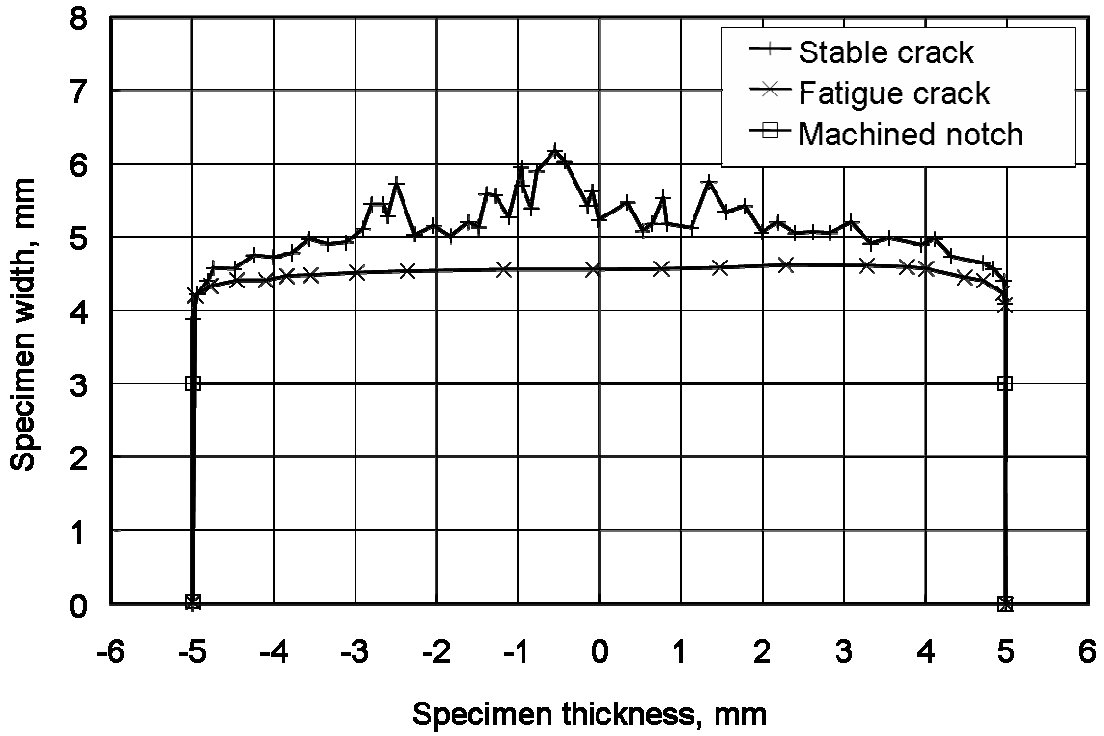

Figure 4 — Details of the area average measurement of crack length as applied to a precracked Charpy specimen

8 Evaluation of fracture mechanics parameters

8.1 The adequacy of fracture toughness parameters depends on the fracture behaviour of the test specimen as reflected in the force-displacement diagrams described in Table 2. Therefore the measured force displacement or force-time diagram shall be assigned to one of the diagram types shown in Figure 1.

8.2 In the case of unstable fracture as in Figure 1 - Types I or II, the applicable evaluation method depends on the oscillations superimposed on the force signal. If there are more than 3 oscillations during the fracture process [7-9], or if their amplitude is small (less than ±15 %) compared with the mean value at $t = t_f$, fracture toughness shall be evaluated according to the quasistatic approach of ISO 12135. Impact velocity may be reduced in order to obtain a force signal with reduced oscillations. Otherwise, the dynamic evaluation method described in Annex C shall be employed.

8.3 In the case of stable crack extension as in Figure 1 - Types III or IV, either multi-specimen or single-specimen techniques described in Annexes D and E, respectively, are to be used to determine the R-curve.

8.3.1 Multi-specimen methods and the corresponding evaluation of R-curves are described in Annex D. Using these methods either J-Δa R-curves or δ-Δa R-curves may be determined.

8.3.2 Single-specimen tests require numerical or analytical determinations of the J-Δa R-curve. Appropriate methods are suggested in Annex E. Other evaluation methods may be applied if their reliability can be shown experimentally and theoretically. Single specimen methods shall be validated by comparison with multi-specimen methods.

NOTE J-Δa R-curves evaluated from just a single force-displacement diagram are necessarily approximations, but their accuracy may be sufficient for many practical purposes.

8.4 The determination of characteristic fracture toughness values from dynamic crack resistance curves is described in Annex F.

8.5 Crack-tip loading rate

As indicated in Table 2, fracture toughness values shall be stated with the corresponding loading rate added in parentheses. The latter may be estimated as follows:

Type I:
$$\frac{dK_I}{dt} = \frac{K_{Id}}{t_f} \tag{4}$$

Type II:
$$\frac{dJ}{dt} = \frac{J_{cd}}{t_f} \quad \text{or} \quad \frac{dJ}{dt} = \frac{J_{ud}}{t_f} \tag{5}$$

Type III and IV:
$$\frac{dJ}{dt} = \frac{F_m v_0}{B_N (W - a_0)} \eta_{pl} \left(\frac{a_0}{W} \right) \tag{6}$$

$$\frac{d\delta}{dt} = \frac{0{,}4(W - a_0) v_0}{S} \tag{7}$$

8.6 The dynamic yield stress at the relevant strain rate may be required for certain evaluation procedures and validity checks, and may be determined using the ESIS Procedure P7-00 [10]. The relevant strain rate may be estimated in accordance with Annex B.

9 Test report

9.1 The test report shall include the following general information:

a) reference to this International Standard;

b) specimen dimensions;

c) specimen identification [grade, cast no, etc.....];

d) specimen location and crack plane orientation according to ISO 3785;

e) initial crack length a_o;

f) amount of stable crack extension Δa;

g) method used to measure crack length;

h) irregular crack front if applicable;

i) fatigue precracking details;

j) identification and type of test apparatus;

k) striker impact velocity v_o;

l) nominal energy of the striker at velocity v_o;

m) test temperature and tolerance limits, in °C (test temperature range in case the "Cleavage R-curve method" is used, see Annex D - D.3);

n) effective energy absorbed KV according to ISO 148 Part 1 in J.

9.2 The test report shall specify the fracture parameters determined as:

a) value of K_{Id} obtained, if applicable;

b) value of dK/dt obtained, if applicable;

c) value of J and/or δ obtained, if applicable;

d) value of dJ/dt or $d\delta/dt$ obtained, if applicable;

e) type of force-time diagram, with reference to Figure 1 - Types I – IV;

f) a copy of the test record.

Annex A
(informative)

Test machines suitable for each test procedure

A.1 This annex gives guidance on the general types of testing machines used to perform the tests detailed in this International Standard. It shall be noted that not all machines can perform all types of tests.

The preferred testing machine is the instrumented Charpy pendulum impact testing machine according to ISO 14556, modified to have a variable pendulum release position. The machine shall have a variable striking velocity up to 5,5 ms^{-1}.

Other pendulum machines may be used, with either fixed anvil/moving striker or fixed striker/moving anvil, and fixed or moving test specimen. The pendulum release position for such machines is normally variable, and the striker or anvils are normally instrumented to provide force-time or force-displacement records. The machine should have a variable striking velocity up to 5,5 ms^{-1}.

A.2 Falling weight testing machines, which may be spring assisted, have no restrictions on impact velocity or mass of falling weight. The striker is normally instrumented to provide force-time or force-displacement records.

A.3 For tests evaluated by the impact response curve or crack tip strain gauge methods of Annex C, the standard non-instrumented Charpy pendulum impact testing machine of ISO 148 Part 2 may be used. The machine will have a striking energy of 300 ± 10 J or such lower energy as permitted, with a fixed striking velocity between 5,0 and 5,5 ms^{-1}. For such machines, independent methods to determine the moment of impact and time to fracture are required.

A.4 Other testing machines which comply with the calibration and other requirements are not excluded.

Annex B
(informative)

Estimation of strain rate

The loading rate in fracture mechanics tests is characterised in terms of the rate of change of a fracture mechanics quantity with time; e.g. dK/dt. Usually, the strain rate at the crack tip is not known. The required strength value R_{pd} at the temperature of the fracture mechanics test has to be determined in a tensile test at a strain rate that is representative of the fracture mechanics test, recognizing that R_{pd} can differ significantly from the quasi-static value R_p. An approximate equivalent strain rate for the fracture mechanics test may be calculated from [11,12]:

$$\frac{d\varepsilon}{dt} = \frac{R_p}{t_f E} \tag{B.1}$$

where R_p and E are values at the temperature of the fracture mechanics test, and t_f is the time to fracture in the case of small scale yielding, or the time interval of the initial linear part of the force-time record in the case of distinct elastic-plastic material behaviour.

Equation (B.1) provides strain rate values at the edge of the plastic zone ahead of the crack tip.

Annex C
(normative)

Dynamic evaluation of fracture toughness

C.1 General

The evaluation of test records and calculation of results varies in detail depending on the particular test performed. However all the tests have certain common characteristics involving time to fracture, $CTOD$ and force-time or force-displacement responses. The Impact Response Curve and the Crack Tip Strain Gauge procedures are both fully developed and provide accurate and repeatable results.

C.2 Impact Response Curve Method

C.2.1 The Impact Response Curve Method is a fully dynamic measuring technique [3-5]. It is applicable to any test condition, particularly higher impact velocities or low temperatures, and is strictly applicable to ferritic steels only. The procedure is illustrated in Figure C.1. Times to fracture less than 25 µs shall be evaluated with caution; in particular it shall be proven that the measurement of the time to fracture t_f is reliable.

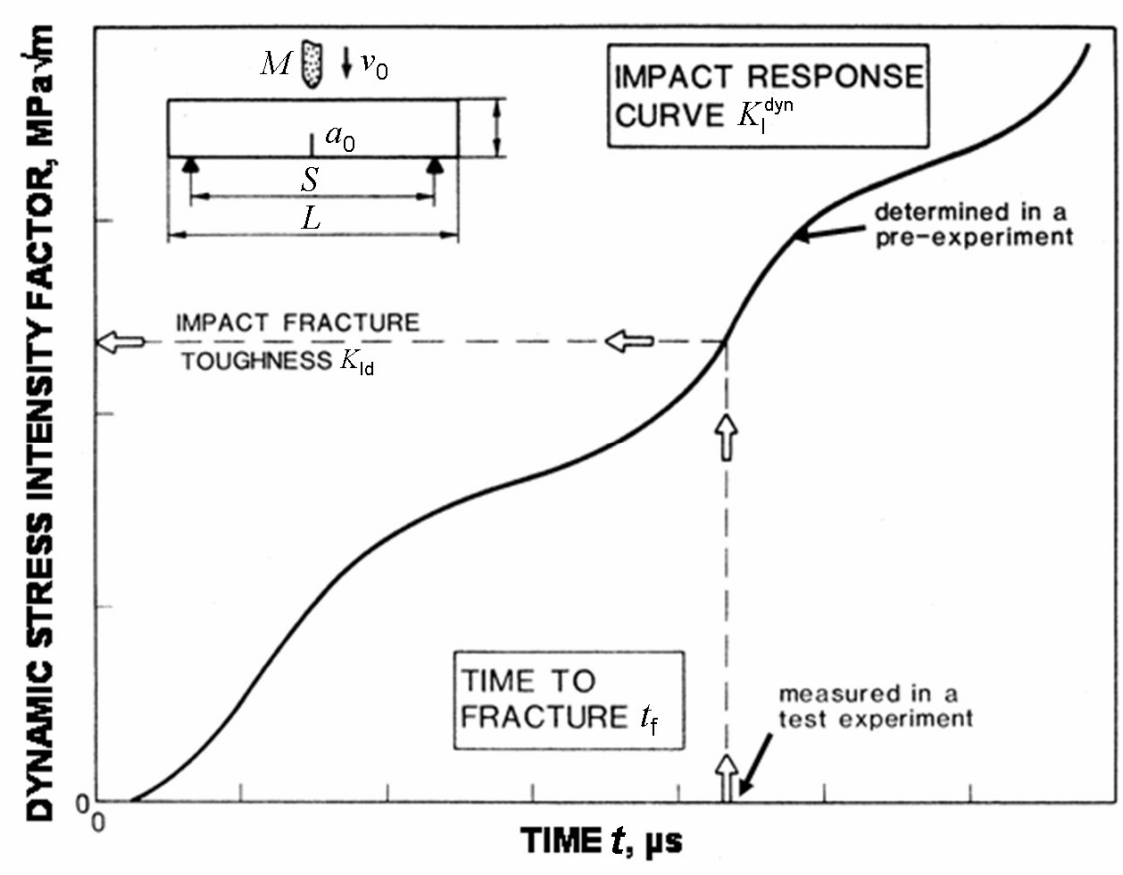

Figure C.1 — Schematic illustration of the Impact Response Curve method

The leading edge of the force signal marks the beginning of the impact event t_o. The time at the onset of crack propagation, t_i, is determined as described in C.2.2 and C.2.3. The time to fracture t_f is the interval between the two times t_i and t_o, see Figure C.2.

C.2.2 A strain gauge is bonded on the specimen close to the crack tip, as shown in Figure C.2. This strain gauge does not require calibration. The onset of crack extension is defined as a sudden drop of at least 20 % in the gauge signal.

C.2.3 A magnetic sensor, which may be simply a coil, is placed close to but not in contact with the test specimen, near its crack tip. The onset of crack initiation is indicated by a sudden rise of the magnetic signal at the moment of instability, as shown in Figure C.2.

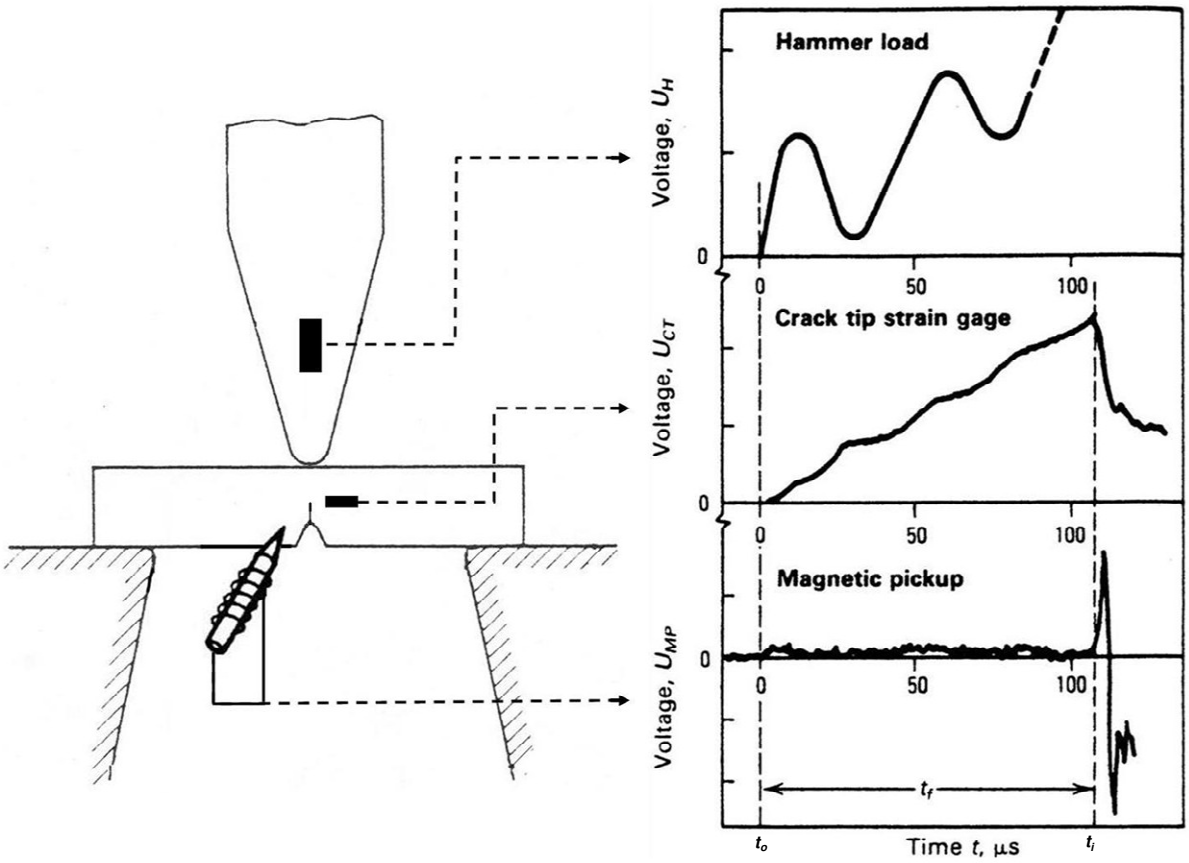

Figure C.2 — Typical striker force, crack-tip strain gauge and magnetic pickup signals during impact. The onset of crack extension is defined as a sudden drop in the gauge signal or a sudden rise in the pickup voltage.

C.2.4 When there is a sufficiently long time to fracture, $t_f > 3\tau$ [7-9], crack initiation is defined as a sudden drop of at least 5 % of the force registered at the instrumented tup, for which a quasistatic evaluation may be performed.

C.2.5 The stress intensity factor - time history $K_I^{dyn}(t)$ constitutes the Impact Response Curve [3]. Using the measured t_f, the impact fracture toughness K_{Id} is determined as:

$$K_{Id} = K_I^{dyn}\left(t = t_f\right) \tag{C.1}$$

Impact Response Curves for three particular impact velocities v_o = 2,0, 3,8 and 5,0 ms^{-1} are shown in Figure C.3. The curves scale with velocity.

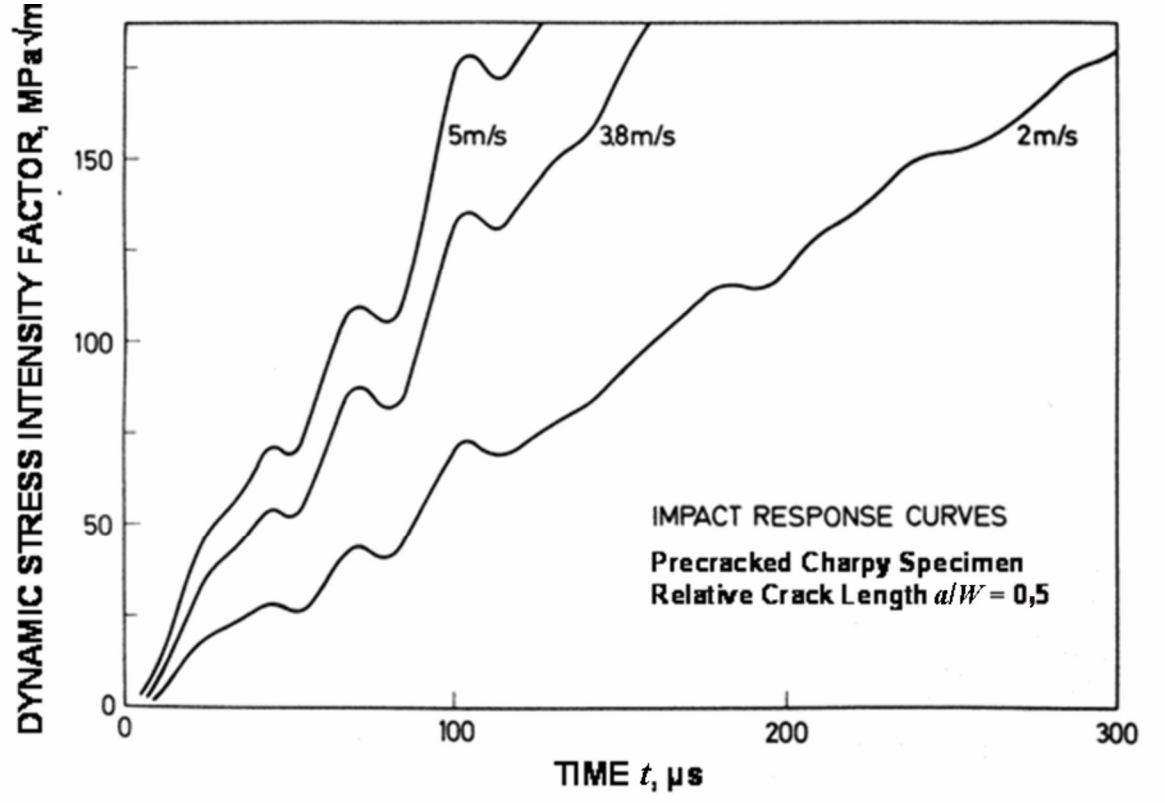

Figure C.3 — Impact Response Curves at velocities v_o = 2,0, 3,8 and 5,0 ms^{-1}.

For practical applications use the expression:

$$K_I^{dyn} = Rv_0 f(t') \tag{C.2}$$

where the constant R = 301 GN/$m^{5/2}$ and the correction factor $f(t')$ is found in Table C.1, with

$$t' = t\left[1 - 0{,}62\left(\frac{a}{W} - 0{,}5\right) + 4{,}8\left(\frac{a}{W} - 0{,}5\right)^2\right] \tag{C.3}$$

where t is the measured physical time and t' is a modified time which compensates for variations of the initial crack length in the range 0,45 < a_o/W < 0,55. The correction factor is less than 5 % for t > 110 µs, and thus the $f(t')$-correction is limited to t' ≤ 110 µs (~2τ). $f(t')$ = t' for t' > 110 µs.

Table C.1 — Functions for the determination of K_I^{dyn} [3,5]

t' (µs)	$t'' = f(t')$ (µs)	t' (µs)	$t'' = f(t')$ (µs)	t' (µs)	$t'' = f(t')$ (µs)
0	0	40	45	80	69
2	0	42	46	82	70
4	2	44	47	84	75
6	4	46	46	86	81
8	6	48	45	88	88
10	9	50	45	90	94
12	13	52	46	92	100
14	17	54	49	94	106
16	20	56	53	96	111
18	24	58	57	98	116
20	28	60	61	100	118
22	30	62	65	102	119
24	33	64	69	104	118
26	35	66	72	106	117
28	36	68	73	108	115
30	38	70	73	110	115
32	39	72	72		
34	40	74	70		
36	42	76	69		
38	43	78	68		

NOTE This value of the constant R applies for stiff pendulum test devices according to ISO 148 with a machine compliance C_m = 8,1 x 10^{-9} m/N. If the actual compliance of the test device differs from this value, the resulting influence can be taken into account by multiplying the given value of R by the first-order correction factor 1,276 / (1 + 0,276 · C_m · 8,1 x 10^{-9} m/N). Procedures for determining the machine compliance of impact test devices are described in [3,7].

C.3 Crack Tip Strain Gauge method

C.3.1 The Crack Tip Strain Gauge method uses the output of a small strain gauge mounted on one or both sides of the test specimen close to, and with its centre aligned with, the fatigue crack tip, with its grid direction perpendicular to the crack as shown in Figure C.4. The background to this method is given in reference [13].

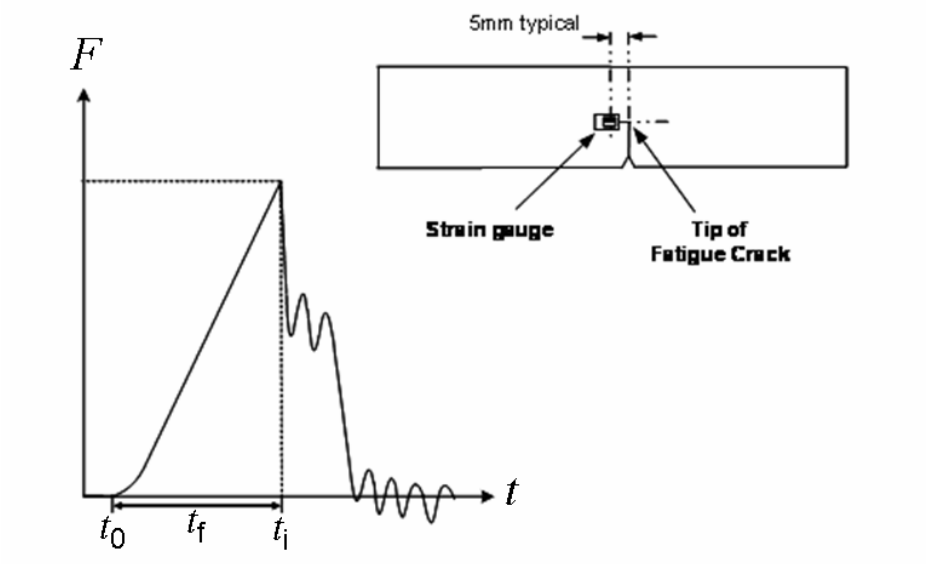

Figure C.4 — Typical crack tip strain gauge record

C.3.2 The strain gauge shall have a grid size of not more than 1,5 mm × 1,5 mm and be bonded preferably using hot-cured solvent-thinned epoxy adhesive to obtain the thinnest possible glue line. The gauge is connected to a high frequency response amplifier using the 3-wire quarter bridge configuration; the recommended frequency response is 1 MHz. Gauge energisation voltage shall be low enough to minimise thermal drift; 1 - 4 volts is usual.

C.3.3 The specimen is first loaded statically in bending to obtain a calibration record of the strain gauge amplifier output against applied force. At least six values of output voltage and force are required, up to the maximum pre-cracking stress intensity factor K_{fmax}. This calibration is preferably performed in the same testing machine as the impact test.

C.3.4 Without removing the specimen from the machine, the impact test is performed with the strain gauge output signal recorded. A typical test record is shown in Figure C.4.

C.3.5 When there is a sufficiently long time to fracture, $t_{\mathrm{f}} > 3\tau$ [7-9], crack initiation is defined as a sudden drop of at least 5 % of the force registered at the instrumented tup and a quasistatic evaluation is performed.

C.3.6 If $t_{\mathrm{f}} \leq 3\tau$, the equivalent applied force at fracture F_{cd} is defined as a sudden drop of at least 20 % of the strain gauge record, using a conversion factor determined by a preliminary static calibration. K_{Id} is then calculated from Equation (H.5) of Annex H.

Annex D
(normative)

Determination of resistance curves at impact loading rates by multiple specimen methods

D.1 General

These methods make it possible to determine fracture toughness parameters in those cases where stable crack extension occurs, Figure 1 – Types III and IV. The multi-specimen procedure involves loading a series of nominally identical specimens to selected displacement levels, resulting in corresponding amounts of stable crack extension. Each specimen tested provides one point on the resistance curve. Six or more favourably positioned data points are required to generate one resistance curve, thus making it possible to determine fracture toughness near the onset of physical crack initiation.

NOTE Loading the first specimen to a point just beyond maximum force will help to determine the energy levels needed to position the points in subsequent tests. The choice of a test temperature sufficiently far above the transition from cleavage to ductile fracture will avoid brittle fracture and thus the loss of some specimens.

D.2 Low-blow test

D.2.1 This test procedure is intended to limit the available impact energy W_0 of a pendulum hammer or a drop weight such that it is sufficient to produce a certain stable crack extension, but not sufficient to fully break the specimen. By selecting different energy levels W_0 in a series of tests on nominally identical specimens, a series of different crack extensions Δa_i are produced. From the corresponding J-values or δ-values, J-Δa or δ-Δa curves are constructed.

D.2.2 The following procedure is recommended.

a) Prepare 7 – 10 specimens to nominally the same initial crack length a_0.

b) Perform a full blow instrumented impact bending test on one of the specimens. Evaluate the energy at maximum force and the total fracture energy, W_m and W_t, in accordance with ISO 14556.

c) Determine the energy spacing as $\Delta W_0 = 2W_m/N$, where N is the number of available specimens.

d) Perform an impact test by setting the release position of the pendulum hammer, or the height of the drop weight, such that $W_0 = 2W_m/N$. Avoid a second impact of the hammer.

e) Repeat the test on the remaining specimens, increasing the available fracture energy W_0 by the amount $\Delta W_0 = 2W_m/N$ at each test.

f) In order to mark the crack extension, fatigue cycling or heat tinting may be used.

g) Break all specimens open after testing. Care is to be taken to minimize post-test specimen deformation. Cooling ferritic steels may help to ensure brittle behaviour during specimen opening.

h) Measure a_0 and $\Delta a_s = \Delta a_i$ (where 'i' is the test index, with $1 \le i \le N$-1) in accordance with Clause 7.7.

i) Calculate J_i using Equation (H.1) with F_i, W_i and $a_i = a_0 + \Delta a_i$ replacing F_c , W_c, and a, respectively.

j) Plot the resulting N-1 pairs of values (J_i, Δa_i) in a J-Δa diagram or (δ_i, Δa_i) in a δ-Δa diagram and determine the J-R or δ-R curve according to ISO 12135.

NOTE The differences in impact velocity and loading rate between the various tests are small enough to have a negligible influence on the results and can be ignored.

D.3 Cleavage R-curve method

This test method can only be used for steels that exhibit a brittle-ductile transition. The test temperature is varied within the ductile-to-brittle transition zone so that stable crack extensions of varying lengths Δa_s are obtained from tests terminated by cleavage fracture. J_{ud} calculated using Equation (H.1) with the corresponding Δa_s represent points on the cleavage J-Δa curve which can be fitted by a power law of the type J=A+C·Δa^D.
The difference between the temperatures of the various resistance points can be neglected, provided it doesn't exceed 50 K. Details of this method are given in [14,15].

Annex E
(normative)

Estimation of J-Δa R-curves by single specimen methods

E.1 General

Since, at the present time, there is no generally accepted way to measure and record crack extension during impact fracture, determination of the J-Δa R-curve from a single specimen is necessarily a theoretical approximation.

The methods described in the following Clauses E.1 and E.2 have been shown in several comparative investigations [16-18] to be easily implemented without special equipment, and to deliver reproducible, reliable and often sufficiently accurate results. These methods are also applicable to Figure 1 - Type III behaviour and to multiple specimen tests such as low-blow tests performed according to D.1, if Δa_s > 1,6 mm. In the latter case, the normalization technique described in ASTM E 1820 [19] can be applied as a third alternative, see E.3.

NOTE 1 It is suggested that, if possible, all three estimation methods are used, and that the lowest values obtained be used in order to provide a conservative fracture analysis.

NOTE 2 Presently, no single-specimen method is available for estimating the δ-Δa R-curve.

E.2 Basic Key Curve Method

This method is based on references [20-22]:

$$J(\Delta a(s)) = \frac{\eta(a_0)}{B_N(W-a_0)}\int_0^s F(s)ds \tag{E.1}$$

where Δa is obtained by integrating the following equation:

$$\frac{da}{ds_{pl}} = \frac{W-a}{2}\left(\frac{1}{n\cdot s_{pl}} - \frac{dF/F}{ds_{pl}}\right) \tag{E.2}$$

where: n is the strain hardening exponent of the Ramberg-Osgood material law
s_{pl} is the plastic component of displacement s (calculated in accordance with ISO 14556)
$\frac{dF/F}{ds_{pl}}$ is the normalized slope of the force-displacement curve

NOTE To evaluate Equation (E.2), a mathematical approximation of the force-displacement diagram by a polynomial may be advantageous to reduce the effect of scatter [23].

E.3 Analytical 3-Parameter Approach

E.3.1 Type IV fracture

According to the derivations in [24,25], the J-Δa R-curve may be estimated from a continuous force-displacement diagram as a function of Δa by:

$$J(\Delta a)=\left(\frac{2}{p}\right)^{p}\frac{\eta(a_0)}{B_N(W-a_0)^{1+p}}\cdot W_t^{\,p}\cdot W_{mp}^{1-p}\cdot\left[1-\frac{(0{,}75\eta\cdot a_0-1)\cdot\Delta a}{W-a_0}\right]\cdot\Delta a^{p}+\frac{K_I^2(F_m,a_0)}{E}\left(1-\nu^2\right) \quad \text{(E.3)}$$

with:

$$p=\frac{3}{4}\left(1+\frac{W_{mp}}{W_t}\right)^{-1} \quad \text{(E.4)}$$

$W_{mp}=W_m-\dfrac{F_m^2}{2k(a_0)}$: the non-recoverable part of W_m (see Figure E.1)

k : slope of the initial elastic line (linear regression line in the range $0 < F < F_{gy}$)

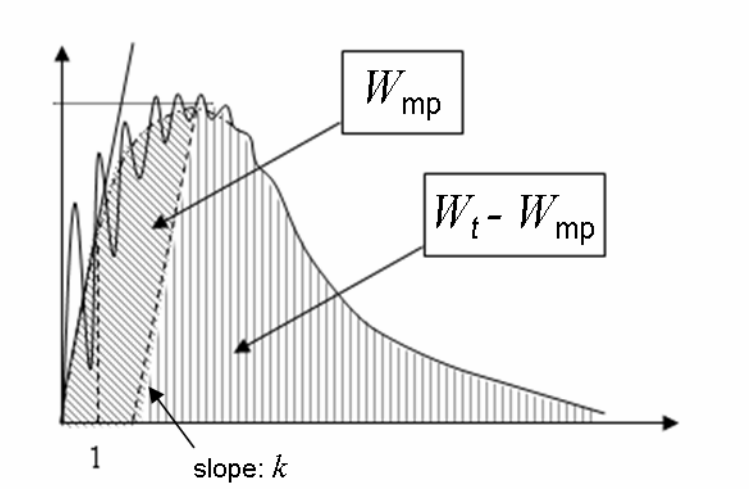

Figure E.1 — Definition of parameters used for the evaluation of Equation(E.3)

E.3.2 Type III fracture or multiple specimen tests

If ductile tearing is interrupted at a crack extension Δa_s >1,6 mm by the onset of cleavage or in the case of a low-blow test, then W_t in eq. (E.3) shall be replaced by its extrapolated value $W_{t/ext}$, which is obtained by:

$$W_{t/ext}=\frac{W_t(W-a_0)^2}{2(W-a_0)\cdot\Delta a_s-\Delta a_s^2} \quad \text{(E.5)}$$

E.4 Normalization Method

E.4.1 The normalization method (NM), which is documented in [26], is derived from the basic key-curve method. The procedure described below is adopted mainly from ASTM E 1820 [19].

E4.2 The first step of the J-Δa R-curve determination is the measurement of initial and final crack lengths according to Clause 7.7. Subsequently, each $F_{(i)}$ load value up to, but not including F_m, is normalized using the following expression:

$$F_{N(i)} = \frac{F_{(i)}}{WB_e\left[\frac{W - a_{b(i)}}{W}\right]^{\eta}} \tag{E.6}$$

The value of η for a three-point bend specimen is given in Equation (H.2). The effective thickness B_e is defined as

$$B_e = B - \frac{(B - B_N)^2}{B} \tag{E.7}$$

$a_{b(i)}$ is the blunting corrected crack length calculated as follows:

$$a_{b(i)} = a_0 + \frac{J_{(i)}}{2R_{fd}} \tag{E.8}$$

$$J_{(i)} = \frac{K^2_{I(i)}\left(1-\nu^2\right)}{E} + J_{pl(i)} \tag{E.9}$$

$$J_{pl(i)} = J_{pl(i-1)} + \left[\frac{2\left(W_{pl(i)} - W_{pl(i-1)}\right)}{\left(W - a_{(i-1)}\right)B_N}\right]\left[1 - \frac{a_{(i)} - a_{(i-1)}}{W - a_{(i-1)}}\right] \tag{E.10}$$

where R_{fd} is the dynamic flow stress, i.e., the average between dynamic yield and ultimate tensile strengths (see Annex F). $K_{I(i)}$ is obtained from eq. (H.5) as $K_{I(i)} = K_I(F_i, a_{b(i)})$.

The normalized plastic displacement for each point is calculated from the load-line displacement s_i as follows:

$$s'_{pl(i)} = \frac{s_{pl(i)}}{W} = \frac{s_{(i)} - F_{(i)}C_{(i)}}{W} \tag{E.11}$$

where $C_{(i)}$ is the elastic load-line compliance of the specimen based on the crack length $a_{b(i)}$ and is given by:

$$C_{(i)} = \frac{1}{EB_e}\left(\frac{S}{W - a_{b(i)}}\right)^2\left[1{,}193 - 1{,}98\left(\frac{a_{b(i)}}{W}\right) + 4{,}478\left(\frac{a_{b(i)}}{W}\right)^2 - 4{,}443\left(\frac{a_{b(i)}}{W}\right)^3 + 1{,}739\left(\frac{a_{b(i)}}{W}\right)^4\right] \tag{E.12}.$$

E4.3 In this manner data points up to, but not including, the maximum force are normalized. In order to obtain the final point, the same equations are employed, but instead of the initial crack length, the final crack length is used. The normalized plastic displacement values above 0,001 up to maximum force, excluding the F_{max} value itself, and the point obtained with the use of the final crack length shall be used for the normalization function fit. The normalization function may be analytically expressed in the form:

$$F_N = \frac{C_1 + C_2 s'_{pl} + C_3 s'^2_{pl}}{C_4 + s'_{pl}} \tag{E.13}$$

where C_1, C_2, C_3, C_4 are fitting coefficients. After the fitting parameters are determined, an iterative procedure is further applied to force all $F_{N(i)}$ data to lie on the fitted curve by $a_{(i)}$ adjustment. After the crack lengths are determined, the J-Δa R-curve and the critical J-integral value are evaluated.

E4.4 When the Normalization Method is to be applied, the following requirements shall be satisfied: evenly distributed data points shall be within the fitting range, a minimum of 10 data points shall be available, all fitted points shall be within 1 % deviation from measured data and the maximum permissible crack extension evaluated with the use of this procedure is 15 % of the initial uncracked ligament.

E4.5 In order to confirm the applicability of the Normalization Method for the material investigated, at least one additional specimen shall be tested. Using the previously obtained J-Δa R-curve, deflection of the specimen corresponding to 0,5 mm crack extension is to be determined. The specimen is loaded under identical conditions as previous specimens up to that deflection, and the crack extension optically measured shall be 0,5 ± 0,25 mm.

Annex F
(normative)

Determination of characteristic fracture toughness values $J_{0,2Bd}$ or $\delta_{0,2Bd}$

F.1 General

From J-Δa R-curves determined according to Annex D or E, or from δ-Δa R-curves determined according to Annex D, characteristic fracture toughness values can be determined analogous to ISO 12135. In particular, the $J_{0,2Bd}$ or $\delta_{0,2Bd}$ value is obtained at the intersection of the J-Δa or δ-Δa R-curve with the 0,2 mm-offset construction line. Some dynamic adjustment of the construction line is required, and the following procedures are suggested.

NOTE Fracture toughness values $J_{0,2Bd}$ or $\delta_{0,2Bd}$ are regarded as engineering estimates of the onset of stable crack extension. They cannot be regarded as material properties independent of specimen size and are not transferable to larger structures. The use of $J_{0,2Bd}$ or $\delta_{0,2Bd}$ values in safety assessments may result in non-conservative results. Nevertheless, $J_{0,2Bd}$ or $\delta_{0,2Bd}$ values can be used for research and development of materials, in quality control and service evaluation and to establish the variation of properties with test temperature.

F.2 Dynamic construction line for $J_{0,2Bd}$

Adapting the definition of the construction line of ISO 12135 to dynamic testing gives:

$$J(\Delta a) = 3{,}75 \cdot R_{md} \cdot \Delta a \tag{F.1}$$

where R_{md} is the dynamic ultimate tensile strength of the material. This shall preferably be obtained from dynamic tensile tests, provided that it can be demonstrated that the corresponding loading rate is equivalent to that of the fracture toughness tests. Alternatively, an estimation of the dynamic ultimate tensile strength can be obtained from the force-displacement test record of the Charpy test as [27]:

$$R_{md} = \frac{0{,}729 \cdot F_m \cdot S}{(W - a_0)^2 B_N} \qquad \text{for a 2 mm radius striker} \tag{F.2}$$

or

$$R_{md} = \frac{0{,}683 \cdot F_m \cdot S}{(W - a_0)^2 B_N} \qquad \text{for a 8 mm radius striker.} \tag{F.3}$$

NOTE For plane-sided specimens, $B_N = B$.

F.3 Dynamic construction line for $\delta_{0,2Bd}$

Adapting the definition of the construction line of ISO 12135 to dynamic testing gives:

$$\delta(\Delta a) = 1{,}87 \cdot \frac{R_{md}}{R_{pd}} \cdot \Delta a \tag{F.4}$$

where R_{md} is estimated from Equation (F.2) and R_{pd}, the dynamic yield strength of the material, shall preferably be obtained from dynamic tensile tests or, alternatively, from the force-displacement test record of the Charpy test using [27]:

$$R_{md} = \frac{0{,}729 \cdot F_m \cdot S}{(W - a_0)^2 B_N} \quad \text{for a 2 mm radius striker} \tag{F.5}$$

or

$$R_{md} = \frac{0{,}683 \cdot F_m \cdot S}{(W - a_0)^2 B_N} \quad \text{for a 8 mm radius striker.} \tag{F.6}$$

NOTE For plane-sided specimens, $B_N = B$.

Annex G
(normative)

Validity criteria

G.1 General

Fracture toughness values determined according to this International Standard are considered to be valid if $a > 0{,}45W$ and the following criteria are met.

G.2 Plain strain fracture toughness

$$K_{Id} \leq \sqrt{0{,}4(W - a_0)} \cdot R_{pd} \tag{G.1}$$

where R_{pd} denotes the dynamic yield strength at the test temperature. If an experimentally determined value of R_{pd} is not available, it may be estimated from Equation (F.5) or Equation (F.6).

G.3 Initiation of cleavage fracture

$$J_{cd}, J_{ud} \leq \frac{R_{fd}(W - a_0)}{100} \tag{G.2}$$

where R_{fd} denotes the plastic flow stress at the actual strain rate and test temperature; i.e., the dynamic equivalent of the static flow stress used in ISO 12135.

If experimentally determined values of R_{pd} and R_{md} are not available, R_{fd} may be estimated by averaging the values of the dynamic yield and ultimate tensile strengths given by Equations (F.5) or (F.6) and Equations (F.2) or (F.3) respectively.

G.4 Onset of ductile tearing

$$J_{0,2Bd} \leq \frac{R_{fd}(W - a_0)}{25} \tag{G.3}$$

$$\delta_{0,2Bd} \leq \frac{W - a_0}{35} \tag{G.4}$$

NOTE J_{cd}, J_{ud}, $J_{0,2Bd}$ and $\delta_{0,2Bd}$ cannot be considered transferable to larger structures. J_{cd} and J_{ucd} values determined in the transition range are size-sensitive parameters and only valid for the thickness of the specimen tested, see ISO 12135.

Annex H
(normative)

Fracture mechanics parameters

H.1 If a beam containing a stationary edge-crack of length a is quasistatically loaded in 3-point bending up to a generic load-line displacement s and a corresponding force F_s, then the J-integral is given by:

$$J = \frac{\eta(a)\cdot W_{sp}}{B_N(W-a)} + \frac{K_I^2(F_s,a)}{E}\left(1-\nu^2\right) \tag{H.1}$$

where:

$$\eta = 1{,}857 + 0{,}143\frac{a}{W} \tag{H.2}$$

$$W_{sp} = W_s - \frac{F_s^2}{2k(a)} \tag{H.3}$$

is the non-recoverable fracture energy at the actual force F_s;

$$W_s = \int_0^s F_s\,ds \tag{H.4}$$

is the actual total fracture energy (area under the force – displacement diagram up to the actual displacement s);

$k(a)$ is the slope of the linear regression line of the initial elastic part of the force versus load-line displacement curve and shall be determined according to ISO 14556;

$K_I(F_s, a)$ is the stress intensity factor given by:

$$K_I = \frac{F_s S}{\sqrt{BB_N W^3}}\, f\left(\frac{a}{W}\right) \tag{H.5}$$

with:

$$f\left(\frac{a}{W}\right) = \frac{3\cdot\sqrt{\frac{a}{W}}}{2\cdot\left(1+2\cdot\frac{a}{W}\right)\cdot\left(1-\frac{a}{W}\right)^{3/2}}\cdot\left(1{,}99-\frac{a}{W}\cdot\left(1-\frac{a}{W}\right)\cdot\left(2{,}15-3{,}93\cdot\frac{a}{W}+2{,}7\cdot\left(\frac{a}{W}\right)^2\right)\right) \tag{H.6}$$

H.2 If stable crack extension from a_0 to $a = a_0 + \Delta a_s$ occurred during the loading up to s, then Equation (H.1) shall be replaced by:

$$J = \frac{\eta(a_0)\cdot W_{sp}}{B_N(W-a_0)}\left[1-\frac{(0.75\eta(a)-1)\cdot\Delta a_s}{W-a_0}\right] + \frac{K_I^2(F_s, a=a_0+\Delta a_s)}{E}\left(1-\nu^2\right) \tag{H.7}$$

H.3 Under the same conditions (i.e. stable crack extension Δa_s occurring up to displacement s), the crack-tip opening displacement can be calculated as follows:

$$\delta = \left[\left(\frac{S}{W}\right)\frac{F_s}{\sqrt{BB_N W}} f\left(\frac{a_0}{W}\right)\right]^2 \left[\frac{1-\nu^2}{2R_{pd}E}\right] + \frac{0{,}6\Delta a_s + 0{,}4(W-a_0)\cdot s_{pl}}{0{,}6(a_0+\Delta a_s)+0{,}4W+z} \quad \text{(H.8)}$$

where R_{pd} can be measured experimentally or estimated using Equation (F.5) or Equation (F.6).

NOTE For plane-sided specimens, $B_N = B$.

Bibliography

[1] T. L. Anderson, Dynamic and Time-Dependent Fracture, in "Fracture Mechanics – Fundamentals and Applications", Second Edition, CRC Press, 1995, pp. 205-225.

[2] ASTM E 1921, Standard Test Method for Determination of Reference Temperature, T_o, for Ferritic Steels in the Transition Range, ASTM Book of Standards, Volume 03.01.

[3] J. F. Kalthoff, S. Winkler, W. Böhme, A Novel Procedure for Measuring the Impact Fracture Toughness K_{Id} with Pre-cracked Charpy Specimens, Int. Conf. DYMAT 85, 2-5 Sep 1985, Paris, France, in: Journal de Physique, Coll. C5, Suppl. No. 8, Tome 46, pp.179 -186, 1985.

[4] W. Böhme, Dynamic Key Curves for Brittle Fracture Impact Tests and Establishment of a Transition Time, 21st Nat. Symp. on Fracture Mechanics, Annapolis, Maryland, USA, 28. 30.06.1988, in: ASTM STP 1074, Eds. J. P. Gudas, J. A. Joyce, and E. M. Hackett, Am. Soc. for Testing and Materials, Philadelphia, pp. 144 -156, 1990.

[5] J. F. Kalthoff, Fracture Behaviour under High Rates of Loading, Engineering Fracture Mechanics Vol.23 No.1 pp. 289-298, 1986.

[6] E. Lucon, R. Chaouadi, and E. van Walle, Different Approaches for the Verification of Force Values Measured with Instrumented Charpy Strikers, in "Pendulum Impact Machines: Procedures and Specimens", ASTM STP 1476, Eds. T. A. Siewert, M. P. Manahan, Sr., and C. N. McCowan, ASTM, 2006, pp. 95-103.

[7] D.R. Ireland, Procedures and Problems Associated with Reliable Control of the Instrumented Impact Test, in "Instrumented Impact Testing", ASTM STP 563, Ed. T. S. DeSisto, Am. Soc. for Testing and Materials, Philadelphia, 1974.

[8] D.R. Ireland, Fracture Toughness Data for Ferritic Nuclear Pressure Vessel Materials, ETI Technical Report TR75-37 for EPRI, 1975.

[9] D.R. Ireland, A Review of the Proposed Standard Method of Test for Impact Testing Precracked Charpy Specimens of Metallic Materials, C.S.N.I. Specialist Meeting on Instrumented Precracked Charpy Testing, EPRI NP-2102-LD, Project 1757-1, C.S.N.I. No.67, Proceedings, November 1981, pp. 1.25-1.64.

[10] ESIS Procedure P7-00, Procedure for Dynamic Tensile Tests.

[11] G. R. Irwin, Crack-Toughness Testing of Strain-Rate Sensitive Materials, Transaction of the ASME, Journal of Engineering for Power, October 1964, pp. 444-450.

[12] A.K. Shoemaker, Factors Influencing the Plane-Strain Crack Toughness Values of a Structural Steel, Transactions of the ASME, Journal of Basic Engineering, Sep 1969, pp. 506-511.

[13] H. J. MacGillivray and D. F. Cannon, The Development of Standard Methods for Determining the Dynamic Fracture Toughness of Metallic Materials, in "Rapid Load Fracture Testing", ASTM STP 1130, Eds R. Chona and W. Corwin, Am. Soc. for Testing and Materials, Philadelphia, pp. 161-179, 1992.

[14] W. Böhme, Experience with Instrumented Charpy Tests obtained by a DVM Round Robin and further Developments, ESIS 20, Ed. E. van Valle, MEP Publications, London, 1996, pp. 1-23.

[15] B. K. Neale, An assessment of fracture toughness in the ductile to brittle transition regime using the Euro fracture toughness dataset, Engineering Fracture Mechanics 69 (2002) 497-509.

[16] W. Böhme, and H.J. Schindler, Application of Single Specimen Methods on Instrumented Charpy Tests: Results of DVM Round Robin Exercises, *Pendulum Impact Testing: A Century of Progress*,

ASTM STP 1380, T. Siewert and M.P. Manahan, Sr. Eds., American Society for Testing and Materials, West Conshohocken, PA, 1999, 327 – 336.

[17] H.J. MacGillivray, Report on ESIS TC5 First Round-Robin Test Programme on Dynamic J_{1c} and J-R Curve Determination, October 1993.

[18] E. Lucon, The Use of Single-Specimen Techniques for Measuring Upper Shelf Toughness Properties under Impact Loading Rates, SCK•CEN Open Report BLG-1016, September 2005.

[19] ASTM E 1820, Standard Test Method for Measurement of Fracture Toughness, ASTM Book of Standards, Volume 03.01.

[20] H. Ernst, P.C. Paris, M. Rossow and J.W. Hutchinson, Analysis of load-displacement relationship to determine J-R curve and tearing instability material properties, *Fracture mechanics*, ASTM STP 677, C. W. Smith, Ed., ASTM, 1979, pp. 581-599.

[21] J.A. Joyce, Static and dynamic J-R curve testing of A533B steel using the Key-curve analysis technique, *Fracture Mechanics: 14th symposium, Volume I: Theory and Analysis*, ASTM STP 791, J.C.Lewis and G. Sines, Eds., ASTM, 1983, pp. I-543-I-560.

[22] K. Brüninghaus, R. Twickler, A. Heuser, D. Memhard and W. Dahl, Application of the Key Curve Method on Static and Dynamic JR-Curve Determination with CT- and SENB-Specimens, Proc. 6th Europ. Conf. Fracture, (ECF 6), Amsterdam, 1986, S. 429.

[23] R. Ott and W. Böhme, Anwendung der Key-Curve Methode zur bruchmechanischen Analyse von instrumentierten Schlagbiegeversuchen, Fraunhofer-IWM-Report Z 18/92, Freiburg, December 1999 (in German).

[24] H. J. Schindler, Estimation of the dynamic J-R-curve from a single impact bending test, Proceedings of 11th European Conf. on Fracture (ECF11), Poitiers, 1996, EMAS, pp. 2007-2012.

[25] H. J. Schindler, Estimation of fracture toughness from Charpy tests – theoretical relations, *Pendulum Impact Testing: A Century of Progress*, ASTM STP 1380, T. Siewert and M. P. Manahan, Sr. Eds., American Society for Testing and Materials, West Conshohocken, PA, 1999, 337-353.

[26] J. D. Landes, Z. Zhou, K. Lee and R. Herrera, Normalization method for developing J-R curves with the LMN function, Journal of Testing and Evaluation, Vol. 19, No. 4, July 1991, pp. 305-311.

[27] W. L. Server, General Yielding of Charpy V-Notch and Precracked Charpy Specimens, Journal of Engineering Materials and Technology, Vol. 100, Apr 1978, pp. 183-188.

ANNEX 4

Sections of IAEA CRP-8 Final Report related to loading rate effects (Topic Area #2)

4. LOADING RATE EFFECTS AND QUALIFICATION OF IMPACT FRACTURE TOUGHNESS TESTING

4.1 Background

The Master Curve (MC) approach procedure standardised in ASTM E 1921-08 is defined for quasi-static loading conditions. However, the use of the MC method for dynamic test is obvious. Namely impact toughness results on different RPV steels were already obtained in the frame of previous CRPs. Dynamic and impact tests conducted by Wallin [4-1], Joyce and Tregoning [4-2,4-3], Viehrig [4-4] suggest that dynamic fracture toughness values confirm the MC course. Wallin [4-5] proposed an empirical relationship between loading rate dK/dt and increase of the reference temperature ΔT_0 (in K) based on the analysis of a large database mostly consisting of RPV steels.

$$\Delta T_0 = \frac{T_{01} \cdot \ln\left(\frac{dK_I}{dt}\right)}{\Gamma - \ln\left(\frac{dK_I}{dt}\right)} \tag{4.1}$$

where: T_{01} reference temperature measured under quasi-static conditions (in K)
Γ empirical function based on the Zener-Holloman Strain Rate parameter given by

$$\Gamma = 9.9 \cdot \exp\left[\left(\frac{T_{01}}{190}\right)^{1.66} + \left(\frac{R_{el}}{722}\right)^{1.09}\right] \tag{4.2}$$

with: R_{eL} = quasi-static yield strength (in MPa).

To exclude the influence of the loading rate on the measured reference temperature a range is given in the ASTM E1921-08 standard. In a previous version of ASTM E1921 (2003) the allowed loading rate was specified in terms of time take to reach 40% of the limit load (between 0.1 and 10 min). Investigations by Wallin [4-6], Hall and Yoon [4-7,4-8] and Joyce et al. [4-9] have clearly shown that within this range the variation in T_o is significantly larger than 10 K. In order to remain within this limit the allowed range was reduced in the current version of ASTM E1921 to dK/dt between 0.1 and 2 MPa√m/s. At the same time the ASTM Technical Committee responsible for E1921 is working on developing an appendix for higher loading rates up to impact testing. The results of this CRP Topic Area will provide a significant contribution to this effort with test results covering the range between quasi-static loading rates (0.1 to 2 MPa√m/s) and impact loading rates (10^5 MPa√m/s using instrumented impact pendulum machines).

Impact toughness tests on precracked Charpy specimens have been performed by many institutions for several decades now. Indeed, the instrumentation of the striker made it possible to use the simple Charpy test for dynamic fracture mechanics testing and, thus to apply the results for the structural integrity assessment. In the range of lower shelf and the lower ductile-to-brittle transition (DBT) region, J-integral-based fracture toughness values,

K_{Jc}, can be determined at the onset of cleavage crack initiation. The onset of cleavage fracture appears on the measured force versus time trace as a force drop.

The execution of the tests and the calculation of dynamic fracture toughness data of precracked Charpy specimens have not yet been defined by any official international standard. However, there are procedures and draft standards published by the Electric Power Research Institute (EPRI) in the report EPRI NP-119 [4-10,4-11] and the Draft International Standard: ESIS, European Structure Integrity Society: "Proposed Standard Methods for Instrumented Pre-cracked Charpy Impact Testing of Steels – Combined K_{Id}, J_{Id} and CTOD Tests Methods", respectively. The state-of-the-art in the dynamic fracture toughness measurement using pre-cracked Charpy size specimens was summarised by Lucon [4-12]. Based on these references, a set of guidelines has been developed for impact tests performed within Topic Area #2 of this CRP.

4.2 Investigation of loading rate effects

4.2.1 Data sets analyzed

CRP-8 participants were required to perform and evaluate the tests in accordance with the current version of ASTM E1921. The Master Curve data sets supplied by the participants for different blocks of JRQ and national steels are summarised in Table X and Y of Appendix B. Figures 4-1 and 4-2 show the values T_0 as a function of loading rates ranging from quasi-static to impact. The most comprehensive data are available for the JRQ steel (Figure 4-1), whereas for the national steels (Figure 4-2) the limited data available for each steel can only provide information about the general trends.

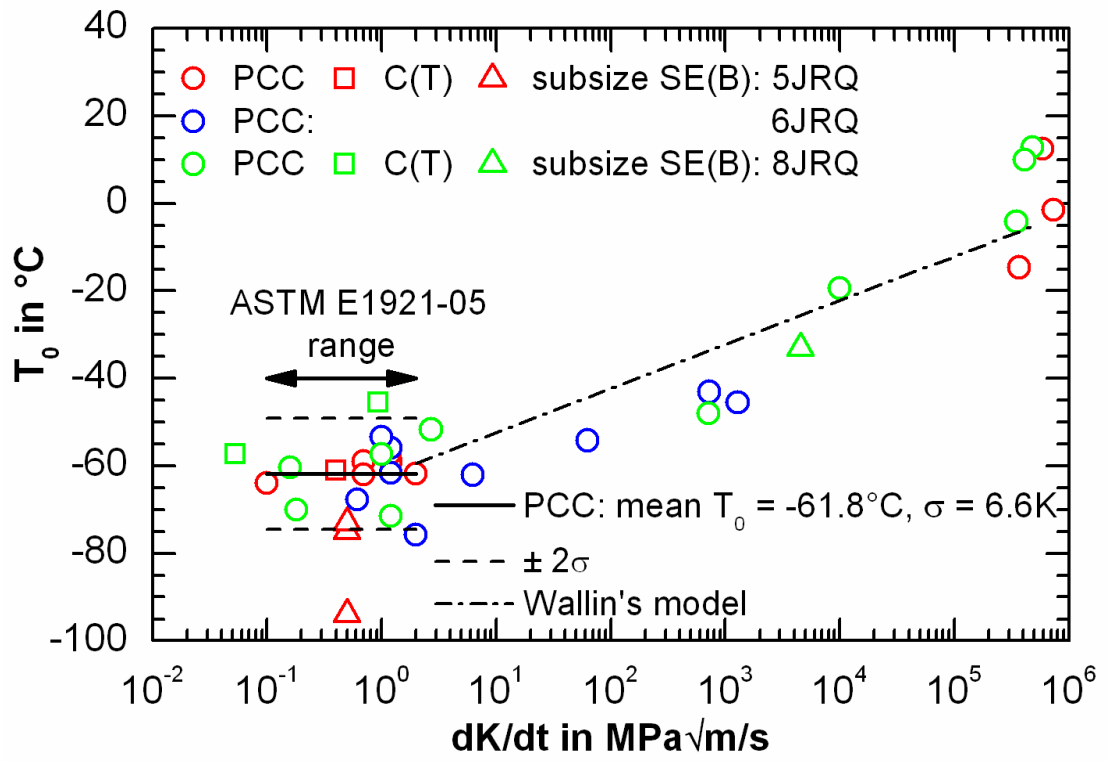

Figure 4-1. Reference temperature T_0 vs. loading rate for different JRQ blocks (PCC specimens only) and comparison with the predictions of Eq. (4.1) (Wallin's model).

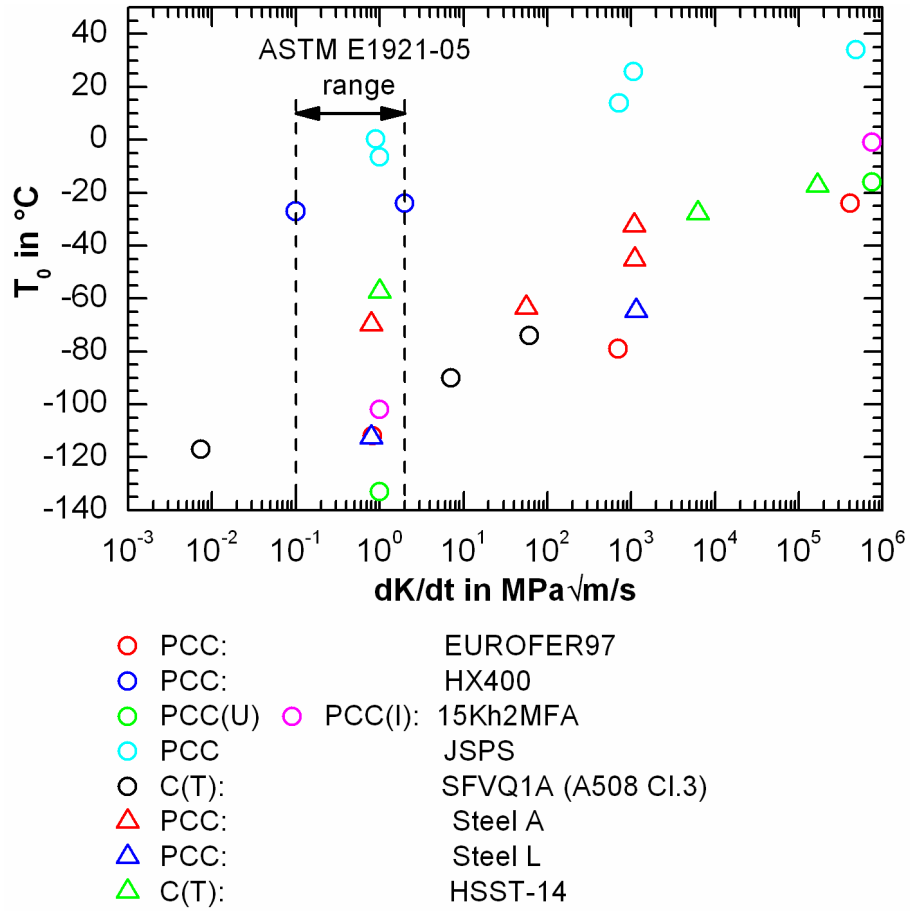

Figure 4-2. Reference temperature T_0 vs. loading rate for the national steels.

4.2.2 Variation of T_o within the quasi-static loading range (0.1 – 2 MPa√m/s)

As shown by Figures 4-1 and 4-2, there is no systematic variation of T_0 within the quasi-static loading range prescribed by ASTM E1921-08 (0.1 to 2 MPa√m/s). For JRQ, all T_0 values are within the $\pm 2\sigma$ scatter band. The observed scatter is likely a result of variations between different JRQ plates, different specimen geometries (PCC and C(T)) and testing in different laboratories. The T_0 values determined with PCC specimens of the 5JRQ plate fall within a small scatter band, even through the tests were performed by different laboratories (Figure 4.1). This statement is substantially confirmed by the results obtained within the quasi-static range for the HX400 and JSPS steels (Figure 4.2).

4.2.3 Variation of T_o outside the quasi-static loading range (below 0.1 MPa√m/s and above 2 MPa√m/s)

Above the 2 MPa√m/s limit, there is a clearly defined trend to increasing T_0 values with increasing loading rates [4-2, 4-4, 4-5, 4-6, 4-13]. As depicted in Figure 4-1, the shift of T_0 with increasing dK/dt for the JRQ steel can be satisfactorily predicted using Wallin's empirical relationship, Eq. (4.1). This correlation predicts an increase of about 52 K between the upper limit of the quasi-static loading rate (2 MPa√m/s) and an impact loading rate of about 3.5×10^5 MPa√m/s, corresponding to impact loaded PCC specimens (round robin

exercise, see below). This variation is about 15 K lower than experimentally determined in the round robin exercise (see Table 4-3 below). The trend to higher T_0 values with increasing loading rate can also be observed for the national steels, but the results shown in Figure 4-2 indicate that the slope is material-dependent. Namely, JSPS, steel A and HSST-14 show a shallower slope compared with JRQ, EUROFER 97 and steel L.

4.3 Impact Fracture Toughness Round-Robin Exercise (RRE) on Precracked Charpy Size Specimens

The round robin exercise involves 12 labs. General guidelines specified by the topic area leaders are reported in the following.

4.3.1 Test conditions and analysis procedures

The test conditions and requirements were:

- Loading rate: 1.2 m/s
- Test temperature range : -30 to 10 °C
- Specimen geometry: SE(B), Charpy-type, Charpy V-notch + sharpened notch (for crack initiation) = total depth 2.5 mm; specimens 20% side-grooved
- 10 specimens to be tested by each laboratory
- Minimum response frequency of the acquisition system: 100 kHz
- Minimum sampling rate: 2 µs
- Precracking conditions: initiation of fatigue crack K_{max} = 25 MPa√m; finish sharpening K_{max} = 18.5 MPa√m.
- Side-grooving: according to E1921, §7.7.
- Pre-test dimensional measurements: B, B_N, W (precision: 0.01 mm)
- Status of machine/thermocouple calibration and temperature control/conditioning times/transfer time: in accordance with ASTM E23
- Post-test crack size measurements: a_o, a_f (9-point average method, precision 0.01 mm)

From the dynamic test record, the absorbed impact energy is calculated from the area under the force-displacement curve up to the onset of cleavage fracture. Force is directly measured and displacement is calculated, by double numerical integration of force/time data according to Eqs. (1) and (2).

$$V(t) = V_0 - \frac{1}{m}\int_{t_0}^{t} F(t)dt \tag{4.3}$$

$$s(t) = \int_{t_0}^{t} V(t)dt \tag{4.4}$$

m mass of the pendulum hammer
F impact force measured at the pendulum striker
V actual velocity of the pendulum hammer
V_0 initial impact velocity of the pendulum hammer
s deflection of the specimen

The J integral at the onset of cleavage fracture, Eq. (5), is determined per ASTM E1921-08 in analogy to the standards ISO/DIS 12135 "Metallic Materials – Unified Method of Test for the Determination of Quasistatic Fracture Toughness" and ASTM E1820 "Standard Test Method for Measurement of Fracture Toughness".

$$J_c = J_{el} + J_{pl} = \frac{K_c{}^2(1-\nu^2)}{E} + \frac{2W_{c(pl)}}{B_N b_0} \tag{4.5}$$

B_N specimen net thickness between side grooves
b_0 specimen ligament
E Young's modulus calculated as a function of test temperature T using:

$$E = 207000 - (T-20)\cdot 87 \quad \text{in MPa}$$

J_{el} elastic component of the J-integral
J_p plastic component of the J-integral
K_c stress intensity at the onset of cleavage failure
$W_{c(pl)}$ plastic part of the area under the force-deflection curve
ν Poisson's ratio

$$K_c = \left[\frac{F_c \cdot S}{\sqrt{B \cdot B_N . W^3}}\right] \cdot f(a/W) \tag{4.6}$$

where
F_c force at cleavage failure determined at the onset of the force drop in the force deflection curve
S span value of the anvils (for a DIN 300 J pendulum: 42 mm)
B specimen thickness
W specimen width
f(a/W) specimen stress intensity function for SE(B) specimens

$$f(a_0/W) = \frac{3\cdot\sqrt{\frac{a_0}{W}}\cdot\left[1.99 - \left(\frac{a_0}{W}\right)\cdot\left(1-\frac{a_0}{W}\right)\cdot\left(2.15 - 3.93\cdot\left(\frac{a_0}{W}\right) + 2.7\cdot\left(\frac{a_0}{W}\right)^2\right)\right]}{2\cdot\left(1+\frac{2a_0}{W}\right)\cdot\left(1-\frac{a_0}{W}\right)^{1,5}} \tag{4.7}$$

The total absorbed impact energy W_{tot} is calculated from the area under the force-displacement curve up to the onset of cleavage fracture. This energy value contains some contributions not related to fracturing the specimen. The true specimen initiation energy, $W_{c(pl)}$, is determined according to Eq. (8).

$$W_{c(pl)} = W_{tot} - \frac{C_0 \cdot F_c{}^2}{2} \tag{4.8}$$

with C_0 = reciprocal of the initial elastic slope.

The initial elastic slope is determined according to the ESIS draft on "Proposed standard methods for instrumented pre-cracked Charpy impact testing of steels".

Acceptable force values F_c are obtained when the inertial oscillations have been sufficiently dampened, namely after 3 complete oscillations (3τ, with τ = period of force oscillation) [4-10,4-11,4-12].

J_c values are transformed into values of plain strain stress intensity factor K_{Jc} according to ASTM E 1921-08 using Eq. (9).

$$K_{Jc} = \sqrt{\frac{E \cdot J_c}{1-\nu^2}} \tag{4.9}$$

The calculated K_{Jc} are used to evaluate the reference temperature T_o following ASTM E1921-08.

For the tests performed in the framework of the RRE, the loading rate dK/dt has been calculated in MPa√m/s as the ratio between K_{Jc} and the time to fracture t_f. This is the recommended approach according to the investigation detailed in Appendix B, Section B.1.

Dynamic yield strength properties for the calculation of the validity limit K_{lim} has been evaluated according to:

$$\sigma_{yd} = \frac{4 \cdot F_{gy}}{C \cdot B_N (W-a_0)^2} \cdot \frac{S}{4} = \frac{C' \cdot F_{gy}}{B_N \cdot (W-a_0)^2} \cdot \frac{S}{4} \tag{4.10}$$

where:

a_0 initial crack length

C constraint factor (C' = C/4); for pre-cracked Charpy size SE(B): ISO-tup C'= 3.13; ASTM-tup C' = 2.98

F_{gy} force at general yield (in N).

Additional options available for estimating yield strength in case of elevated loading rates are described in Appendix B, Section B.3.

4.3.2 Results of the RRE

Twelve organizations signed up for the round-robin exercise (see Table 4.1); each of them received from JRC Petten 10 precracked and side-grooved Charpy specimens of JRQ material (plate 8JRQ44). Later, one of the participants pulled out due to the unavailability of the testing machine. Consequently, the round-robin exercise counted eleven participants.

Each participant sent in his results using the data reporting Excel spreadsheets supplied by the topic area leaders.

4.3.2.1 Master Curve results provided by the participants

Table 4-3 summarizes the original results of the Master Curve analyses provided by the round-robin participants (number of specimens tested N, number of valid data r, sum of weighting factors $\sum n_i$, reference temperature T_o, standard deviation σ_{To}, average loading rate dK/dt). For reference purposes, the Table also reports the results obtained by FZD at quasi-static loading rate (1.2 MPa√m/s) on PCVN specimens of the same plate (8JRQ44).

Each participant tested 10 specimens; lab 4 supplied only 8 valid results, due to a fault in the acquisition system. Lab 11 used a higher impact speed (1.6 m/s) than prescribed. All participants provided valid reference temperatures ($\sum n_i \geq 1$); invalid tests ranged from a minimum of 0 to a maximum of 3.

Table 4-3. Results supplied by the round-robin exercise participants.

Lab #	N	r	$\sum n_i$	T_o (°C)	σ_{To} (°C)	dK/dt (MPa√m/s)
1	10	9	1.40	-1.6	6.0	3.51×10^5
2	10	9	1.40	1.6	6.0	3.21×10^5
3	10	7	1.12	-9.9	6.8	3.70×10^5
4	8	8	1.18	10.0	6.6	4.14×10^5
5	10	10	1.57	2.1	5.7	3.29×10^5
6	10	9	1.32	4.6	6.0	3.44×10^5
7	10	8	1.33	-20.4	6.4	2.69×10^5
8	10	9	1.40	-1.1	6.0	3.36×10^5
9	10	7	1.07	-2.5	6.8	4.25×10^5
10	10	9	1.40	-3.8	6.0	5.02×10^5
11	10	10	1.57	-2.6	5.7	4.66×10^5
Average values			1.34	-2.1	6.2	3.75×10^5
FZD	8	8	1.29	-71.4	6.4	1.2

T_o values reported by participants range from -20.4 to 10.0 °C, corresponding to a maximum difference of 30.4 °C. The difference between impact (average value) and quasi-static reference temperature is 69.3 °C.

Individual Master Curves for RRE data sets are compared in Figure 4-3.

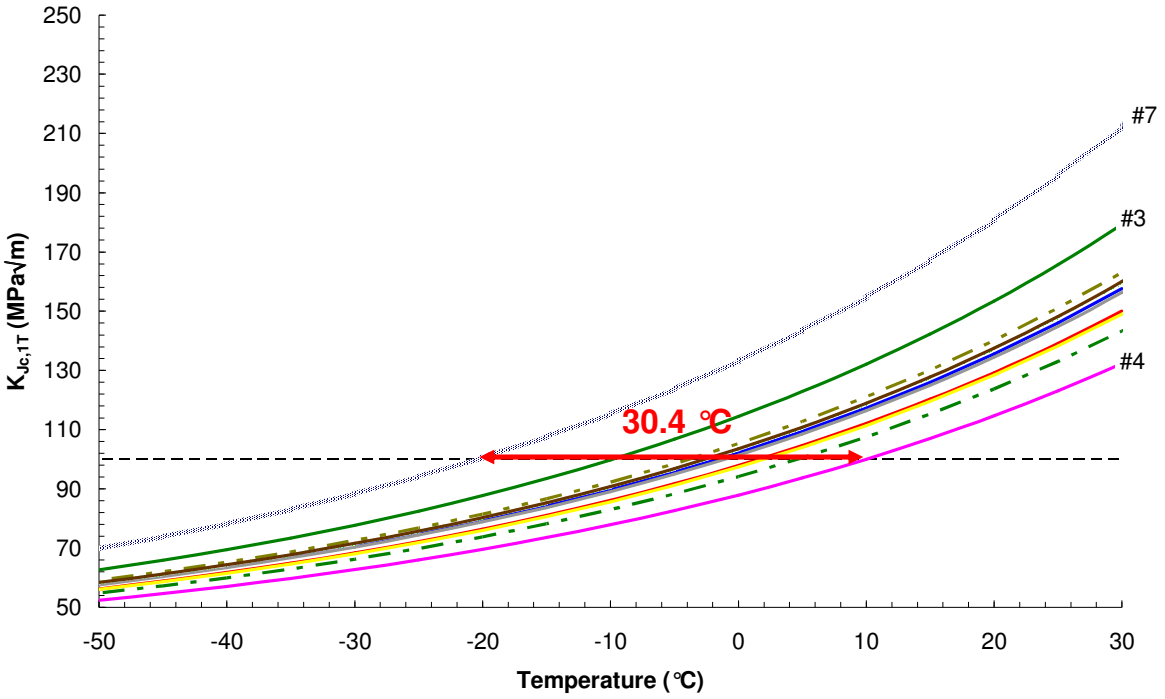

Figure 4-3. Master Curves supplied by the round-robin participants.

Individual K_{Jc} test results (normalized to 25 mm reference thickness), including quasi-static data, are plotted in Figure 4-4 as a function of the difference between test temperature and reference temperature reported by the corresponding lab ($T_{o,lab}$). This

normalized representation shows that impact fracture toughness values measured in the round-robin exercise effectively follow the Master Curve and its tolerance bounds.

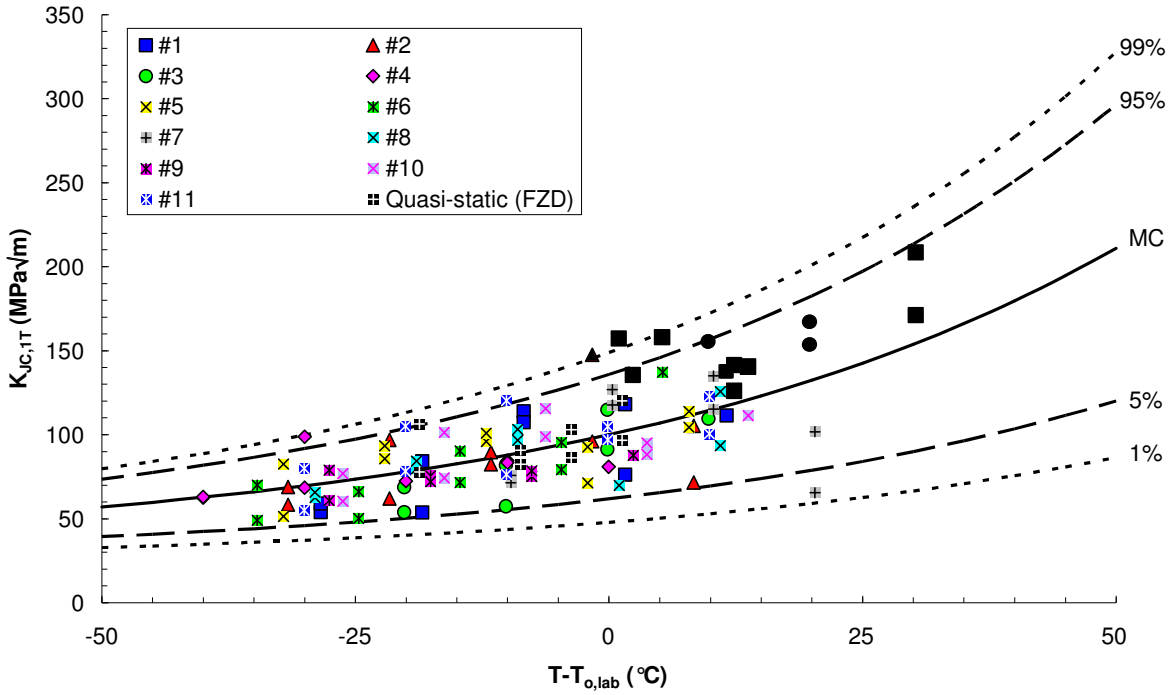

Figure 4-4. Normalized fracture toughness values measured in the round-robin exercise compared to the Master Curve and its tolerance bounds. Black symbols represent invalid (censored) data. Quasi-static data measured by FZD are also included.

An overall Master Curve analysis was performed on the individual K_{Jc} values supplied by the participants (108 data points, 95 valid). The results are shown in Table 4-4 and Figure 4-5. The increase with respect to the quasi-static value (-71.4 °C) is now 67.4 °C.

Table 4-4. Results of the overall Master Curve analysis performed on the round-robin dataset.

N	r	$\sum n_i$	T_o (°C)	σ_{To} (°C)
108	95	14.79	-4.0	1.8

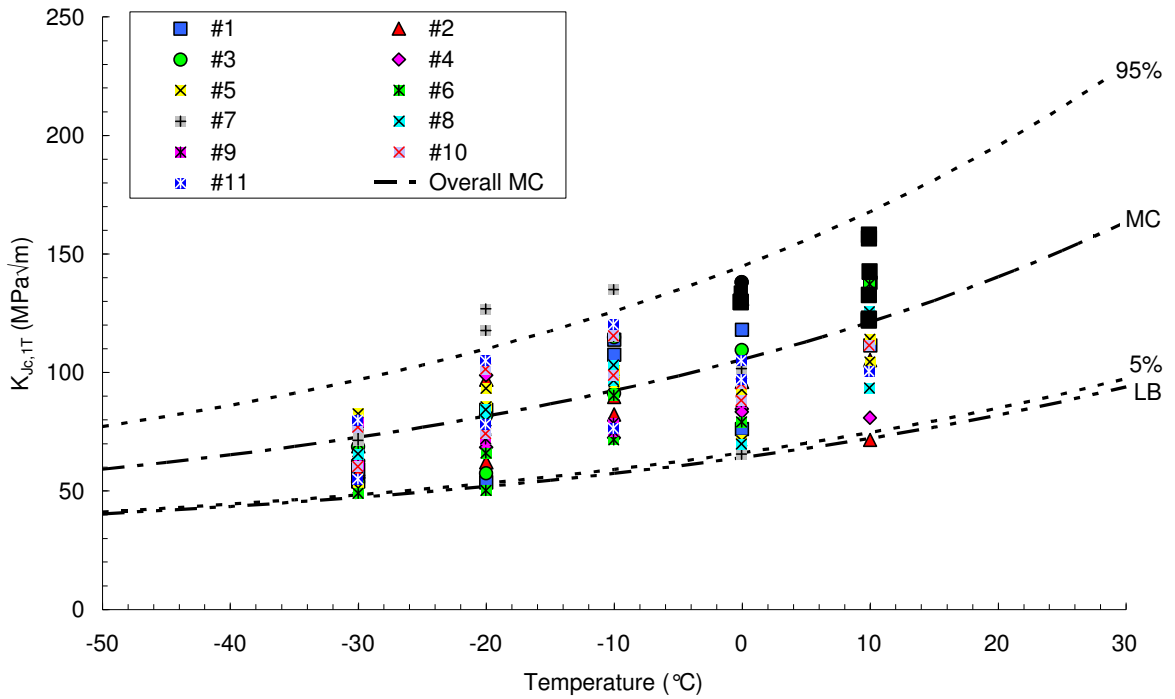

Figure 4-5. Overall Master Curve analysis of the round-robin data set (with 5%-95% tolerance bounds and margin-adjusted 5% tolerance bound). Black symbols represent invalid (censored) data.

Individual T_o values supplied by the participants, with ±2σ error bars, are compared in Figure 4-6 with the result of the overall analysis ($T_{o,all}$ ± 2σ).

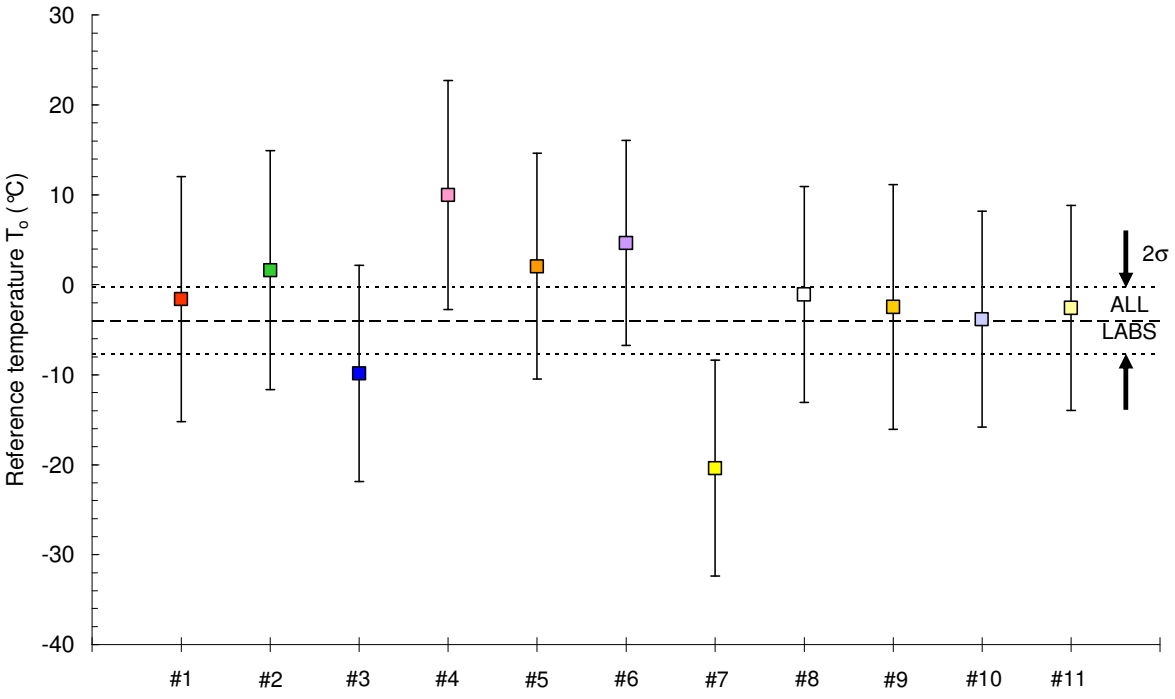

Figure 4-6. Comparison between individual and overall Master Curve reference temperatures with ±2σ error bars.

It is noted that for one data set (lab 7), the error bars do not overlap with the 95% confidence interval around $T_{o,all}$. Furthermore, examination of Figures 4-3 and 4-5 shows that lab 7 has supplied data which fall way above the general trend and could therefore be considered potential outliers (K_{Jc} values too high, T_o too low).

If this datasets is excluded, the maximum difference between individual reference temperature drops to 19.8 °C; the results of the updated overall Master Curve analysis are shown in Table 4-5 and Figure 4-7. Figure 4-8 also shows that, after removing the potential outlier, the error bands of all remaining data sets do overlap with the overall analysis. Furthermore, it can be noted that the lowest and the highest reference temperatures (from labs 3 and 4 respectively) are <u>not</u> statistically different at the 95% (±2σ) confidence level.

A more detailed investigation, which confirms the nature of the outlier data set, is presented in Appendix B, Section B.5.1.

Table 4-5. Results of the updated overall Master Curve analysis after excluding data from lab 7.

N	r	$\sum n_i$	T_o (°C)	σ_{To} (°C)	dK/dt (MPa√m/s)
98	87	13.55	-0.9	1.9	3.86E+05

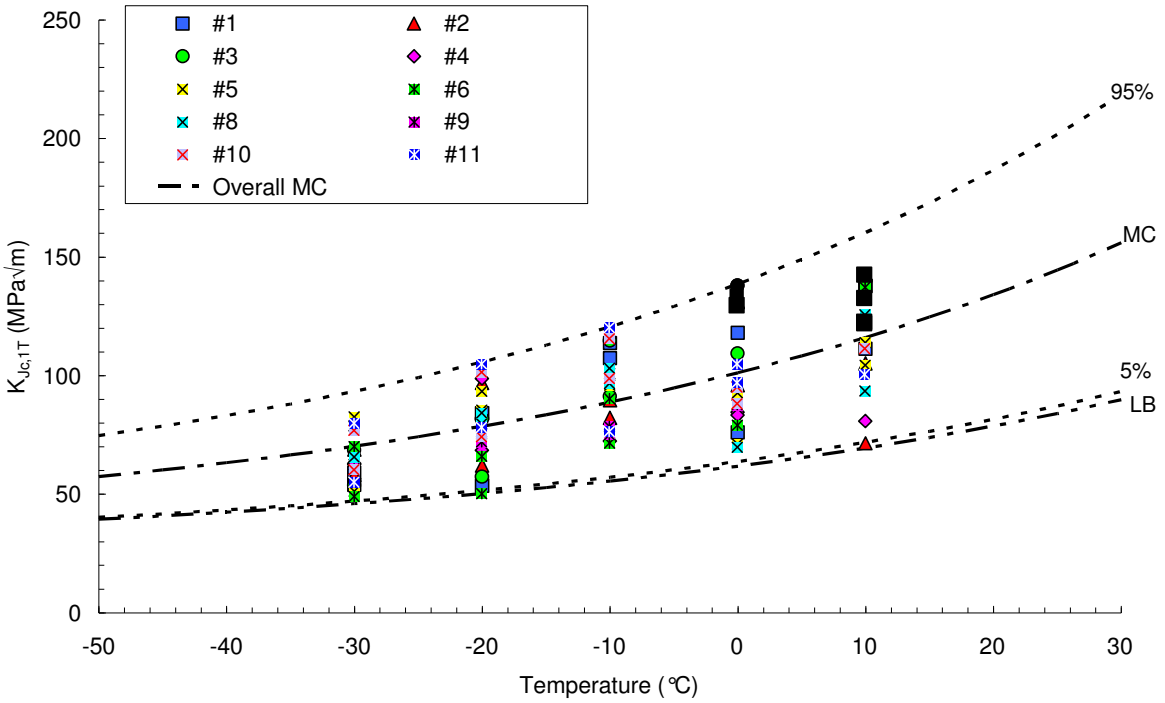

Figure 4-7. Overall updated Master Curve analysis of the round-robin data set after excluding data from lab 7. Black data points represent invalid (censored) data.

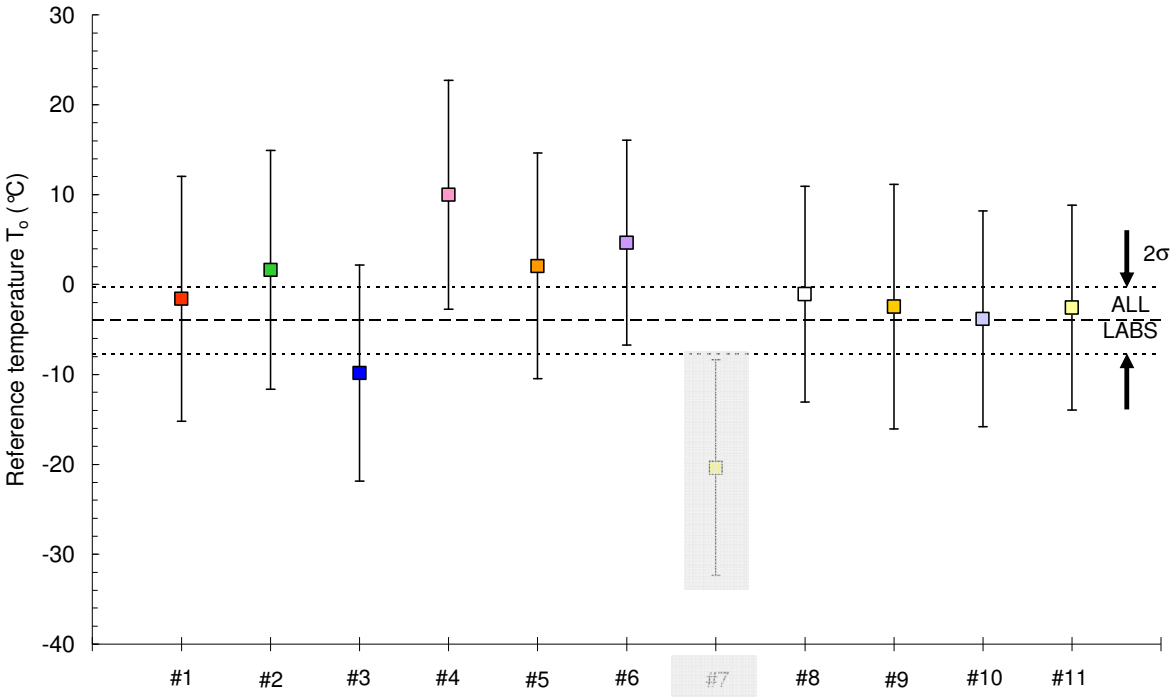

Figure 4-8. Comparison between individual and overall Master Curve reference temperatures after removing data from lab 7.

4.3.2.2 Common re-evaluation of the RRE data sets

In order to investigate the influence of possible subjective interpretations of the analysis method, all individual test results were reanalyzed by Forschungszentrum Dresden-Rossendorf (FZR) in strict accordance with the guidelines given in §4.3.1. Reanalysis consisted in re-evaluating all individual K_{Jc} results (on the basis of original time, displacement and force data supplied by participants) and re-calculating individual T_o values according to ASTM E1921-08.

The re-analysis was conducted using two different approaches for the evaluation of the elastic and plastic components of the energy absorbed up to cleavage (and therefore of the J-integral):

(a) using the fitted slope of the initial elastic portion of the force/displacement record;

(b) using the theoretical compliance C_o, calculated as the sum of the specimen compliance C_S (obtained by FZD using FEM for a precracked Charpy specimen with a/W = 0.5) and the machine compliance C_M, which was requested to each participant as one of the input data.

Re-evaluated T_o using the two approaches are compared to original values in Table 4-7. In the case of approach (b), T_o could be re-evaluated only for those participants who provided the value of machine compliance in the Test Report form (7 out of 11).

Variations up to 17.3 °C (lab #10) for approach (a) and up to 16.1 °C (lab #3) for approach (b) were obtained; in most cases, variations are of the same order of magnitude as the standard deviations σ_{To} or lower. In general, recalculated T_o were found to be slightly higher than the original submissions (average differences = 4.4 and 6.9 °C for the two approaches respectively). Such variations should not be attributed to the Master Curve calculations (which were carried out using the same EXCEL97 subroutine for all participants), but to differences in the calculation of individual K_{Jc} values based on the original time/displacement/force data supplied by the participants.

Again, the reference temperature obtained by FZD at quasi-static strain rates is indicated in Table 4-7. The dynamic increase of T_o is now 75.9 °C using the measured compliance and 78.3 °C using the theoretical compliance.

Table 4-7. Comparison between original ($T_{o,or}$) and re-calculated ($T_{o,re}$, using approaches (a) and (b)) values.

Lab #	$T_{o,or}$ (°C)	$T_{o,re(a)}$ (°C)	$T_{o,re(a)} - T_{o,or}$ (°C)	$T_{o,re(b)}$ (°C)	$T_{o,re(b)} - T_{o,or}$ (°C)
1	-1.6	3.5	5.8	6.5	8.8
2	1.6	3.7	2.1	-0.5	-2.1
3	-9.9	-5.2	4.7	3.4	13.3
4	10.0	1.6	-8.4	3.0	-8.4
5	2.1	1.7	-0.4	-	-
6	4.6	11.8	7.2	8.5	3.9
7	-20.4	-22.3	-1.9	-	-
8	-1.1	-1.3	-0.2	-	-
9	-2.5	11.3	13.8	10.2	12.7
10	-3.8	15.6	19.4	-	-
11	-2.6	6.1	8.7	3.2	5.8
Average	-2.1	2.2	4.4	6.9	6.9
Quasi-static loading rate (FZD tests) T_o = -71.4 °C					

After re-analysis according to approach (a), the maximum difference between individual T_o values increases from 30.4 to 35.8 °C (Figure 4-9). A normalized representation of the re-analyzed data set, using the differences between test temperatures and recalculated T_o, is given in Figure 4-10 (including quasi-static data). These and the following analyses cannot be repeated for approach (b) since the theoretical compliance is not available for all participants.

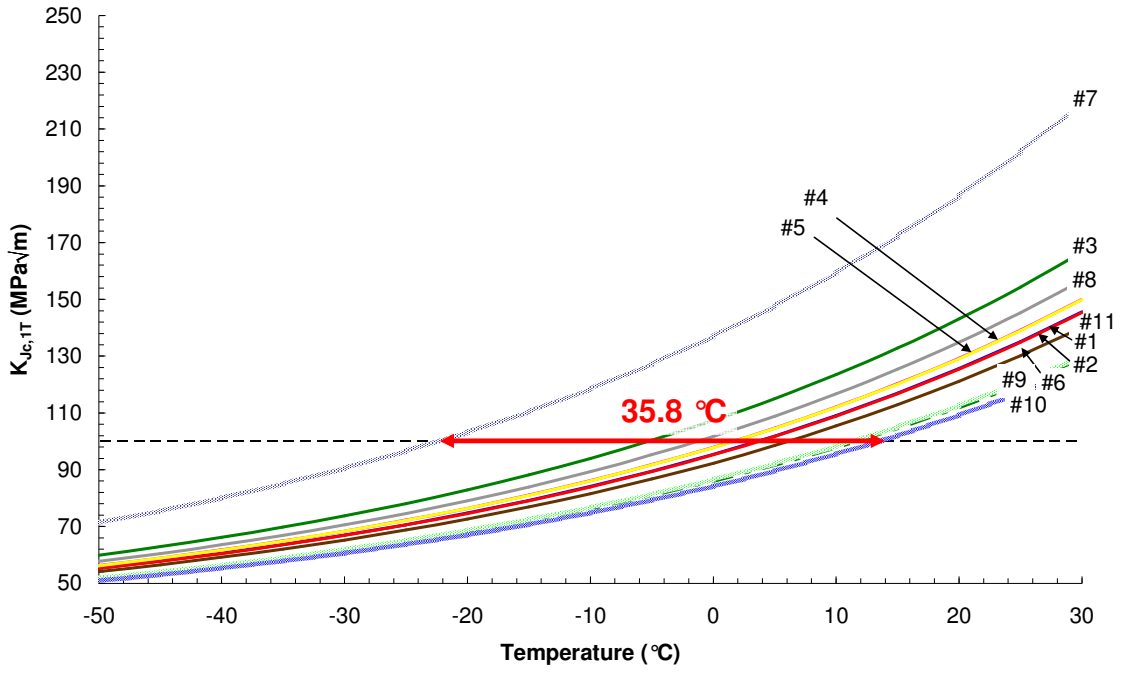

Figure 4-9. Individual Master Curves for round-robin participants after re-analysis by FZD.

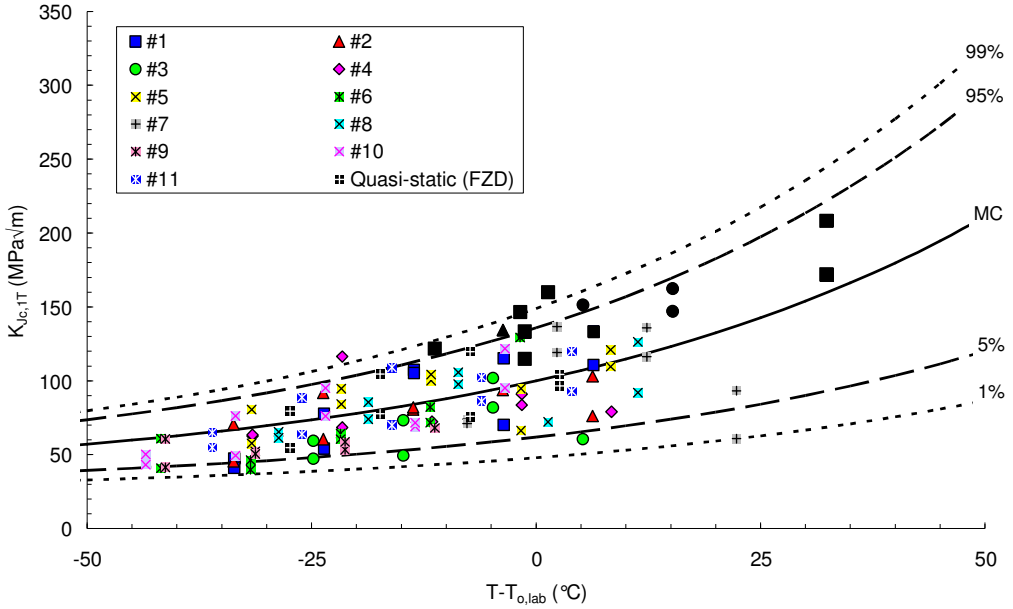

Figure 4-10. Normalized fracture toughness values measured in the round-robin exercise after re-analysis by FZD. Black symbols represent invalid (censored) data.

Results of the overall Master Curve analysis of the re-analyzed data set are provided in Table 4-8 and Figure 4-11. The overall reference temperature slightly increases.

Table 4-8. Results of the overall Master Curve analysis performed on the round-robin data set after re-analysis by FZD.

N	r	$\sum n_i$	T_o (°C)	σ_{To} (°C)
108	97	15.12	-1.6	1.8

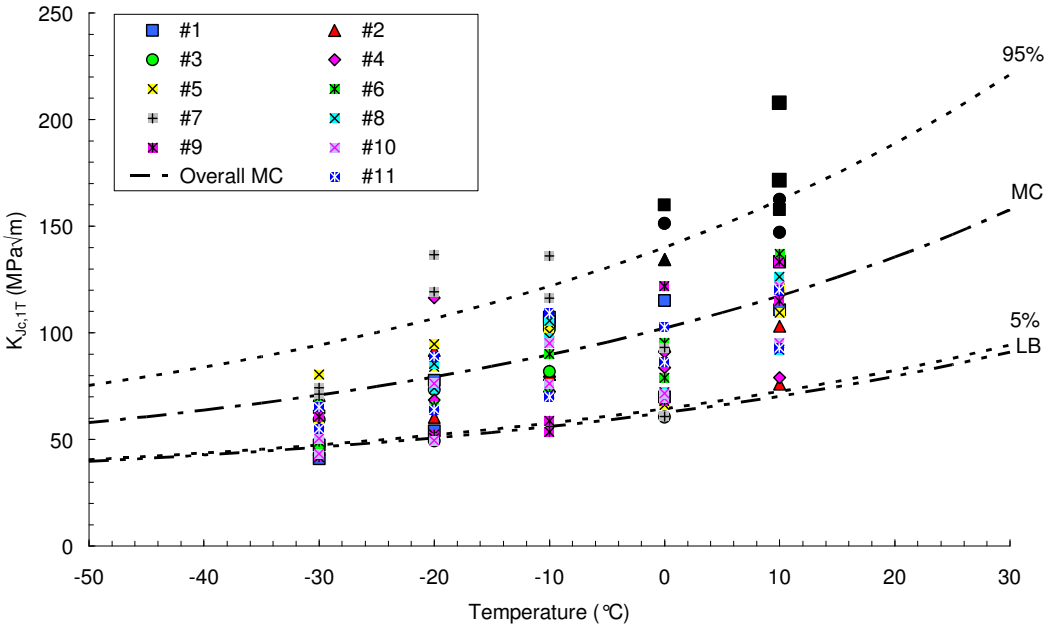

Figure 4-11. Overall Master Curve analysis of the round-robin data set, after re-analysis by FZD.

Re-calculated T_o values, with $\pm 2\sigma$ error bars, are compared in Figure 4-12 to the outcome of the overall Master Curve analysis.

Even after re-analysis, the potential outlier nature of lab 7 is confirmed.

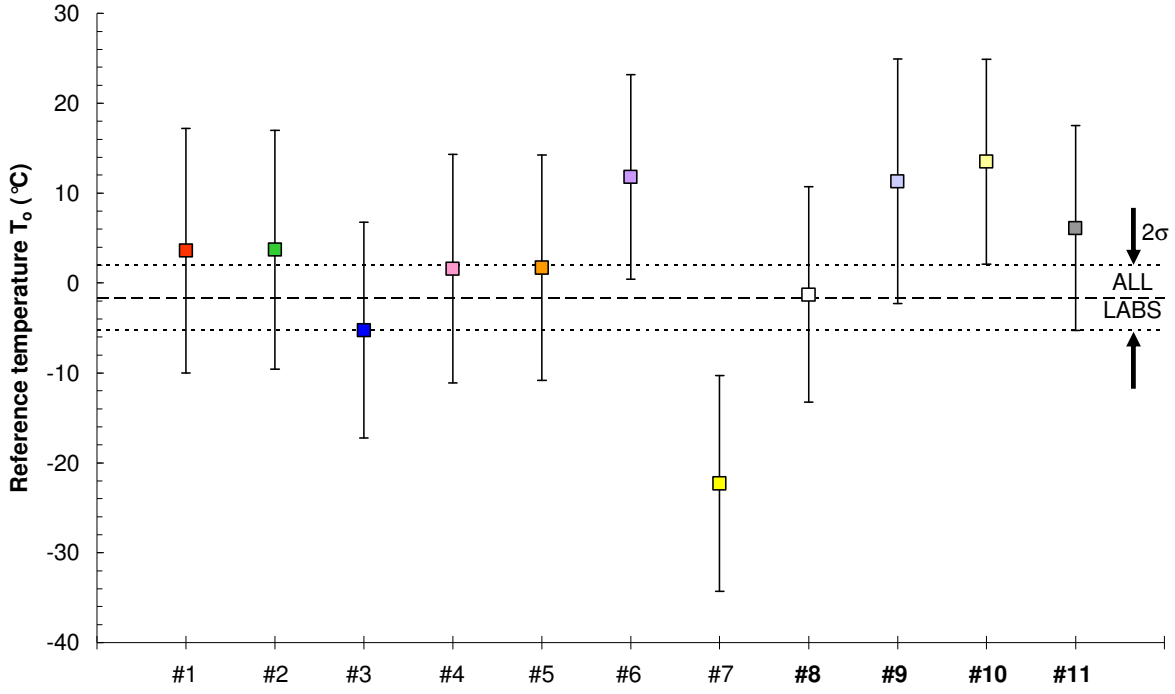

Figure 4-12. Comparison between individual and overall Master Curve reference temperatures ($T_o \pm 2\sigma$) after re-analysis by FZD.

4.3.2.3 Influence of pendulum striker radius on the reference temperature

Three of the RRE participating laboratories (#3, #8 and #10) used an instrumented striker conforming to the ASTM E23 standard, i.e. with a tup radius of 8 mm. The remaining eight labs used a 2 mm striker, i.e. conforming to the ISO 148 standard.

The values of Master Curve reference temperature obtained by the individual labs allow assessing a possible influence of striker radius on the results of impact toughness testing. Note that lab #7 is not included in this assessment.

Using the original T_o and K_{Jc} values reported by participants, the assessment is shown in Figure 4-13 (T_o vs striker radius) and Figure 4-14 (comparison between Master Curves obtained by separately analyzing 2mm and 8mm striker data). The corresponding analyses on RRE data reanalyzed by FZD (§4.3.2.2) are shown in Figures 4-15 and 4-16.

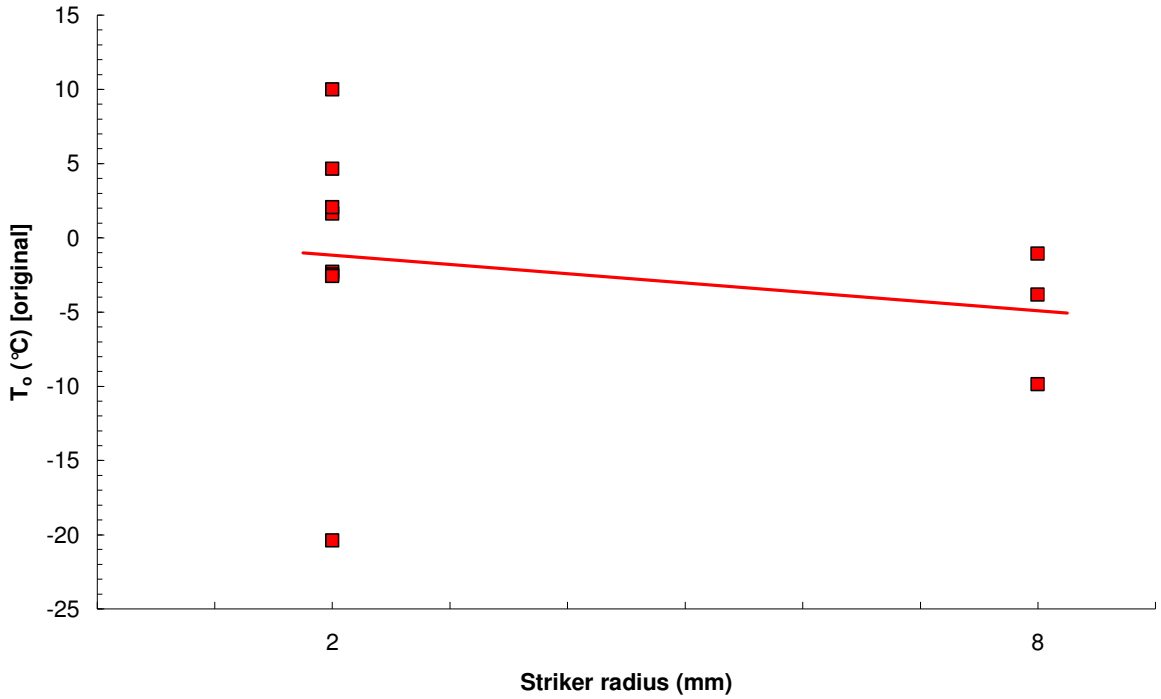

Figure 4-13. Influence of striker radius on T_o (original RRE submissions).

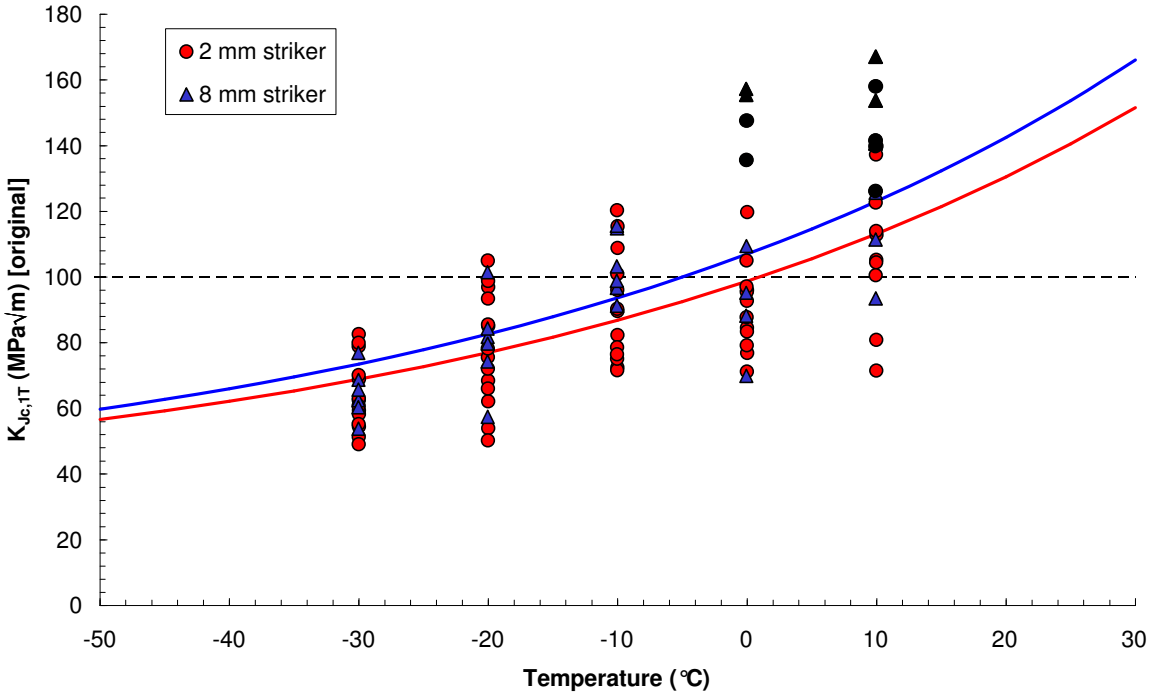

Figure 4-14. Master Curves obtained from 2mm and 8mm striker test results (original RRE submissions). Black symbols are invalid (censored) data.

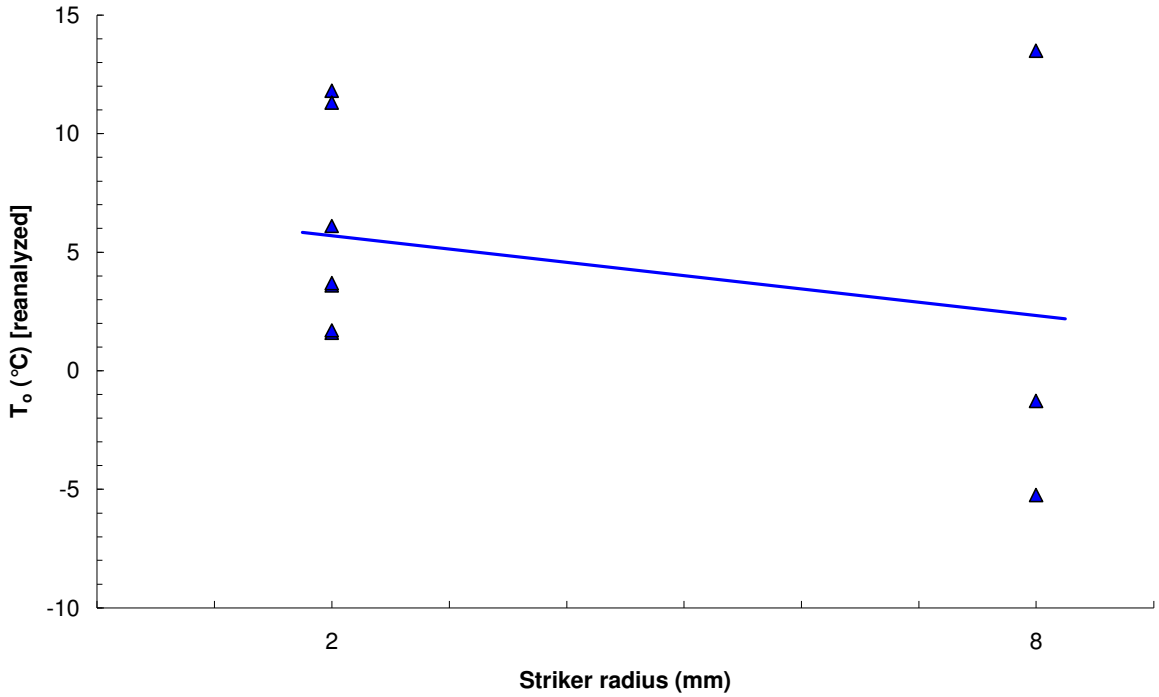

Figure 4-15. Influence of striker radius on T_o (RRE data reanalyzed by FZD).

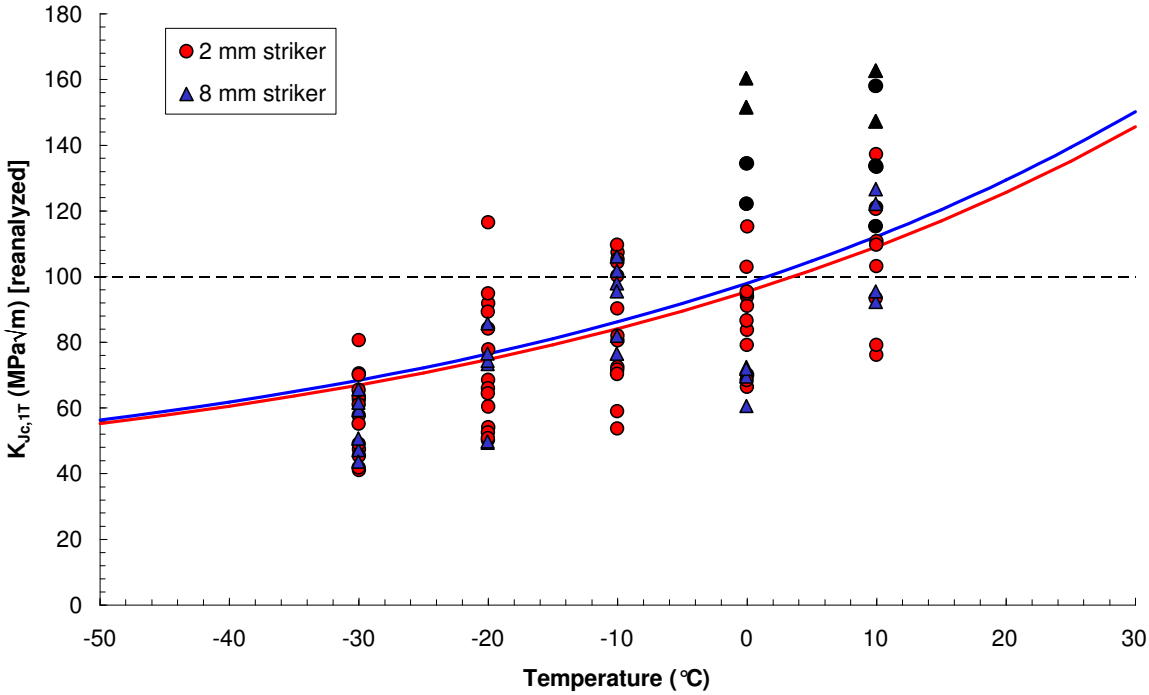

Figure 4-16. Master Curves obtained from 2mm and 8mm striker test results (RRE data reanalyzed by FZD). Black symbols are invalid (censored) data.

Original RRE data show a decrease of T_o with striker radius, but if reanalyzed data are considered the effect becomes negligible (see also the Master Curves in Figure 4-16). However, when considering overall reference temperatures with $\pm 2\sigma$ ($\pm 95\%$) confidence limits (Table 4-9), T_o values from both strikers are statistically undistinguishable.

Table 4-9. Results of overall Master Curve analyses on 2mm and 8mm striker data, using original and reanalyzed RRE data.

RRE data	Striker radius (mm)	No. of labs	T_o (°C)	σ_{To} (°C)
Original	2	7	1.1	2.3
	8	3	-5.0	3.6
Reanalyzed	2	7	3.6	2.3
	8	3	1.5	3.5

4.3.2.4 Conclusions from the round-robin exercise

1) Except for one laboratory (which appears to have striker calibration problems), the results supplied by the participants are very consistent and show reasonable scatter.
2) The Master Curve approach has proven to be fully applicable to impact fracture toughness measurements obtained in the ductile-to-brittle transition region.
3) Despite the lack of an official test standard, the guidelines supplied to the participants for the execution and evaluation of the tests have proven to be reliable and can be easily implemented by the testing laboratories.
4) The quality of impact fracture toughness measurements strongly depends on the quality of force values. Hence, a reliable calibration of the instrumented striker is of primary importance.
5) Although the JRQ material is known to be a fairly inhomogeneous material (particularly through the plate thickness), the results obtained from the round-robin exercise are quite satisfactory and can be probably considered above expectations.
6) No clear influence of instrumented striker radius (2mm vs 8mm) on impact toughness results has been detected.

An additional investigation concerning the impact of possible requirements on time to fracture or general yield ($t_f > 3\tau$ or 5τ, with τ = period of oscillation) is presented in detail in Appendix B, Section B.5.2. It results that the requirement currently proposed in the draft ASTM and ISO standards, i.e. $t_f > 5\tau$, is too restrictive and can cause significant non-conservatism in the Master Curve analyses. The less stringent requirement ($t_f > 3\tau$) should therefore be recommended.

4.3.3 Force Interlaboratory Comparison (ILC) using ERM specimens

As previously stated, the RRE results had shown the existence of an outlier laboratory (#7); the most likely cause appeared to be an incorrect calibration of the instrumented striker, which provided excessively high force values.

It was therefore decided to perform an Interlaboratory Comparison (ILC) among the RRE participants based on general yield (F_{gy}) and maximum (F_m) force measurements, using ERM (European Reference Materials) Charpy-V specimens from the high energy level (KV ~ 150 J) supplied by the Institute for Reference Materials and Measurements (IRMM) in Geel, Belgium. The specimens were purchased and distributed to all participating laboratories by JRC-IE, Petten; each laboratory received two ERM specimens to be tested in as-received

condition using the same pendulum machine and instrumented striker used for the RRE and full impact velocity (i.e. 5-5.5 m/s).

Instrumented force measurements were returned by 10 of the 11 institutes which took part in the RRE. Lab #6 was unable to provide data on the machine used for the RRE, which was a small-capacity 80 J pendulum which cannot be used to test ERM high energy specimens; however, tests were performed using another impact test machine with 407 J capacity. Lab #11 did not provide results.

For each one of the 22 instrumented tests performed, the following information was provided:

- force at general yield, F_{gy}
- maximum force, F_m
- absorbed energies KV (encoder or dial reading) and W_t (integrated).

The availability of the two latter values (KV and W_t) allowed investigating the so-called "dynamic force adjustment" approach, which consists in adjusting force and deflection values until absorbed energies from the pendulum encoder (KV) and under the instrumented test record (W_t) are equal [4-23].

The most accurate way to apply this procedure is by iteratively correcting force values until KV = W_t, since deflections are calculated from time and force measurements, as well as using the pendulum mass and the initial impact velocity. However, in a first approximation forces can be adjusted by simply using the ratio KV/W_t as a correction factor. Within this ILC, reported values of F_{gy} and F_m have been corrected using the accurate procedure mentioned above, with the exception of lab #8, which did not provide raw force/time data; in this case, the approximate procedure was employed. The aim was to verify whether the interlaboratory consistency improved or became worse.

Table 4-10 reports the original ILC results in terms of force and absorbed energy values. Figures 4-17 and 4-18 show the original (uncorrected) data provided by the participants for F_{gy} and F_m respectively. Significant scatter is observed; the standard deviations are 10.0% for F_{gy} and 13.9% for F_m with respect to the mean values. Moreover, lab #7 is confirmed as an outlier with force values which once again appear too high.

Table 4-11. Original results of the ILC.

Lab #	Striker rad.(mm)	Spec. id	F_{gy} (kN)	F_m (kN)	KV (J)	W_t (J)
1	2	16	17.95	22.80	151.70	152.10
		17	17.69	22.93	145.20	145.60
		Mean	17.82	22.86	148.45	148.85
2	2	6	16.29	22.72	160.01	156.54
		7	16.45	22.80	157.21	153.13
		Mean	16.37	22.76	158.61	154.84
3	8	18	19.56	25.47	136.30	139.88
		21	19.35	25.55	137.80	139.70
		Mean	19.46	25.51	137.05	139.79
4	2	19	18.97	26.07	150.30	163.69
		20	18.94	26.00	157.10	172.76
		Mean	18.96	26.04	153.70	168.23
5	2	8	18.61	23.98	149.20	148.10
		27	19.89	23.92	145.10	143.90
		Mean	19.25	23.95	147.15	146.00

Lab #	Striker rad.(mm)	Spec. id	F_{gy} (kN)	F_m (kN)	KV (J)	W_t (J)
6	8	9	18.85	24.96	151.00	151.30
		28	18.40	25.09	151.00	151.30
		Mean	18.63	25.03	151.00	151.30
7	2	1	22.52	32.21	168.19	203.12
		3	22.65	31.95	162.12	194.68
		4	22.25	31.90	159.70	192.74
		5	22.32	31.59	153.50	186.81
		Mean	22.44	31.91	160.88	194.34
8	8	23	20.02	23.14	139.65	134.04
		25	19.25	23.21	145.07	141.82
		Mean	19.64	23.18	142.36	137.93
9	2	22	16.65	20.54	149.70	130.09
		24	16.63	20.38	150.56	129.82
		Mean	16.64	20.46	150.13	129.95
10	8	10	18.95	25.94	134.36	140.33
		26	19.08	26.01	142.63	146.29
		Mean	16.64	20.46	150.13	129.95
Average values			19.15	25.42	149.88	155.35
Standard deviation (abs)			1.92	3.53	8.75	21.42
Standard deviation (%)			10.0%	13.9%	5.8%	13.8%

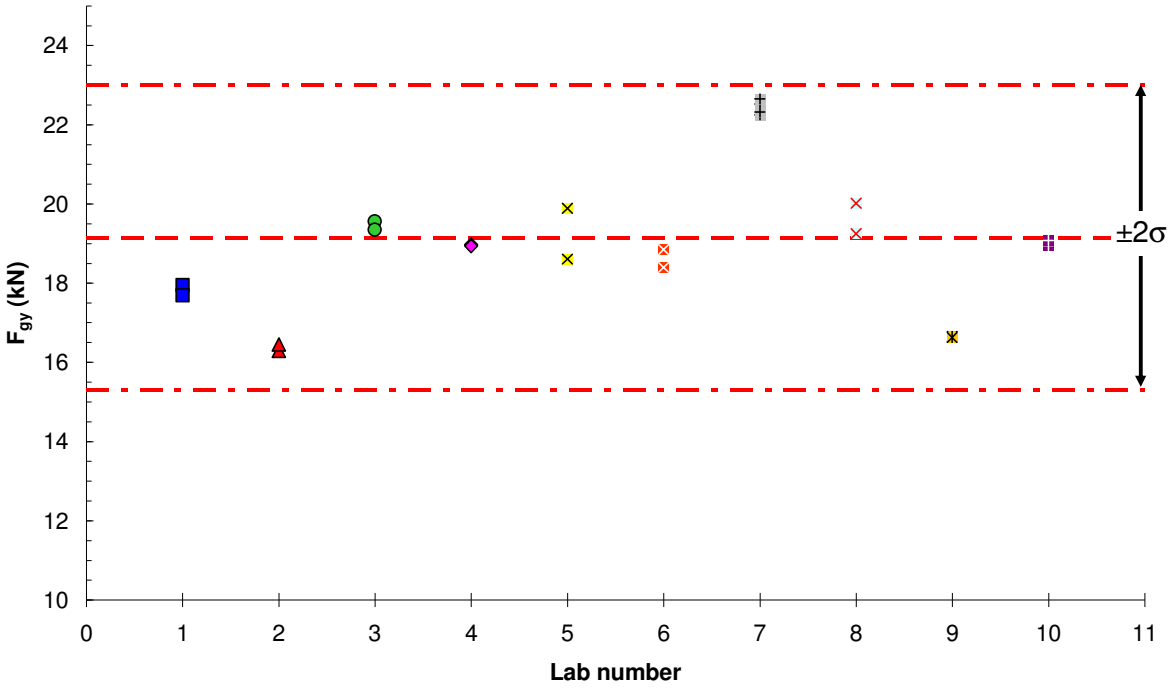

Figure 4-17. Original values of force at general yield returned by ILC participants.

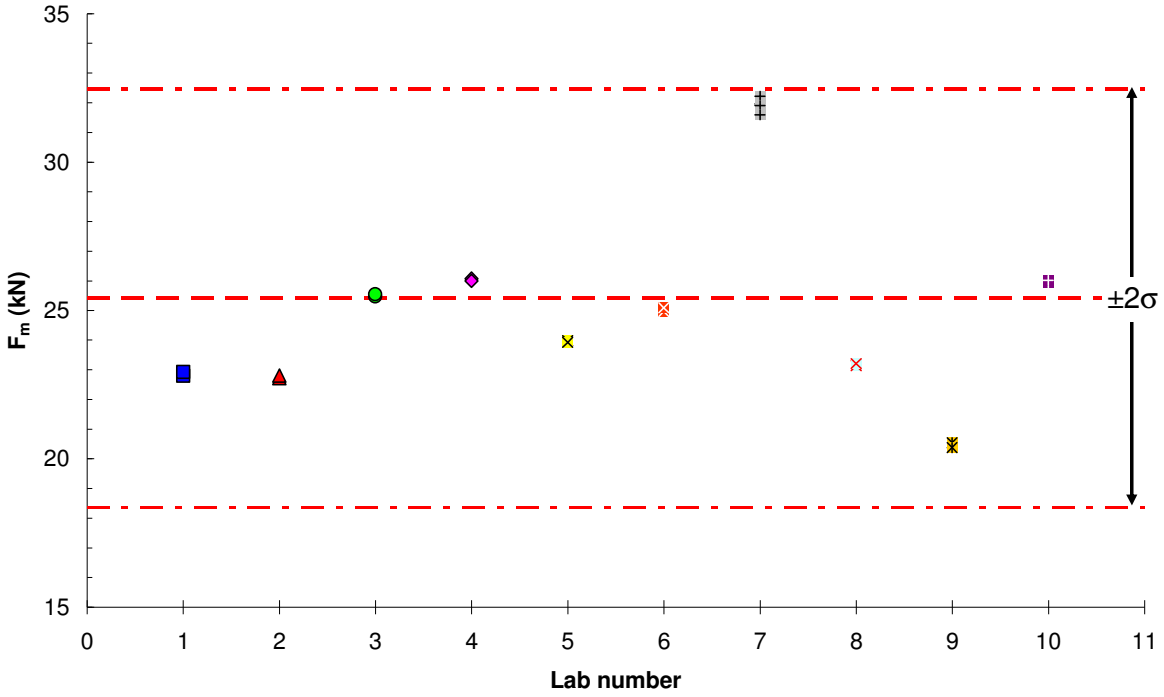

Figure 4-18. Original values of maximum force returned by ILC participants.

As previously stated, the dynamic force adjustment was applied to the original ILC results.

The corrected ILC results are provided in Table 4-12, in terms of correction factor and instrumented force values.

Table 4-12. Corrected ILC results.

Lab #	Spec. id	Corr. factor	F_{gy} (kN)	F_m (kN)
1	16	0.990	17.77	22.57
	17	0.993	17.58	22.77
	Mean		17.68	22.67
2	6	1.028	16.75	23.37
	7	1.034	17.01	23.57
	Mean		16.88	23.47
3	18	0.951	18.60	24.22
	21	0.965	18.68	24.67
	Mean		18.64	24.44
4	19	0.902	17.11	23.52
	20	0.892	16.89	23.19
	Mean		17.00	23.35
5	8	1.010	18.79	24.21
	27	1.011	20.11	24.19
	Mean		19.45	24.20
6	9	0.998	18.81	24.91
	28	0.998	18.36	25.04
	Mean		18.59	24.98

Lab #	Spec. id	Corr. factor	F_{gy} (kN)	F_m (kN)
7	1	0.760	17.12	24.49
	3	0.772	17.49	24.67
	4	0.767	17.06	24.46
	5	0.759	16.94	23.98
	Mean		17.15	24.40
8	23	1.042	20.86	24.11
	25	1.023	19.69	23.74
	Mean		20.27	23.93
9	22	1.135	18.89	23.31
	24	1.142	18.98	23.27
	Mean		18.94	23.29
10	10	0.951	18.02	24.67
	26	0.971	18.52	25.25
	Mean		18.27	24.96
Average values			18.18	24.01
Standard deviation (abs)			1.13	0.74
Standard deviation (%)			6.2%	3.1%

The effect is beneficial for the force at general yield (Figure 4-19), where the standard deviation decreases from 10.0% to 6.2%, and very beneficial for the maximum force (Figure 4-20), where the standard deviation drops from 13.9% to just 3.1%. In both cases, the "anomaly" represented by lab 7 practically disappears.

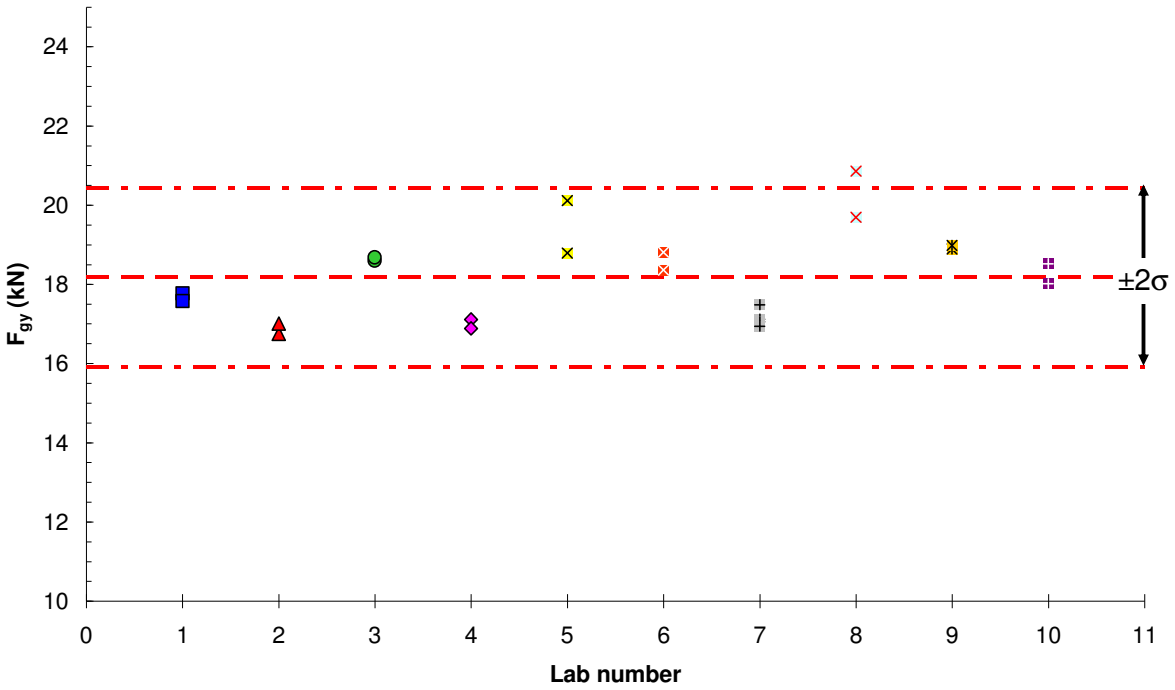

Figure 4-19. Values of F_{gy} after dynamic force adjustment.

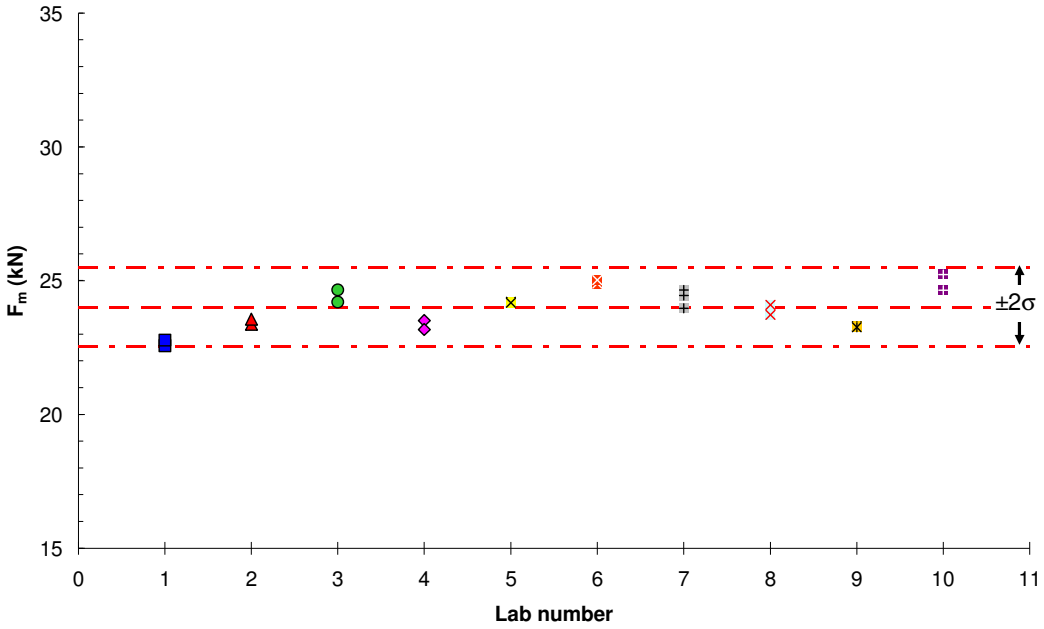

Figure 4-20. Values of F_m after dynamic force adjustment.

It could somehow be expected that the dynamic force adjustment would have a more significant effect on F_{gy} than on F_m, since the former parameter has an intrinsic higher dispersion due to the subjectivity of its determination with respect to the maximum force.

4.3.3.1 Conclusions from the interlaboratory comparison

1) The original results provided by the ILC participants show considerable scatter: standard deviation is 10.5% for F_{gy} and 14.6% for F_m.

2) Laboratory 7 confirms its nature of potential outlier.

3) After applying the "dynamic force adjustment" to the original data, the standard deviation is considerably reduced (to 6.5% for F_{gy} and 2.9% for F_m).

Additional analyses on the ILC results (within-laboratory and between laboratory statistics, influence of striker radius on instrumented forces) are presented in Appendix B, Section B.6.

4.4 Additional items related to loading rate effects

Appendix B addresses some additional items related to loading rate effects, namely:

- comparison between Master Curve reference temperatures measured at quasi-static and impact loading rates (section B.2);
- effect of loading pattern, i.e. monotonic loading vs partial unloading (section B.4);
- relationship between crack arrest forces from instrumented Charpy tests and NDT from Pellini tests (section B.7);
- correlation between T_o and T_{41J} (section B.8).

References

[4-1] Wallin, K. (1995). Summary of the IAEA/CRP3 Fracture Mechanical Results. Proceedings of a Specialists Meeting Organized by the International Atomic Energy Agency and held in Espoo, Finland 23-26 October 1999, IWG-LMNPP-95/5, Volume II, IAEA, Vienna, Austria.

[4-2] Joyce, J. A. (1998). On the Utilization of High Rate Pre-Cracked Charpy Test Results and the Master Curve to Obtain Accurate Lower Bound Toughness Predictions in the Ductile-To-Brittle Transition. Small Specimen Test Techniques, ASTM STP 1329, W.R. Corwin, S.T. Rosinski and E. van Walle, Eds. American Society for Testing Materials, 1998, pp. 253-273.

[4-3] Tregoning, R. L., Joyce, J. A. (2002). Investigation of Censoring Limits for Cleavage Fracture Determination. Fourth Symposium on Small Specimen Test Techniques, to be published in ASTM STP 1405, M. A. Sokolov, J. D. Landes, and G. E. Lucas, Eds., American Society for Testing and Materials, West Conshohocken, PA, 2002

[4-4] Viehrig, H.-W., Böhmert, J. and Dzugan, J. (2002). Use of Instrumented Charpy Impact Tests for the Determination of Fracture Toughness Values. "From Charpy to Present Impact Testing", ESIS-Publication 30, D. Francois, A. Pineau, Eds., Charpy Centenary Conference, 2-5 October 2001, Poitiers, France, Elsevier Science Ltd. and ESIS, pp. 245.

[4-5] Wallin, K. (1997), Effect of Strain Rate on the Fracture Toughness Reference Temperature T_0 for Ferritic Steels, Recent Advances in Fracture, R.K. Mahidhara, et al. (Eds.), The Minerals, Metals & Materials Society, 1997.

[4-6] Wallin, K. (2004). Loading Rate Dependence of T_o, presentation at E08.08.02, Salt Lake City, May, 2004.

[4-7] Hall, J.B., and Yoon, K.K. (2003). Quasi-static Loading Rate Effect on the Master Curve Reference Temperature of Ferritic Steels and Implications, Proceedings of the 2003 ASME Pressure Vessels and Piping Conference, July 28-31, 2003, Cleveland.

[4-8] Hall, J.B., and Yoon, K. K. (2004). Proposed Changes in E1921 for Quasi-static Loading Rate, presentation at E08.08.02, Salt Lake City, May, 2004.

[4-9] Joyce, J.A., Tregoning, R.L. and Roe C. (2006). On Setting Testing Rate Limitations for the Master Curve Reference Temperature, T_o, of ASTM E 1921, Journal of Testing and Evaluation, Vol. 34, No. 2.

[4-10] McCornell, P., Server, W. L. (1980). EPRI Instrumented Impact Test Procedures. In Proceedings C.S.N.I. Specialists Meeting on Instrumented Precracked Charpy Testing. EPRI NP-2102-LD, Prepared by Electric Power Research Institute, Ed. by R. A. Wullaert, Palo Alto, USA, pp. 1-1 to 1-22.

[4-11] Ireland, D. R. (1980). A Review of the Proposed Standard Method of Test for Impact Testing Precracked Charpy Specimen of Metallic Materials. In Proceedings C.S.N.I. Specialists Meeting on Instrumented Precracked Charpy Testing. EPRI NP-2102-LD, Prepared by Electric Power Research Institute, Ed. by R. A. Wullaert, Palo Alto, USA, pp. 1-23 to 1-63.

[4-12] Lucon, E. (1999). Dynamic Toughness Testing of Pre-Cracked Charpy V-Notch Specimens. Report BLG-808, SCK-CEN, April 1999, Mol, Belgium.

[4-13] Shutter, D. M. (2002). Dynamic Fracture Toughness Determination Using Precracked Charpy Specimens, From Charpy to Present Testing, ESIS Publication 30, D. Francois and A. Pineau (Eds.), Elsevier Science Ltd. and ESIS, 2002, pp. 237.

[4-14] Lucon, E., Chaouadi, R. and van Walle, E. (2006). Different Approaches for the Verification of Force Values Measured with Instrumented Charpy Strikers. Journal of ASTM International, Volume 3, Issue 3.

Appendix B

Additional investigations related to loading rate effects

TABLE OF CONTENTS

B.1 Master Curve data sets provided by CRP-8 participants for investigating the effect of loading rate on T_0

Table B-1. Master Curve data sets for JRQ steels.

JRQ Block	Country Code	W mm	B mm	B_N mm	Spec. type	Loading rate MPa√m/s	$T_0^{measured}$ °C	σ_{To} K	$\sum n_i$
5JRQ22	GER (FZD)	10	10	8	PCC	7.36E+05	-1.5	1.9	9.94
5JRQ33	RUS (RRC KI)	10	10	8	PCC	1.20E+00	-59.0	5.2	1.60
5JRQ34		10	10	8	PCC	1.00E-01	-64.0	6.0	1.90
5JRQ34		10	10	8	PCC	7.00E-01	-59.0	5.4	1.40
5JRQ34		10	10	10	PCC	7.00E-01	-62.0	5.7	1.80
5JRQ34		25	12.5	10	C(T)	4.00E-01	-61.0	5.4	1.80
5JRQ34		10	4	4	SE(B)	5.00E-01	-94.0	6.4	1.20
5JRQ34		10	4	3.2	SE(B)	5.00E-01	-75.0	6.6	1.14
5JRQ34		10	4	3.2	SE(B)	5.00E-01	-73.0	6.7	1.20
5JRQ53	CZR (NRI)	10	10	8	PCC	1.99E+00	-61.8	5.7	1.51
5JRQ53		10	10	10	PCC	5.91E+05	12.5	6.0	1.37
5JRQ12	BEL (SCK□CEN)	10	10	8	PCC	1.18E+00	-57.3	6.0	1.50
5JRQ12		10	10	8	PCC	3.67E+05	-14.7	6.8	1.07
6JRQ	JAP (JAEA)	10	10	8	PCC	2.00E+00	-75.8	N/A	N/A
6JRQ		10	10	8	PCC	7.27E+02	-43.1	N/A	N/A
6JRQ12	GER (FZD)	10	10	8	PCC	1.20E+00	-61.6	6.0	1.43
6JRQ12		10	10	8	PCC	1.20E+00	-55.9	6.3	1.19
6JRQ34	ESP (CIEMAT)	10	10	10	PCC	6.10E-01	-67.8	6.8	1.17
6JRQ34		10	10	10	PCC	1.00E+00	-53.5	4.1	3.21
6JRQ34		10	10	10	PCC	6.30E+00	-62.1	6.6	1.19
6JRQ34		10	10	10	PCC	6.30E+01	-54.2	7.1	1.00
6JRQ34		10	10	10	PCC	1.29E+03	-45.5	6.6	1.00
8JRQ33	KOR (KAERI)	10	10	10	PCC	1.00E+00	-57.3	N/A	1.20
8JRQ44		10	10	8	PCC	4.80E+05	12.8		1.20
8JRQ34	MEX (ININ)	20	10	10	C(T)	5.30E-02	-57.4	5.0	2.17
8JRQ34		10	10	10	PCC	1.60E-01	-60.4	5.2	2.00
8JRQ52		50.8	25.4	25.4	C(T)	9.41E-01	-45.5	5.2	1.86
8JRQ34		10	10	10	PCC	1.80E-01	-70.1	6.0	1.50
8JRQ34		10	10	10	PCC	2.70E+00	-51.7	5.2	1.86
8JRQ44	BEL (SCK•CEN)	10	10	8	PCC	7.16E+02	-48.0	5.4	1.71
8JRQ44		4	3	3	PCC	4.54E+03	-33.0	7.7	0.77

JRQ Block	Country Code	W mm	B mm	B_N mm	Spec. type	Loading rate MPa√m/s	$T_0^{measured}$ °C	σ_{To} K	Σn_i
8JRQ44	GER (FZD)	10	10	8	PCC	1.00E+04	-19.3	5.7	1.43
8JRQ44		10	10	8	PCC	1.20E+00	-71.4	6.4	1.29
8JRQ44	JAP (CRIEPI)	10	10	8	PCC	4.10E+05	10.0		8.00
8JRQ44	RRE*	10	10	8	PCC	3.50E+05	-4.2	2.0	13.21

Table B-2. Master Curve data sets for other steels.

Material ID	Code	specimen type	W mm	B mm	B_N mm	Loading rate MPa√m/s	T_0 °C	σ_{To} K	Σn_i
10 CrMo 9 10	GER (FZD	PCC	10	10	8	1.20E+00	-111.4	5.7	1.29
10 CrMo 9 10	GER (FZD)	PCC	10	10	8	1.20E+00	-109.7	5.7	1.43
EUROFER97	BEL (SCK•CEN)	PCC	10	10	8	8.2E-01	-112.0	4.4	2.52
EUROFER97	BEL (SCK•CEN)	PCC	10	10	8	6.95E+02	-79.0	6.4	1.33
EUROFER97	BEL (SCK•CEN)	PCC	10	10	8	4.12E+05	-24.0	5.7	1.52
HX400	FIN (VTT)	PCC	10	10	8	1.00E-01	-27.0	N/A	N/A
HX400	FIN (VTT)	PCC	10	10	8	2.00E+00	-24.0	N/A	N/A
15X2MFA unirrad. (BM)	FIN (VTT)	PCC	10	10	8	1.00E+00	-133.0	6.0	1.50
15X2MFA irrad. (BM)	FIN (VTT)	PCC	10	10	8	1.00E+00	-102.0	6.3	1.40
15X2MFA unirrad. (BM)	FIN (VTT)	PCC	10	10	8	7.50E+05	-16.0	(5)	(>1)
15X2MFA irrad. (BM)	FIN (VTT)	PCC	10	10	8	7.50E+05	-1.0	(6)	(>1)
JSPS	JAP (JAEA)	PCC	10	10	8	9.00E-01	0.3	N/A	N/A
JSPS	JAP (JAEA)	PCC	10	10	8	1.07E+03	25.9	N/A	N/A
JSPS	BEL (SCK•CEN)	PCC	10	10	8	1.00E+00	-6.4	3.0	5.62
JSPS	BEL (SCK•CEN)	PCC	10	10	8	7.16E+02	14.0	5.9	1.45
JSPS	BEL (SCK•CEN)	PCC	10	10	8	4.83E+05	34.0	6.0	1.50
SFVQ1A (A508 Cl. 3)	JAP (CRIEPI)	C(T)	50.8	25.4	25.4	7.40E-03	-117.0	N/A	6.00
SFVQ1A (A508 Cl. 3)	JAP (CRIEPI)	C(T)	50.8	25.4	25.4	7.10E+00	-90.0	N/A	6.00

Material ID	Code	specimen type	W mm	B mm	B_N mm	Loading rate MPa√m/s	T_0 °C	σ_{To} K	Σn_i
SFVQ1A (A508 Cl. 3)	JAP (CRIEPI)	C(T)	50.8	25.4	25.4	6.10E+01	-74.0	N/A	6.00
Steel A	JAP (JAEA)	PCVN	10	10	8	8.00E-01	-69.6	N/A	N/A
Steel A	JAP (JAEA)	PCVN	10	10	8	5.64E+01	-63.4	N/A	N/A
Steel A	JAP (JAEA)	PCVN	10	10	8	1.09E+03	-32.2	N/A	N/A
Steel A	JAP (JAEA)	PCVN	10	10	8	1.10E+03	-45.3	N/A	N/A
Steel L	JAP (JAEA)	PCVN	10	10	8	8.00E-01	-112.5	N/A	N/A
Steel L	JAP (JAEA)	PCVN	10	10	8	1.15E+03	-64.6	N/A	N/A
HSST-14	USA ORNL/USNA	C(T)	50.8	25.4	20.32	1.00E+00	-57.5	5.2	2.00
HSST-14	USA ORNL/USNA	C(T)	101.6	50.8		6.27E+03	-27.8	9.0	0.67
HSST-14	USA ORNL/USNA	C(T)	101.6	50.8		1.69E+05	-17.3	4.8	2.33

B.2 Assessment of the loading rate in a fracture toughness test

For fracture toughness tests in the ductile-to-brittle transition region, the current ASTM standard E1921-05 requires specimens to be loaded using a loading rate *dK/dt* between 0.1 and 2 MPa√m/s during the initial elastic portion. A table is also provided, which allows estimating the testing machine loading rate associated with this allowable range, both in terms of time to control load t_M or specimen load-line displacement rate $\dot{\Delta}_{LL}$. It has been proposed that the standard allow testing at higher loading rates, including precracked Charpy specimens tested with an instrumented pendulum machine (impact toughness tests). The revised version of ASTM E1921 would require test results (K_{Jc} or T_o) to be reported along with the relevant loading rate (*dK/dt*), and should therefore provide guidance on how to assess the value of *dK/dt* in a relatively simple, but reliable manner.

B.1.1 Possible options for evaluating $\dot{K}$ in a fracture toughness test

The loading rate is not constant during a fracture toughness test, particularly once plasticity is evident in the force/displacement record. However, for practical purposes it is necessary to specify a single value of *dK/dt* to be associated to the individual test result and reported with the measured data. This might also be prescribed in a future revision of ASTM E1921 or in the future ISO standard on impact toughness tests. In the present study[1], the following five options have been investigated.

(a) Average value of *dK/dt*, calculated using each individual force/time data point in a test up to cleavage or test termination. This option is the most time-consuming from a computational point of view. In practical terms, for the *N*-th data point $dK = K_N - K_{N-1}$ and $dt = t_N - t_{N-1}$.

(b) Ratio between stress intensity factor and corresponding time at cleavage or test termination (K_c/t_c). Since K_c is always calculated, the only additional parameter that needs to be evaluated is t_c.

(c) Estimation based on Table 3 of ASTM E 1921-05 (reproduced below in Table B-3), which is intended to help the user choose the appropriate value of load-line displacement rate ($\dot{\Delta}_{LL}$) or t_M (time to control force P_M) corresponding to the required loading rate *dK/dt*. In, *a* is the crack size, *W* the specimen width, σ_Y the yield strength at the test temperature, $\dot{K}$ or $\frac{dK}{dt}$ the loading rate and *E* the Young's modulus.

[1] This study has been published in Journal of ASTM International, Vol. 5, No. 3, March 2008 (Paper ID: JAI101467).

Table B-3. Rate estimation for SE(B) and C(T) specimens (Table 3 from ASTM E1921-05).

SE(B) Specimen Rate Estimation			C(T) Specimen Rate Estimation		
a/W	$\frac{t_M \dot{K}}{\sigma_Y \sqrt{W}}$	$\frac{E\dot{\Delta}_{LL}}{\frac{dK}{dt}\sqrt{W}}$	a/W	$\frac{t_M \dot{K}}{\sigma_Y \sqrt{W}}$	$\frac{E\dot{\Delta}_{LL}}{\frac{dK}{dt}\sqrt{W}}$
0.45	0.346	5.064	0.45	0.412	3.475
0.50	0.333	5.263	0.50	0.386	3.829
0.55	0.318	5.522	0.55	0.361	4.212
0.60	0.302	5.851	0.60	0.336	4.635
0.65	0.283	6.267	0.65	0.312	5.118
0.70	0.263	6.798	0.70	0.287	5.696

By fitting the values in the third or sixth column as a function of *a/W* and solving the relationship for *dK/dt*, the loading rate can be easily calculated since all remaining variables (*a*, *W*, *E* and load-line displacement rate) are known.

(d) Ratio between stress intensity factor and corresponding time within the linear elastic region of the test record (K_{el}/t_{el}). This option requires only the determination of K_{el} and t_{el} at an arbitrarily chosen point along the linear elastic slope.

(e) Value of loading rate *dK/dt* at the instant preceding cleavage fracture (or test termination); i.e. if *N* corresponds to the instant of cleavage, the loading rate to be considered would be $(dK/dt)_{N-1} = (K_{N-1}-K_{N-2})/(t_{N-1}-t_{N-2})$.

B.2.2 Investigations performed

The study consisted in analyzing data from 27 fracture toughness tests. More specifically, three steels with significantly different characteristics (all previously described) were chosen:

- EUROFER97;
- JRQ;
- JSPS.

Three displacement (loading) rate regimes were examined:

- quasi-static (machine crosshead displacement rate 0.2 mm/min; sampling time 1 s; digital precision A/D converter = 24 bit);
- intermediate/dynamic (displacement rate = 150 mm/min; sampling time = 0.2 ms; digital precision A/D converter = 24 bit);
- impact (tests performed on precracked Charpy specimens using an instrumented pendulum with impact velocities in the range 1.2 - 1.6 m/s; sampling time = 0.5 µs; digital precision A/D converter = 12 bit).

Tests were performed in accordance with ASTM E1921-05 (quasi-static and dynamic rates) and the ESIS TC5 Test Procedure (impact rates). Typical test records for the three

loading rates are shown in Figure B-1 (JRQ steel in mid transition regime, K_{Jc} = 99 to 133 MPa√m).

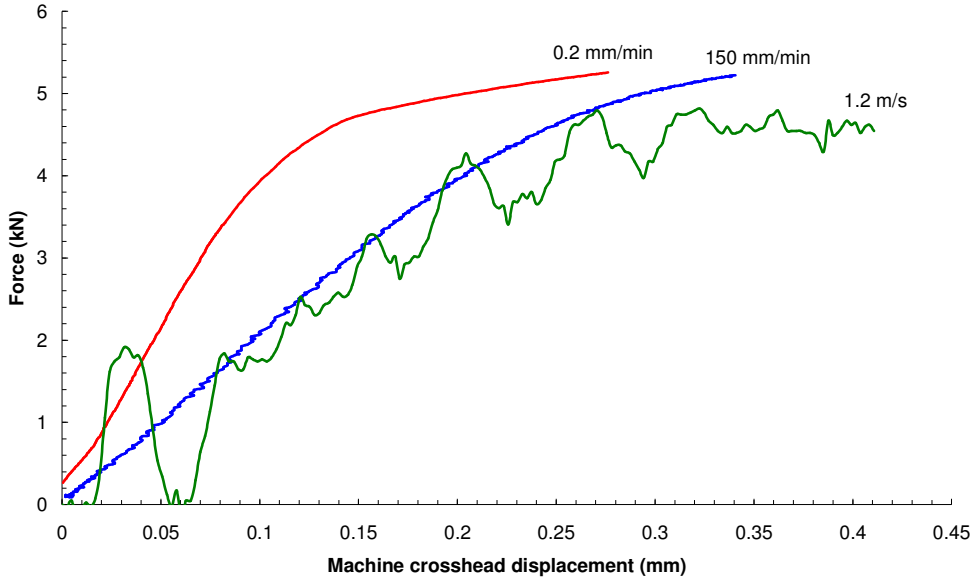

Figure B-1. Typical test records for three different loading rates (JRQ steel).

Three different fracture toughness levels were considered (typical examples of test records are shown in Figure B-2 for the lowest loading rate, i.e. 0.2 mm/min):

- lower transition regime (K_{Jc} = 41 – 88 MPa√m);
- mid transition regime (K_{Jc} = 98 – 133 MPa√m);
- upper transition regime (K_{Jc} = 138 – 241 MPa√m).

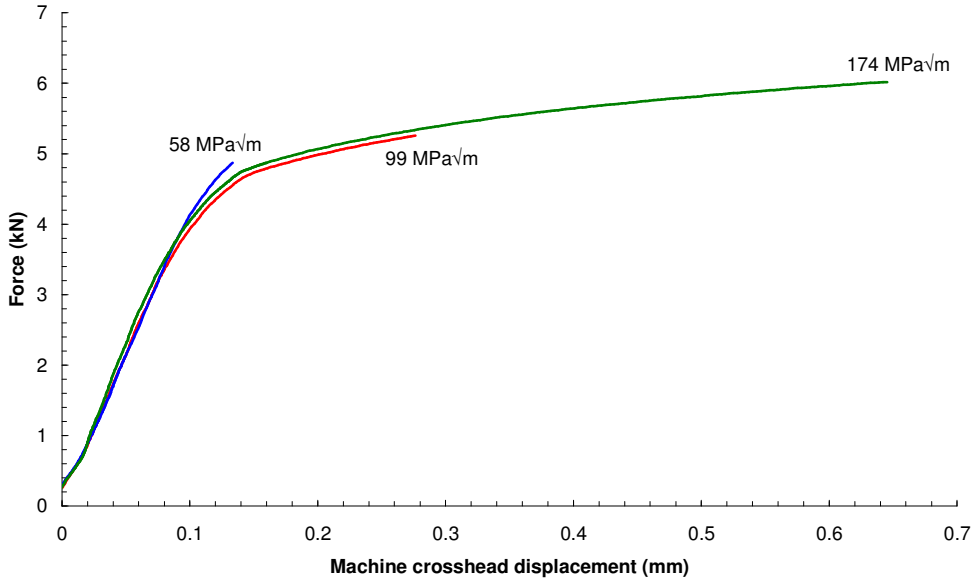

Figure B-2 - Typical test records for the three toughness levels (JRQ steel, 0.2 mm/min).

In order to illustrate four of the five investigated approaches, the force/time record for one of the tests (JRQ steel, 0.2 mm/min, K_{Jc} = 174 MPa√m) is shown in Figures B-3 and B-4 together with the evolution of the loading rate and the stress intensity factor respectively. Options (a) and (e) are depicted in Figure B-3, while Figure B-4 illustrates options (b) and (d).

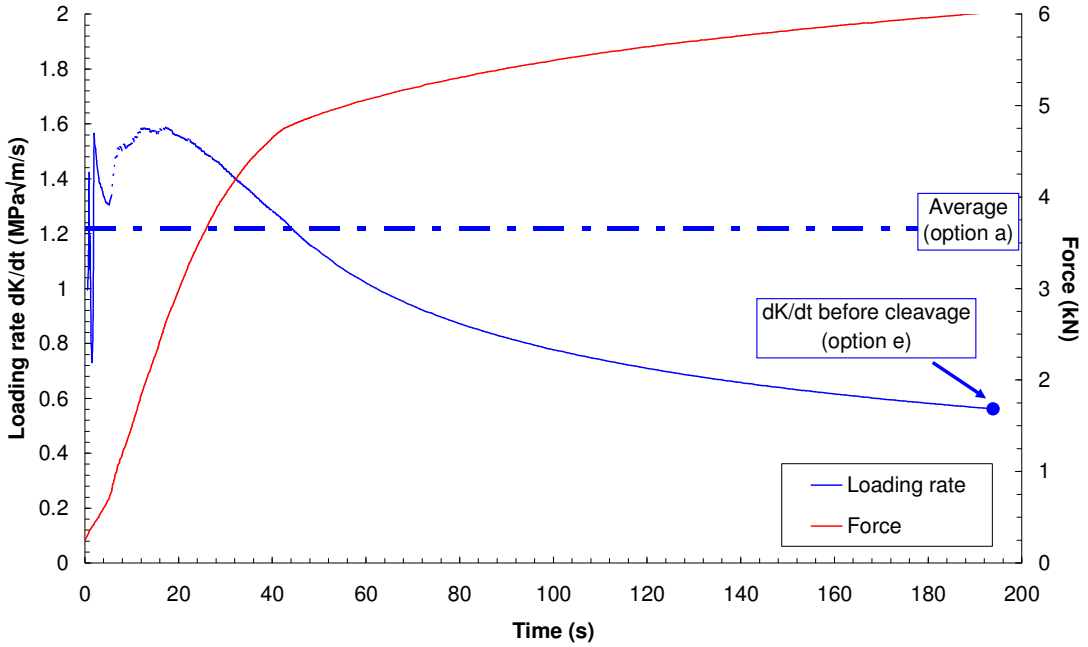

Figure B-3 - Loading rate and test record for a JRQ specimen tested at 0.2 mm/min. Options (a) and (e) are illustrated.

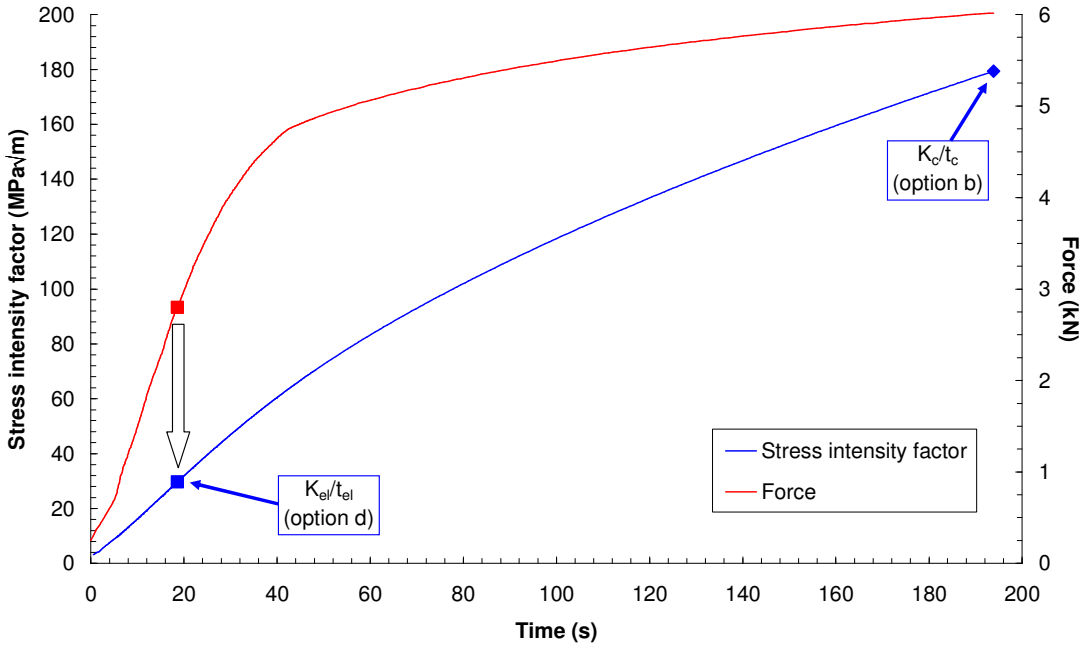

Figure B-4. Stress intensity factor and test record for a JRQ specimen tested at 0.2 mm/min. Options (b) and (d) are illustrated.

As far as option (c) is concerned, the loading rate for a SE(B) specimen can be estimated from the left-hand side of Table B-3 using:

$$\frac{dK}{dt} = \frac{E \cdot \dot{\Delta}_{LL}}{Y \cdot \sqrt{W}} \tag{B.1}$$

where E is in MPa, $\dot{\Delta}_{LL}$ is in m/s, W is in m and Y is a function of a/W obtained by fitting a third-order polynomial curve through the values in the third column in the table and is given by:

$$Y\left(\frac{a}{W}\right) = 24.15 \cdot \left(\frac{a}{W}\right)^3 - 25.31 \cdot \left(\frac{a}{W}\right)^2 + 11.72 \cdot \left(\frac{a}{W}\right) + 2.272 \tag{B.2}$$

B.2.3 Results obtained

The values of loading rate calculated using the five options previously listed for the 27 fracture toughness tests considered are presented in Table B-4.

Table B-4 - Values of loading rate calculated using the 5 different options.

Material	Test speed	K_{Jc} (MPa√m)	Loading rate (MPa√m/s)				
			Average	K_{Jc}/t_c	E1921-05	K_{cl}/t_{el}	dK/dt(cl)
EUROFER97	0.2 mm/min	47	**0.66**	0.72	1.38	0.69	0.79
		106	**0.72**	0.74	1.36	0.69	0.65
		184	**0.69**	0.69	1.33	0.67	0.41
JSPS		53	**1.14**	1.23	1.23	1.27	1.07
		102	**1.09**	1.07	1.26	1.47	0.71
		201	**0.80**	0.73	1.32	1.64	0.39
JRQ		58	**1.34**	1.42	1.39	1.43	1.39
		100	**1.36**	1.25	1.38	1.55	1.36
		174	**1.22**	0.93	1.38	1.60	0.56
EUROFER97	150 mm/min	54	**635**	654	974	634	1615
		99	**742**	752	972	638	1507
		192	**647**	654	985	694	426
JSPS		63	**751**	761	974	673	1728
		98	**760**	777	969	683	-83
		146	**587**	595	950	651	-16
JRQ		60	**674**	693	998	643	-181
		99	**753**	764	967	673	48
		155	**621**	630	932	708	834
EUROFER97	1.6 m/s	41	**8.31E+05**	8.40E+05	6.55E+05	8.42E+05	5.54E+05
		98	**6.78E+05**	6.04E+05	6.51E+05	6.47E+05	2.70E+05
		188	**6.25E+05**	5.04E+05	6.35E+05	6.43E+05	1.40E+05
JSPS	1.5 m/s	75	**6.40E+05**	6.47E+05	5.77E+05	6.38E+05	9.97E+05
		100	**5.53E+05**	5.56E+05	5.79E+05	6.18E+05	5.58E+05
		138	**4.80E+05**	4.82E+05	5.83E+05	6.54E+05	4.29E+05
JRQ	1.2 m/s	88	**3.90E+05**	3.88E+05	4.83E+05	3.86E+05	6.10E+05
		133	**3.85E+05**	3.85E+05	4.75E+05	4.38E+05	2.51E+04
		188	**2.90E+05**	2.90E+05	4.74E+05	4.30E+05	6.15E+04

As an example, results for tests conducted in the lower transition regime (K_{Jc} = 41 to 88 MPa√m) are illustrated in more detail using histograms in Figure B-5 (quasi-static loading rates), Figure B-6 (intermediate/dynamic) and Figure B-7 (impact).

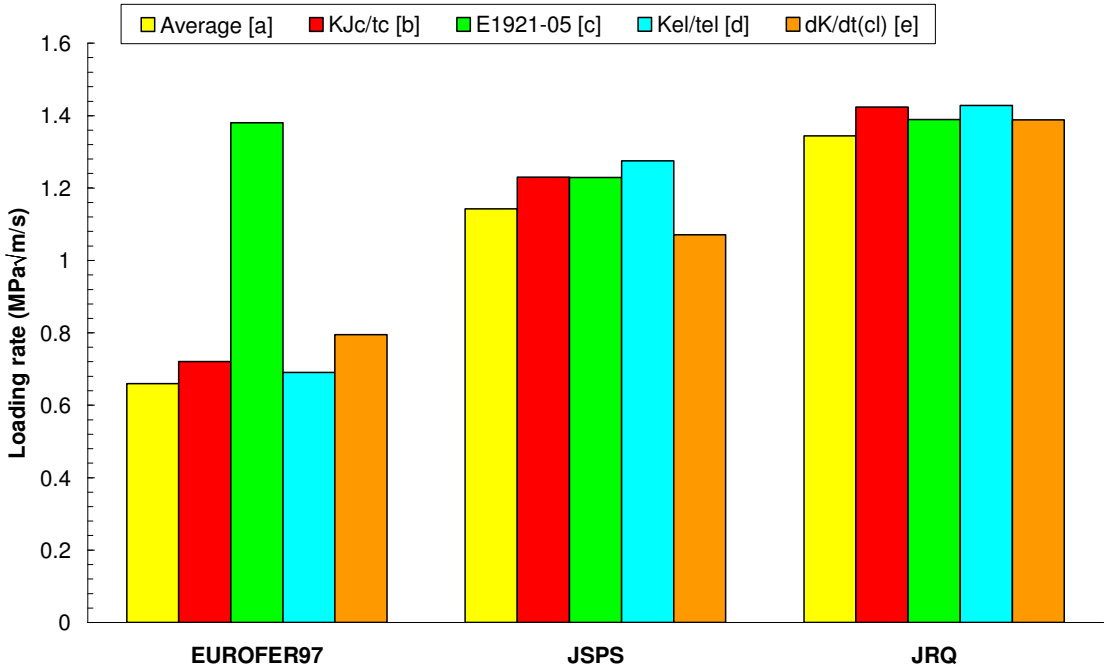

Figure B-5. Comparison between different approaches for evaluating the loading rate under quasi-static conditions for tests conducted in the lower transition regime.

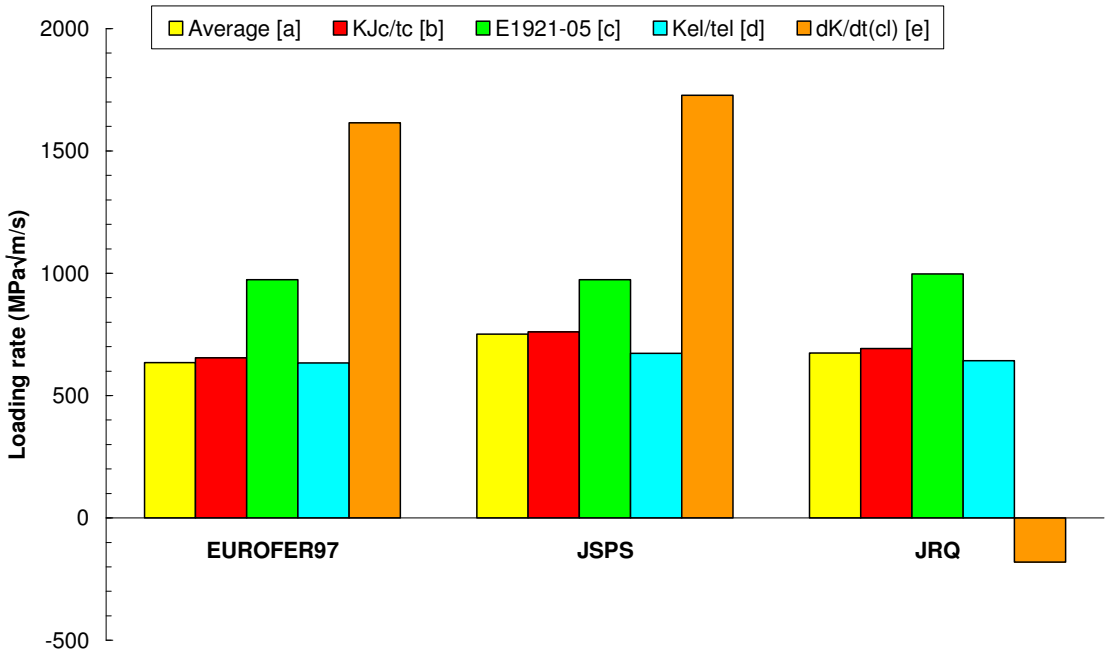

Figure B-6. Comparison between different approaches for evaluating the loading rate under dynamic/intermediate conditions for tests conducted in the lower transition regime.

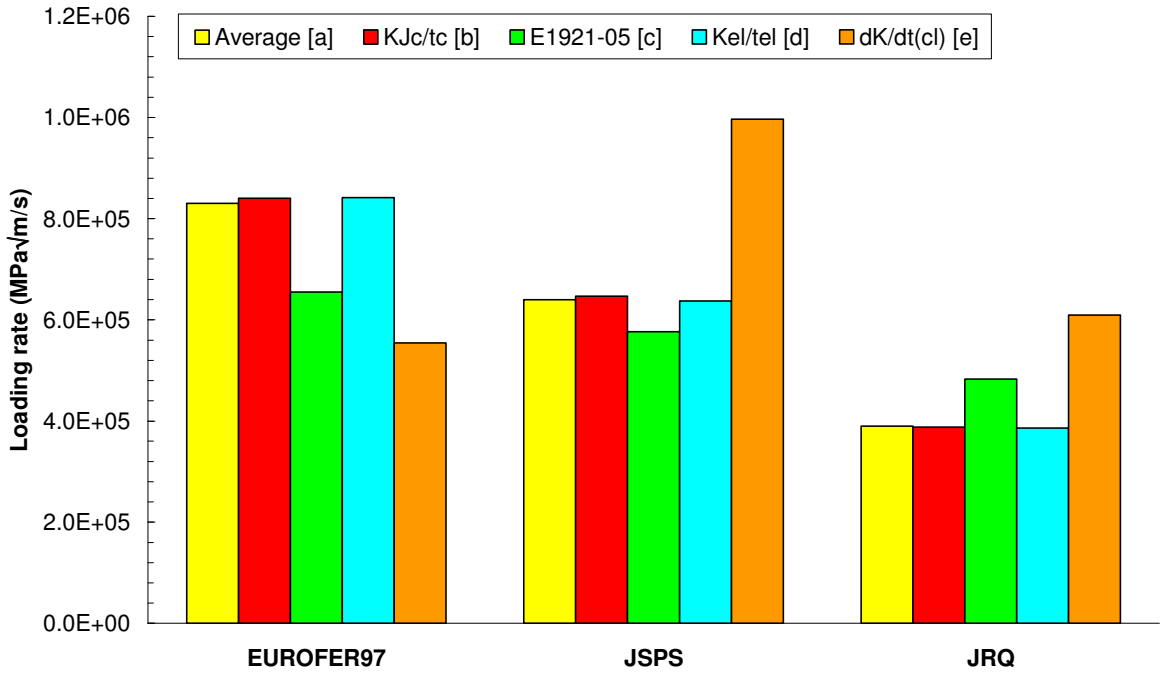

Figure B-7. Comparison between different approaches for evaluating the loading rate under impact conditions for tests conducted in the lower transition regime.

B.2.4 Discussion

It is clear, from the investigations performed but also from a merely intuitive standpoint, that loading rate changes continuously during a fracture toughness test and no "unique" value of *dK/dt* can be defined. However, the results obtained show that options (a) and (b) (and (d) as well, but only in the lower transition regime) provide substantially equivalent results and appear sufficiently representative of the effective loading rate for practical purposes.

In particular, K_c/t_c (option b) offers a straightforward and convenient way to estimate the overall loading rate in a fracture toughness test and, with respect to the average value of *dK/dt* (which can significantly vary during the test, see Figures B-3 and B-8), it offers the advantage of being calculated in relation to the actual fracture event. Moreover, a similar approach is suggested by both ASTM E399-06 (Annex A10) and ASTM E1820-06 (Annex A13). However, one notable exception are tests where partial unloadings are performed in order to evaluate the current crack size; in this case, the time spent during the partial unloadings should be subtracted from the time to cleavage (t_c) used to calculate the loading rate. From a practical point of view, it might be advisable to use for such tests one of the other two approaches, i.e. average *dK/dt* (option a) or K_{el}/t_{el} (option d).

The two approaches which clearly emerge from our investigation as unsatisfactory and therefore should not be recommended are:

- the use of Table 3 from ASTM E1921-05 (option c), which often overestimates the average loading rate of the test, and
- the value of *dK/dt* just before cleavage (option e), which can produce erratic or even negative results since the actual loading rate in some cases oscillates around its mean value, particularly for higher test velocities (an example in Figure B-8).

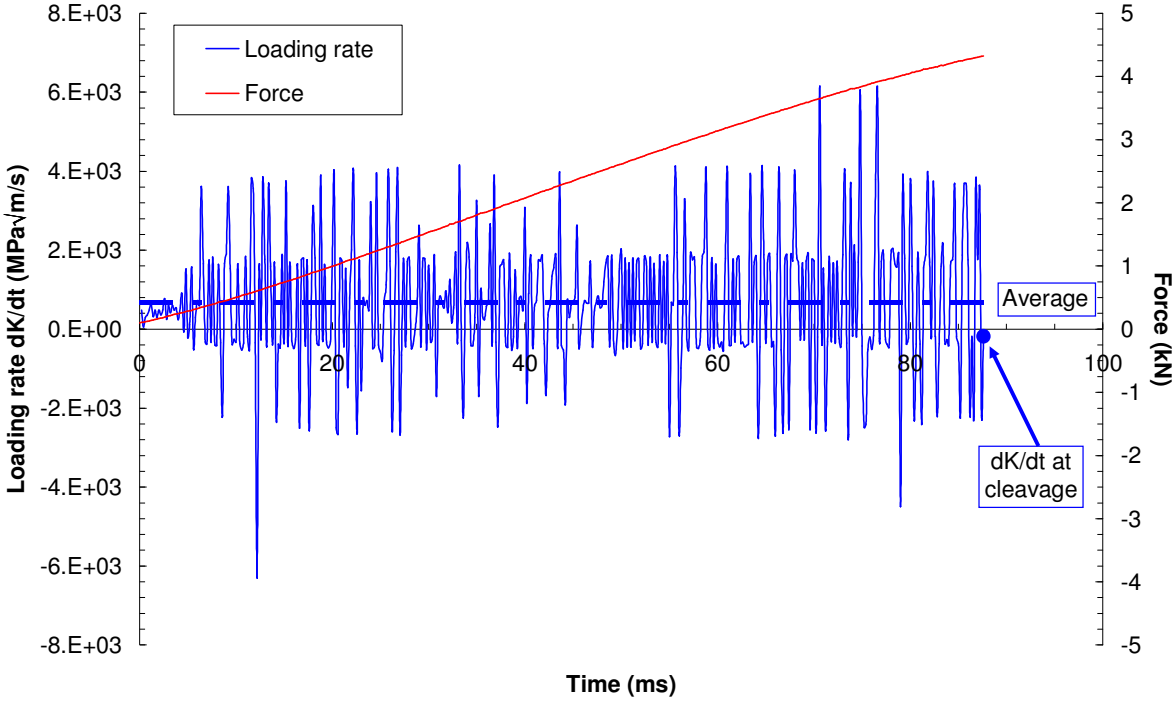

Figure B-8. Loading rate and test record for a dynamic test (150 mm/min) on the JRQ steel.

B.2.5 Conclusions

- Based on the investigations performed, the ratio between stress intensity factor and time at cleavage (or test termination), K_c/t_c, can be used to effectively estimate the average loading rate *dK/dt* in a fracture toughness tests, since:
  - it is sufficiently close to the average loading rate of the test;
  - it requires a minimum of additional computation (i.e. only the determination of the time at cleavage t_c).
- However, in case partial unloadings are performed during the test (for instance during the linear elastic portion), K_c/t_c should not be used and other options (average *dK/dt* excluding the unloading periods or K_{el}/t_{el} evaluated before the first unloading) should be chosen.
- The use of Table 3 from ASTM E1921-05 can grossly overestimate the average loading rate and is therefore not recommended. The reasons of this poor performance are not clear.

- Since the actual loading rate in a test tends to fluctuate around the average value, using *dK/dt* just before cleavage can lead to erratic results, including (albeit only in the case of dynamic tests) negative values which have no physical meaning.

The results obtained do not appear to depend on material type or loading rate.

B.3 Comparison between Master Curve reference temperatures measured at quasi-static and impact loading rates

SCK•CEN has collected reference temperature values obtained on unirradiated and irradiated RPV and ferritic/martensitic steels from tests conducted at quasi-static ($T_{o,qs}$) and impact ($T_{o,imp}$) loading rates using precracked Charpy specimens [B-1]. For the two loading rate regimes, dK/dt corresponds to values of approximately 1 and 4×10^5 MPa$\sqrt{}$m/s respectively.

The data presently included in the SCK•CEN database are shown in Table B-5. Differences between impact and quasi-static reference temperatures are plotted in Figures B-9 and B-10 as a function of $T_{o,qs}$ and $R_{y,Tosq}$ (yield strength measured at $T_{o,qs}$). The latter two parameters are both considered by the empirical model of Wallin [B-2] for predicting the change of reference temperature due to an increase in loading rate.

Fair correlations are observed for the T_o increase in Figures B-9 and B-10, with a significant amount of scatter, particularly for the relationship with $R_{y,Tosq}$. Reference temperature variations appear to decrease as $T_{o,qs}$ increases and $R_{y,Tosq}$ decreases.

Table B-5 - Relationship between T_o measured under quasi-static and impact loading rates (SCK•CEN database).

Material	Condition	$T_{o,qs}$ (°C)	$R_{y,Toqs}$ (MPa)	$T_{o,imp}$ (°C)	ΔT_o (°C)
73W	Baseline	-77	565	-29	48
	Irradiated	24	708	46	22
		39	642	78	39
18MND5	Baseline	-119	694	-71	48
	Irradiated	-85	744	-26	59
JSPS (A533B)	Baseline	-6	468	32	38
JRQ	Baseline	-70	539	-17	53
	Irradiated	15	586	58	43
A302B	Baseline	68	519	81	13
EUROFER97	Baseline	-115	717	-24	91
	Irradiated	-80	777	-13	67
F82H	Baseline	-118	731	-26	92
JRQ (CRP-4)	Baseline	-70	539	-3	67

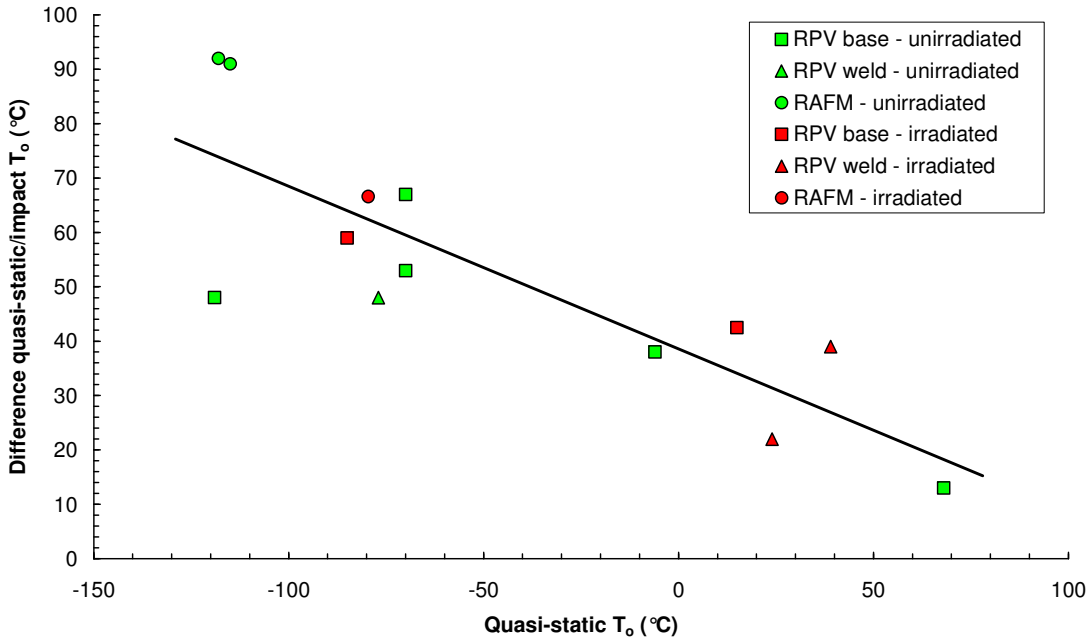

Figure B-9. Influence of quasi-static reference temperature on the increase of T_o.

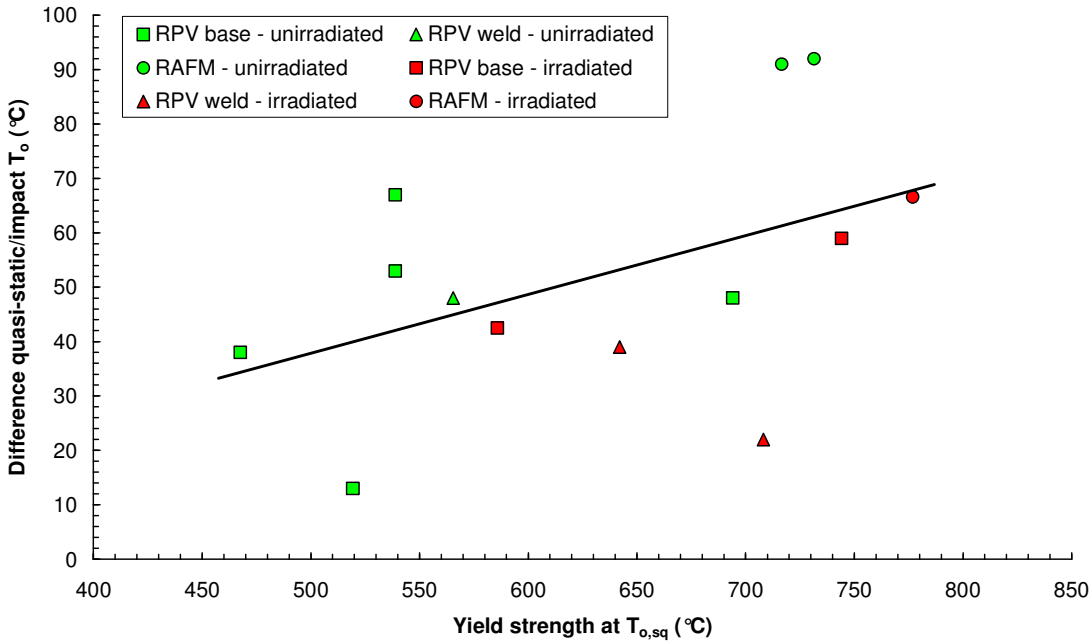

Figure B-10. Influence of yield stress at quasi-static reference temperature on the increase of T_o.

B.4 Yield strength to be used for loading rates higher than quasi-static

In the Master Curve analysis of fracture toughness data, the yield strength σ_{ys} is required for the calculation of the maximum K_{Jc} capacity of a specimen according to the expression:

$$K_{Jc(\text{limit})} = \sqrt{\frac{Eb_o\sigma_{ys}}{30\left(1-\nu^2\right)}} \tag{B.3}$$

where E is Young's modulus, b_o is the specimen uncracked ligament and ν is Poisson's ratio.

Ideally, σ_{ys} to be used in eq.(B.3) should be measured at the same temperature and strain (loading) rate as the fracture toughness test. However, for tests conducted at loading rates higher than quasi-static (0.1 – 2 MPa$\sqrt{}$m/s), representative tensile data might not be available in practice.

In this case, the following options could be used.

1) Using quasi-static tensile results, corresponding to strain rates in the order of 10^{-4} s^{-1}. Such values represent a conservative estimate of the yield strength measured at higher strain rates.

2) Using dynamic tensile results, corresponding to strain rates in the order of 10 s^{-1}, which are considered to be representative of a Charpy impact test. If the fracture toughness test is not performed on a precracked Charpy specimen using an instrumented pendulum, dynamic values represent an unconservative estimate of the actual yield strength and could lead to the calculation of a non-conservative value of the reference temperature, due to a higher censoring limit.

3) Using the Bennett-Sinclair parameter BSP [B-3], which simultaneously accounts for temperature T and loading rate $\dot{\varepsilon}$ in a tensile test:

$$BSP = T\ \ln\left(\frac{A}{\dot{\varepsilon}}\right) \tag{B.4}$$

where A is a frequency factor whose value is around 10^{-8} s^{-1}. Yield strength values corresponding to different temperatures and strain rates can thus be represented on the same plot, as in the example provided in Figure B-11.

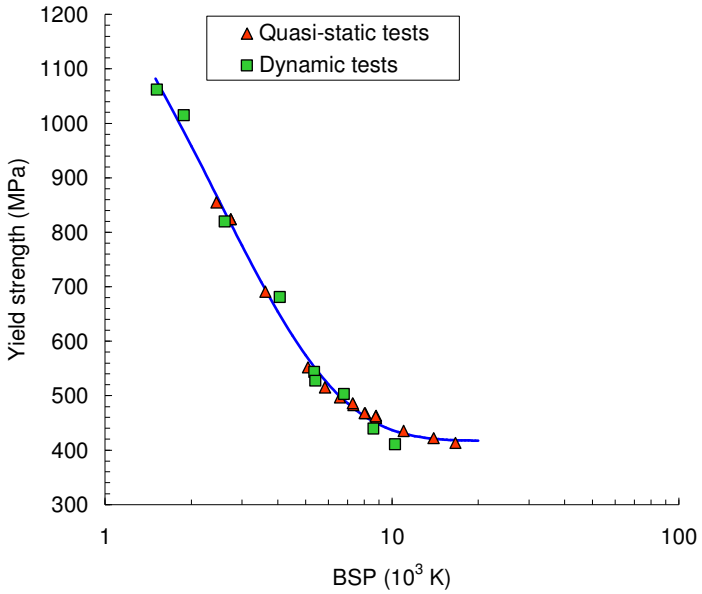

Figure B-11. Example of BSP representation of tensile test results obtained at different temperatures and loading rates.

In the case of quasi-static tests, the loading rate for the fracture toughness test ($\dot{K}$ ~ 1 MPa√m/s) corresponds to a tensile strain rate $\dot{\varepsilon}$ ~ 10^{-4} s^{-1}. For different loading rates, the following relationship holds:

$$\dot{\varepsilon}_{test} = \dot{K}_{test} \frac{\dot{\varepsilon}_{qs}}{\dot{K}_{qs}} \qquad \text{(B.5)}$$

where $\dot{\varepsilon}_{qs}$ and $\dot{K}_{qs}$ are the above mentioned quasi-static values. Using the value of $\dot{\varepsilon}_{test}$ calculated from eq.(B.5) into eq.(B.4), the corresponding value of BSP_{test} can be determined for the test loading rate. The yield strength to be used for the Master Curve analysis can therefore be estimated from a fitting curve like the one shown in Figure B-11 as the ordinate Y corresponding to the ascissa X = BSP_{test}.

The three options described above have been tested on three steels with different characteristics, namely EUROFER97 (9Cr ferritic/martensitic steel for fusion applications), JRQ and JSPS (Japanese A553B steel with low upper shelf toughness). Two loading rates have been investigated: 700 MPa√m/s (all steels) and 4500 MPa√m/s (only JRQ). The overall results are presented in Table B-6 and Figure B-12.

Table B-6 - Master Curve reference temperatures and maximum T_o differences calculated using different values of yield strength.

Material	Loading rate (MPa√m/s)	T_o (°C)			Max Δ (°C)
		Quasi-static	Dynamic	Bennett-Sinclair	
EUROFER97	700 MPa√m/s	-75.0	-79.4	-79.0	4.4
JSPS		14.4	14.4	15.3	0.8
JRQ		-47.9	-48.5	-47.3	1.1
	4500 MPa√m/s	-35.3	-35.7	-33.5	2.2

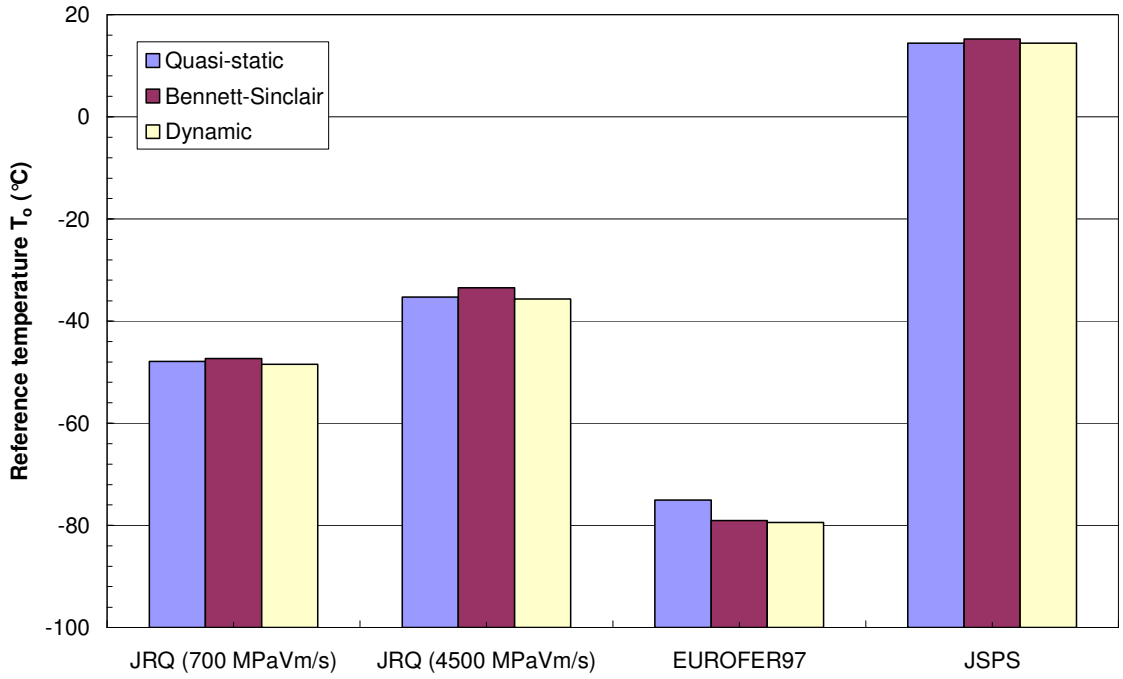

Figure B-12. Master Curve reference temperatures calculated using different values of yield strength.

Differences in terms of T_o for the investigated data sets are small and lower than 5 °C in all cases. This can be also appreciated in Figure B-13, where T_o values are plotted with their respective standard deviations.

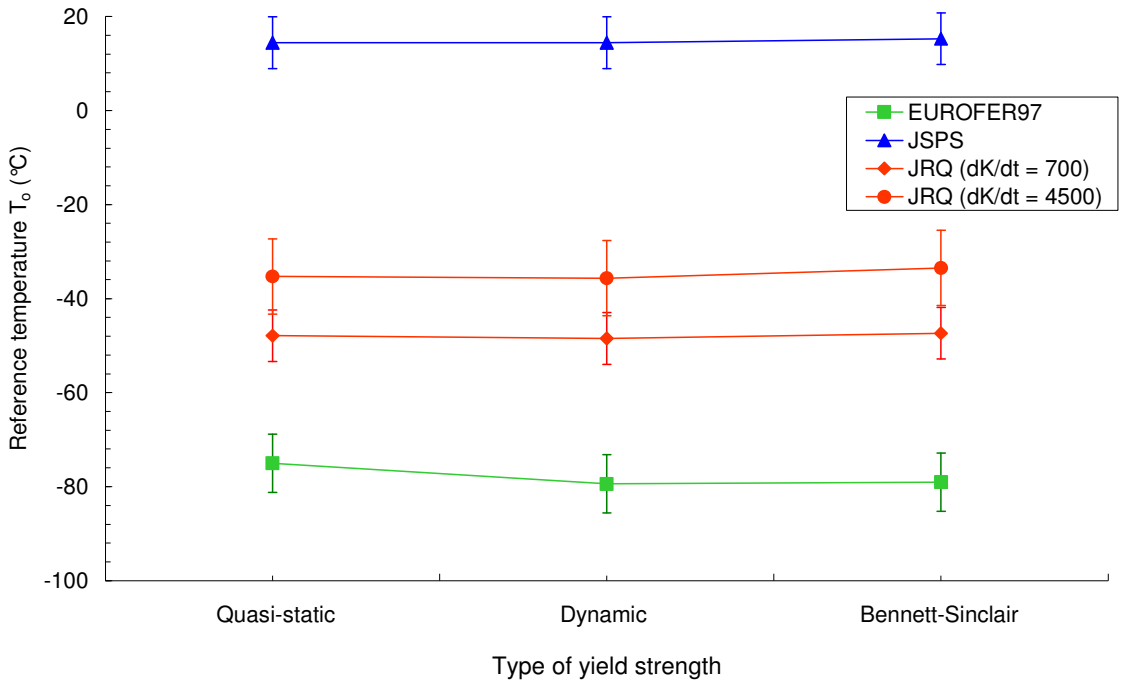

Figure B-13. Master Curve reference temperatures calculated using different values of yield strength, with their corresponding standard deviations.

It is interesting to note that in three out of four cases the highest (most conservative) value of T_o is obtained using the Bennett-Sinclair estimation, rather than the quasi-static value, as might somehow be expected. Conversely, the lowest (less conservative) values of T_o correspond to the dynamic yield strength for three of the four data sets.

B.4.1 Conclusions

1) The differences observed between the calculated values of T_o are smaller than the uncertainties (standard deviations) of the individual reference temperatures. Therefore, a moderate effect of the yield strength choice can be expected, at least for data sets which do not contain a high number of censored data points.

2) From a theoretical point of view, the Bennett-Sinclair approach appears more justified and should therefore be recommended.

3) In the absence of relevant tensile test results, using the quasi-static yield strength is not necessarily the most conservative option.

B.5 Effect of loading pattern (monotonic loading vs partial unloading)

ASTM E1921-05 allows loading test specimens both in the monotonous (M) and in the partial unloading (PU) mode. Partial unloading is recommended in case ductile crack extension needs to be measured.

This raises the question whether the applied loading mode influences the measured fracture toughness and consequently the reference temperature T_o.

PCC specimens of different JRQ blocks and of a German heat resistant steel plate 10 CrMo 9-10 were tested in the M and PU loading mode. Table B-7 contains the values of T_o evaluated by FZD and Figures B-14 to B-16 illustrate test results. Of the 24 monotonously loaded specimens of 5JRQ34, 12 were plane sided. The calculated T_o for the 20% side grooved and plane sided specimens are -59 °C and -62 °C, respectively. Since both values are well within the respective standard deviations (Table B-7), a common evaluation of both datasets was performed (T_o = -60.5 °C).

Table B-7 – Reference temperatures calculated for specimens tested in the monotonic (M) and partial unloading (PU) mode.

Laboratory	Material	Loading mode	Σn_i	T_o (°C)	σ (°C)
GER (FZD)	6JRQ12	PU	1.43	-61.6	6.0
	6JRQ12	M	1.19	-55.9	6.3
	10 CrMo 9-10	PU	1.29	-109.7	5.7
	10 CrMo 9-10	M	1.29	-111.4	5.7
RUS (RRC KI)	5JRQ33, 5JRQ34	PU	3.43	-61.6	3.9
	5JRQ34*	M	3.12	-60.5	4.0

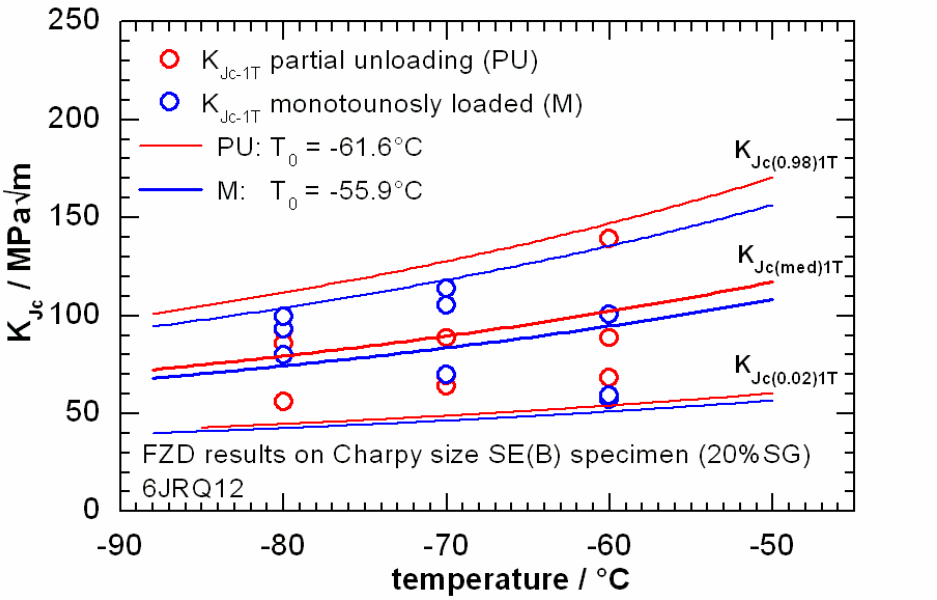

Figure B-14. Master Curve analysis of 6JRQ12 (loading rate PU and M: 1.2 MPa√m/s).

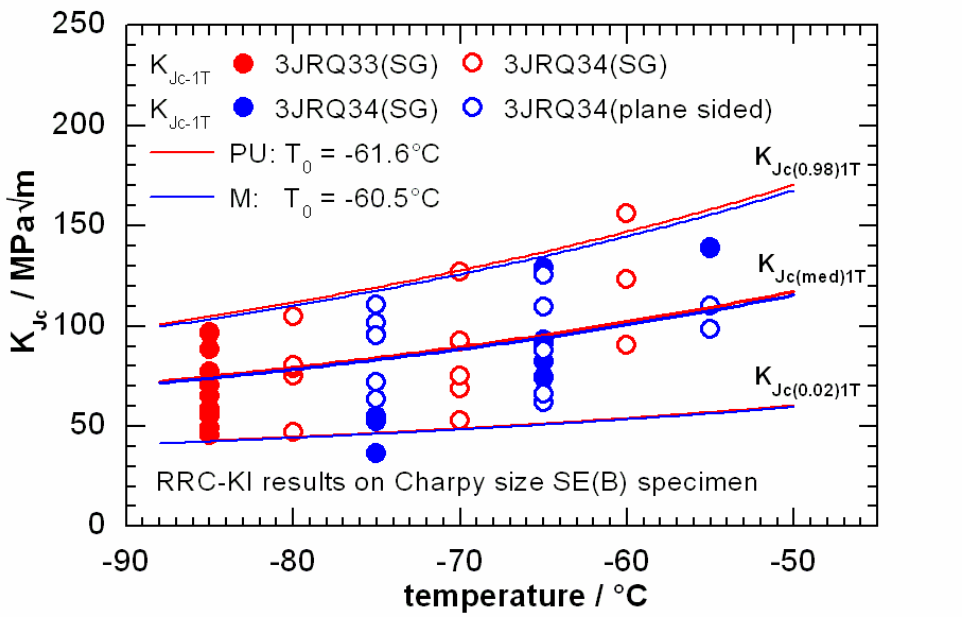

Figure B-15. Master Curve analysis of 5JRQ33 and 5JRQ34 data sets (loading rate PU: 0.1 MPa√m/s and 1.2 MPa√m/s, M: 0.7 MPa√m/s).

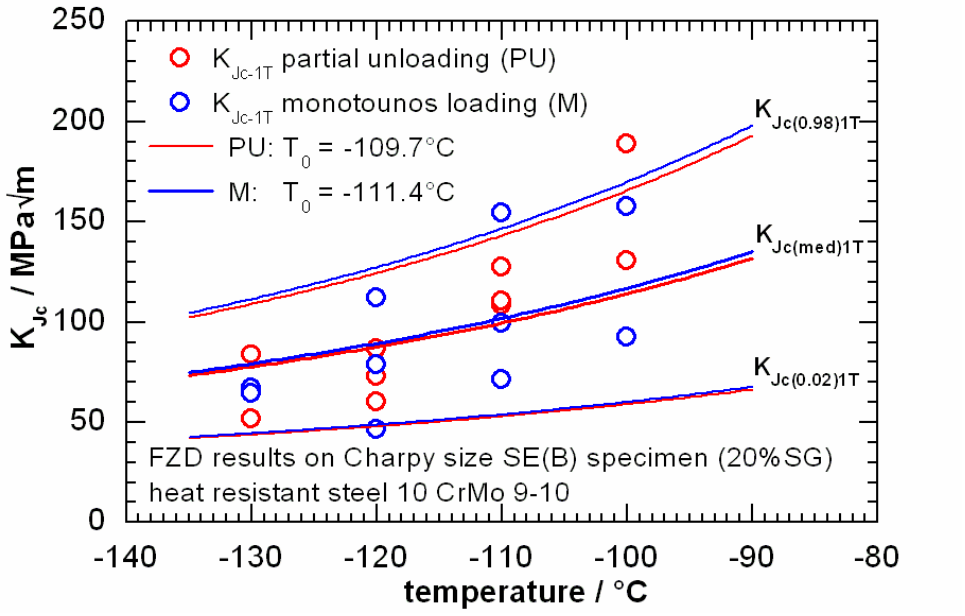

Figure B-16. Master Curve analysis of the German heat resistant steel 10 CrMo 9-10 (loading rate PU and M: 1.2 MPa√m/s).

The variation of the calculated T_o values between the two loading modes is within the standard deviation for the investigated materials, therefore no influence of the loading mode on the Master Curve reference temperature can be detected.

B.6 Additional analyses performed on the Round Robin Exercise (RRE) results

B.6.1 Investigation of the suspect outlier data set (lab 7)

A direct comparison of the RRE results had shown the existence of a suspect outlier laboratory (#7), see Section 4.3.2.1. Further investigations are presented here, aimed at confirming the outlier nature of lab 7 and identifying the cause of such behaviour.

A straightforward comparison of dial energy (KV) values reported by the participants, fitted by simple exponential curves, does not indicate any systematic difference among lab 7 and the others (Figure B-17). This excludes that the outlier behaviour could be caused by material inhomogeneity or improper calibration of the pendulum machine.

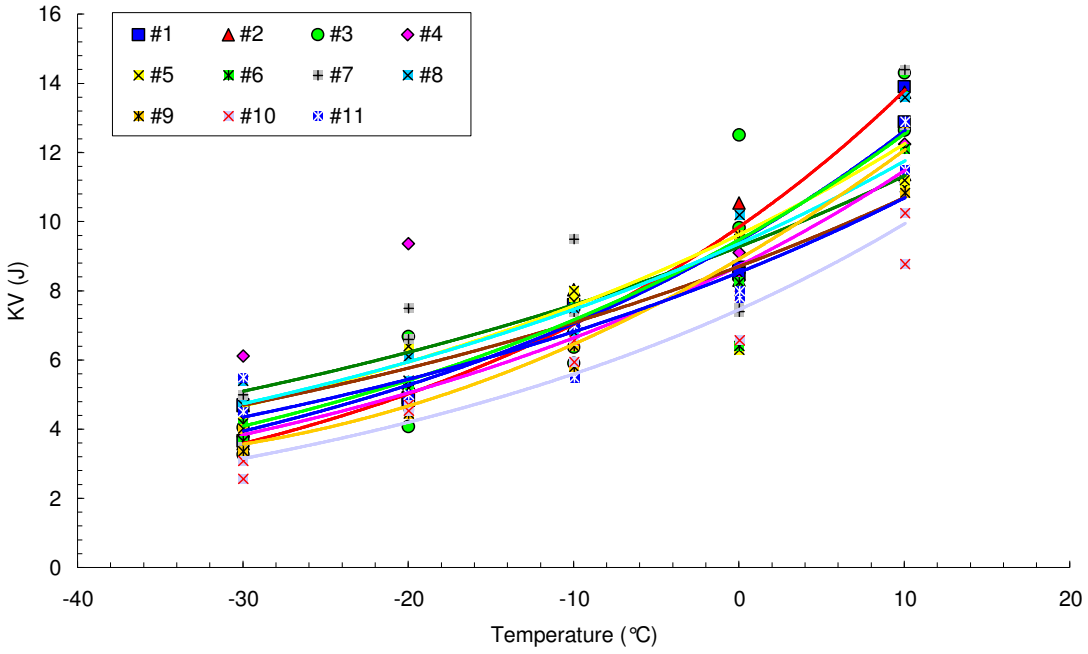

Figure B-17. Dial energy (KV) values reported by RRE participants.

Since K_{Jc} values from impact toughness tests are calculated from time and force measurements and errors in time measurement can be excluded (no systematics are observed in Figure B-18), the observed discrepancies can only derive from incorrect force measurements due to questionable calibration of the instrumented strikers. This appears to be confirmed by Figures B-19 to B-21, which compare test records at -30, -10 and 10 °C for lab 1 and 7 (with lab 1 taken as an example of "normal" or "non-outlier" behaviour).

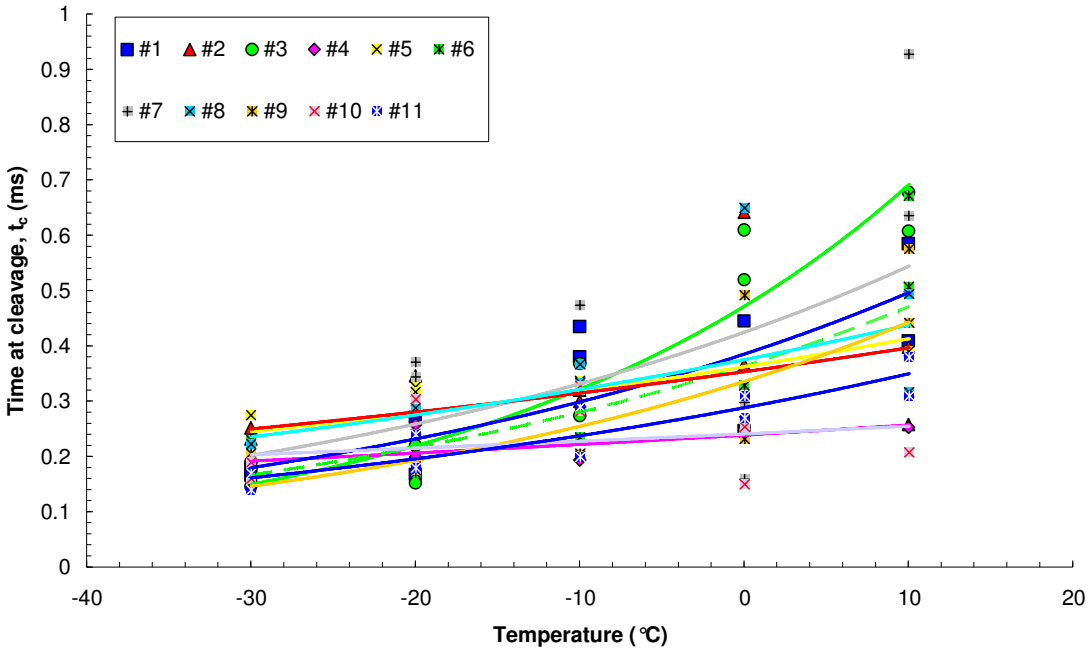

Figure B-18. Values of time at cleavage fracture (t_c) reported by round-robin participants.

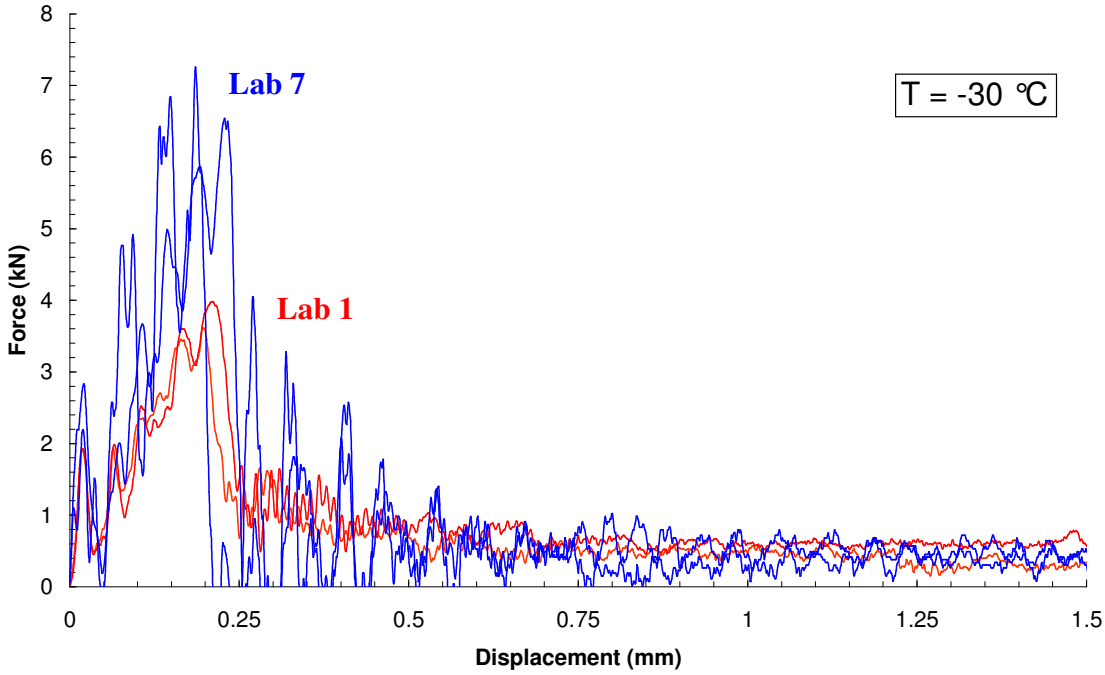

Figure B-19. Test records supplied at -30 °C by labs 1 and 7 (two tests per lab).

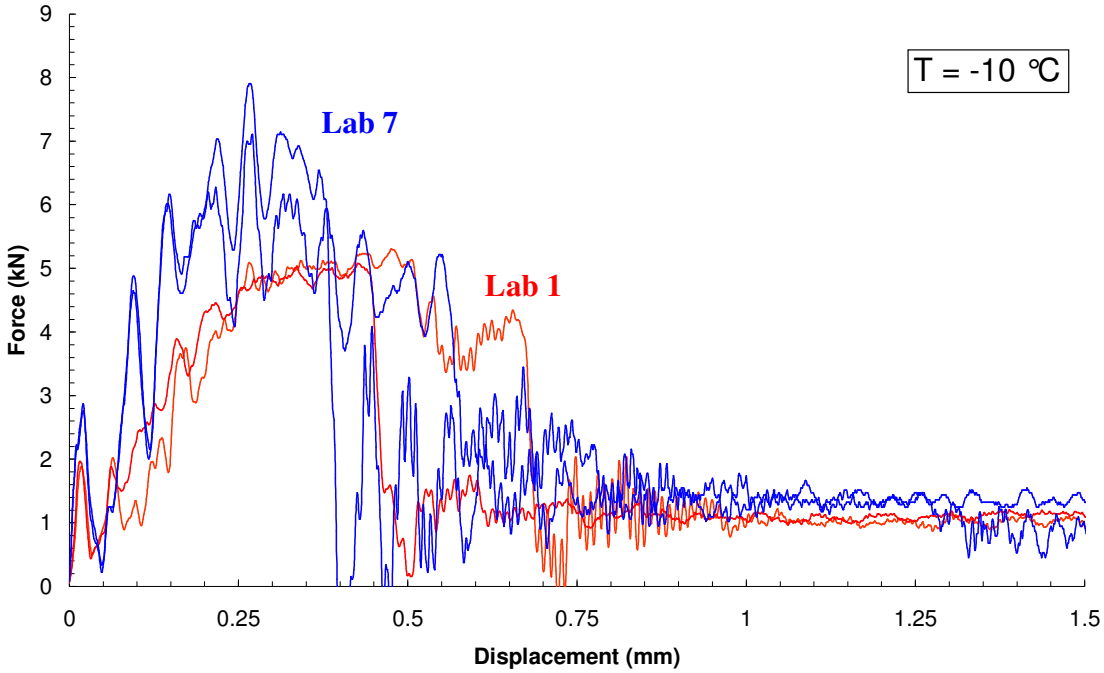

Figure B-20. Test records supplied at -10 °C by lab 1 and 7 (two tests per lab).

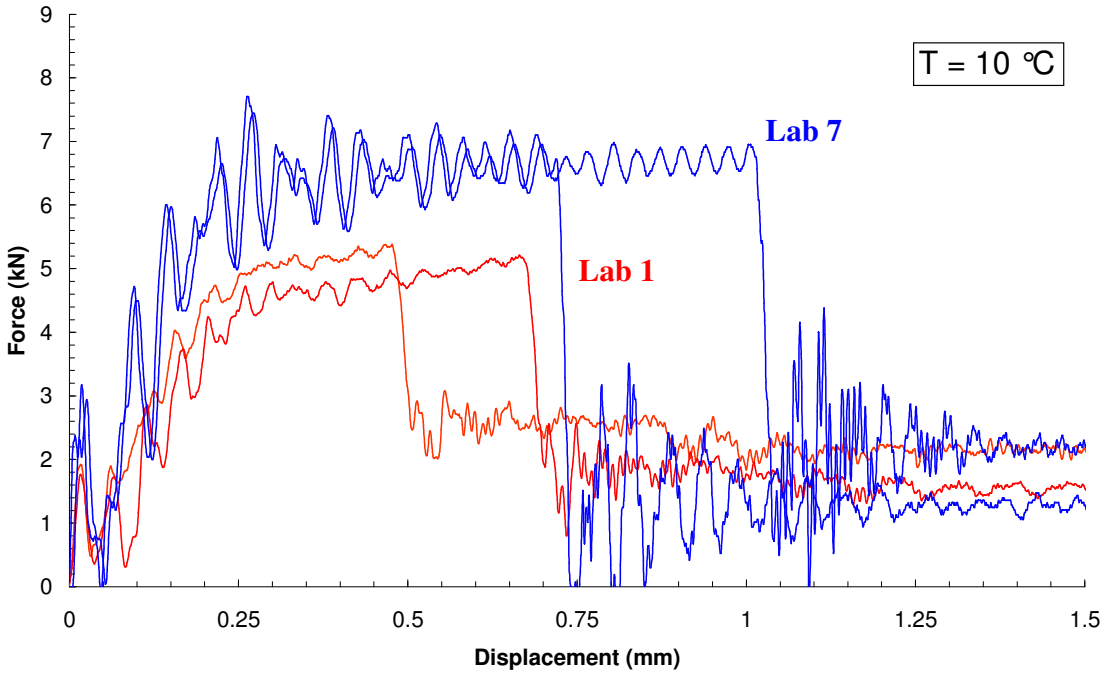

Figure B-21. Test records supplied at 10 °C by labs 1 and 7 (two tests per lab).

Assuming that the striker calibration of lab 1 is reliable, the figures clearly show that force values are too high for lab 7.

An additional assessment of the suspected outlier data set was performed using two recently published extensions of the Master Curve approach for the treatment of inhomogeneous data sets [B-4]:

- the Bi-Modal Master Curve (BMMC), developed for inhomogeneities governed by two separate populations;
- the Multi-Modal Master Curve (MMMC), developed for the analysis of randomly inhomogeneous data sets consisting of multiple populations.

These approaches have been applied to selected individual data sets from the round-robin exercise in order to confirm that the results provided by lab 7 are not homogeneous with the remaining data and should therefore be excluded as outliers. The BMMC approach can also provide an estimation of the percentages corresponding to the two populations (A and B).

The results are summarized in Table B-8 and show that:

- both BMMC and MMMC confirm that the results of lab 7 do not "belong" to the overall population (represented in this case by lab 1);
- both approaches do not detect inhomogeneities between results from labs 1, 2 and 5;
- some indications of inhomogeneity is returned by BMMC for lab 4, although MMMC is unable to detect random heterogeneity.

Table B-8. Application of the bi-modal and multi-modal Master Curve approaches to selected data sets from the round-robin exercise. For BMMC, in case of non-homogeneity percentages for populations A and B are also indicated.

Data sets analyzed	Outcome BMMC	Outcome MMMC
#1 and #7	Not homogeneous (15/85)	Not homogeneous
#1 and #2	Homogeneous	Homogeneous
#1 and #5	Homogeneous	Homogeneous
#1 and #4	Not homogeneous (39/61)	Homogeneous

Following the investigations presented here, an interlaboratory verification exercise was planned, consisting in each participant testing at room temperature two Charpy V-notched samples from the high energy (150 J) batch of Certified Reference Specimens supplied by IRMM (Geel – Belgium). The results from this verification exercise are discussed in detail in Section 4.3.3.

B.6.2 Requirements on the time to fracture/general yield

Impact toughness tests on precracked Charpy specimens are being standardized, at the time of writing, within both ASTM (American Society for Testing and Materials) and ISO (International Standards Organization). Both proposed procedures prescribe the following requirement on the time to fracture/general yield (t_f), if the test is to be analyzed using a quasi-static approach (i.e. using forces and energies calculated from the test record):

$$t_f > 5\tau \tag{B.6}$$

where τ is the period of oscillation of the force signal, which can be analytically evaluated as [B-5]:

$$\tau = 3.36 \cdot \left(\frac{W}{S_0} \right) \cdot \sqrt{E' \cdot B_N \cdot C_S} \tag{B.7}$$

with: W = specimen width, S_0 = speed of sound in steel, E' = plane strain Young's modulus, B_N = specimen net thickness and C_S = specimen compliance. The implication of eq.(B.6) is that, provided fracture occurs after at least five oscillations, inertial effects are sufficiently dampened and a quasi-static loading condition has been reached in the specimen.

In the past, however, a less restrictive criterion had been proposed, i.e.

$$t_f > 3\tau \tag{B.8}$$

This requirement had been suggested by Ireland [B-5,B-6] and later implemented in the EPRI procedures [B-7] and in an ASTM draft standard for dynamic plane strain fracture toughness measurements [B-8]. More recently, model experiments by Böhme [B-9] have shown that for precracked specimens with a/W ~ 0.5 it takes more time (i.e. at least five oscillations) to come to an approximately quasi-static equilibrium of force, and the modified criterion (B.6) was introduced in the experimental procedure issued by ESIS TC5, on which the current ASTM and ISO proposals are based.

If the requirement on time to fracture is not fulfilled, the test has to be evaluated using fully dynamic measuring techniques which do not rely on forces measured by the instrumented striker, such as the Impact Curve Response Method [B-10,B-11] or the Crack Tip Strain Gage Method [B-12].

Using W = 10 mm, S_0 = 5100 m/s, E' = 227472.5 MPa (E = 207000 MPa), B_N = 8 mm and $C_S = 3.79 \times 10^{-5}$ mm/N (calculated by FZD using FEM for a precracked Charpy specimen with a/W = 0.5), eq.(B.7) yields τ = 54.7 µs and the requirements (B.6) and (B.8) become:

$$t_f > 274\ \mu s \tag{B.9}$$

and

$$t_f > 164\ \mu s \tag{B.10}$$

respectively.

Times to fracture for the 108 impact toughness test results provided by RRE participants have been compared to the requirements (B.9) and (B.10).

It emerges that exactly half of the tests performed fail to satisfy the more stringent requirement (B.9), i.e. for 54 out of 108 tests (50%), $t_f \leq 274$ μs; the temperature distribution of the "rejected" tests is: 21 at -30 °C, 14 at -20 °C, 5 at -10 °C, 11 at 0 °C and 3 at 10 °C.

A much smaller portion (only 9 tests, or 8.3%) does not fulfil requirement (B.10), i.e. $t_f \leq 164$ μs; most tests (6) were performed at -30 °C, 1 at -20 °C and 2 at 0 °C.

In order to investigate the effect of a possible t_f requirement on the RRE results, two approaches have been considered prior to performing an overall Master Curve analysis:

(a) simply removing the "invalid" tests, i.e. considering them as "non-tests" (such as specimens with invalid initial crack size in ASTM E 1921);

(b) replacing the measured K_{Jc} with the values corresponding to $t_f = 3\tau$ (52.5 MPa$\sqrt{m}$) or 5τ (90 MPa$\sqrt{m}$), i.e. applying a sort of "censoring" procedure similar to that of ASTM E 1921, whereby if $K_{Jc} > K_{Jc(limit)}$, K_{Jc} is replaced by $K_{Jc(limit)}$ in the analysis.

The impact of the different requirements and approaches on the overall Master Curve analysis results is summarized in Table B-9. For comparison, results of the straightfoward overall analysis (see Section 4.3) are also included.

Table B-9. Influence of time to fracture requirements on the overall Master Curve analysis.

Requirement	Action	N	r	$\sum n_i$	T_o (°C)	σ_{To} (°C)
None	None	108	95	14.79	-4.0	1.8
$t_f > 3\tau$	Remove data	99	86	13.45	-5.2	1.9
	"Censor" data	108	86[2]	13.60	-5.1	1.9
$t_f > 5\tau$	Remove data	54	41	6.81	-12.6	2.8
	"Censor" data	108	41	6.83	-17.2	2.8

Invalidating very short fracture times, i.e. very brittle tests, predictably tends to bias the reference temperature downwards (i.e. non conservatively). The bias is almost negligible (just above 1 °C) in the case of the "old" requirement, and removing or censoring does not make appreciable difference. However, if the more stringent requirement is enforced, the non-conservative shift of T_o is more significant, particularly if the "censoring" approach is applied (shift of 13.3 °C); if invalid data are removed, the resulting bias is less than 10 °C (8.6 °C).

[2] Data with $t_f < 3\tau$ or 5τ are not included in the count of valid data, as in the case of data with $K_{Jc} > K_{Jc(limit)}$.

Therefore, based on the analysis of the RRE results, it appears more convenient to apply the less stringent requirement ($t_f > 3\tau$), in order to avoid significant non-conservatism.

B.7 Additional analyses performed on the Interlaboratory Comparison (ILC) results

B.7.1 Within-laboratory and between-laboratory statistics

A statistical analysis was conducted on the original ILC data in accordance with ASTM E691-05 [B-13], in order to determine their repeatability and reproducibility.

According to the standard, the repeatability concerns the variability between independent test results obtained within a single laboratory; the within-laboratory consistency statistics, *k*, is calculated as:

$$k = \frac{s}{s_r} \tag{B.11}$$

where *s* is the standard deviation for one laboratory and s_r is the repeatability standard deviation of the material, given by:

$$s_r = \sqrt{\frac{\sum_1^p s^2}{p}} \tag{B.12}$$

Figure B-23 shows the values of within-laboratory statistic *k* for F_{gy} and F_m calculated from the original ILC results; the Figure also indicates the critical value of *k* at the 0.5% significance level, which depends on the number of laboratories[3] (10) and the number of tests per laboratory (2); in this case, $k_{crit} = 2.45$.

[3] As mentioned in Section 4.3.3, lab 11 did not provide results.

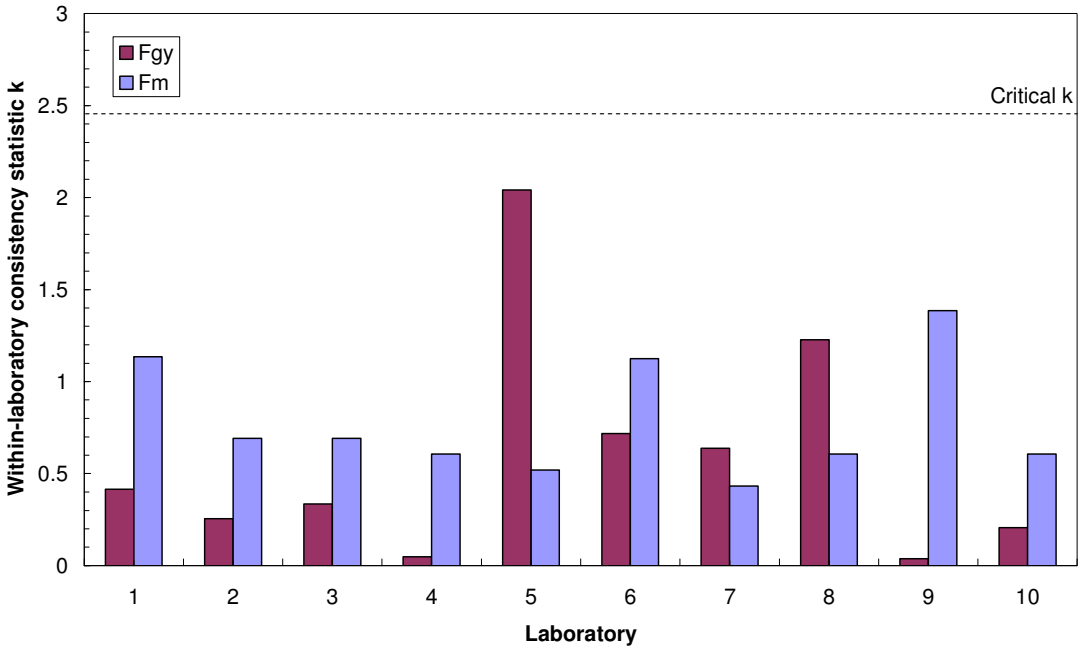

Figure B-23. Within-laboratory consistency statistic *k* for the original ILC data.

On the other hand, reproducibility deals with the variability between single test results obtained in different laboratories. The between-laboratory consistency statistic *h* is calculated as:

$$h = \frac{d}{s_{\bar{X}}} \tag{B.13}$$

where *d* is the deviation of the laboratory average from the average of the laboratory averages and $s_{\bar{X}}$ is the standard deviation of the laboratory averages. The values of *h* calculated for each lab from the original results are shown in Figure B-24, together with the critical values of *h* at the 0.5% significance level, which only depend on the number of labs; in this case, $h_{crit} = \pm 2.29$.

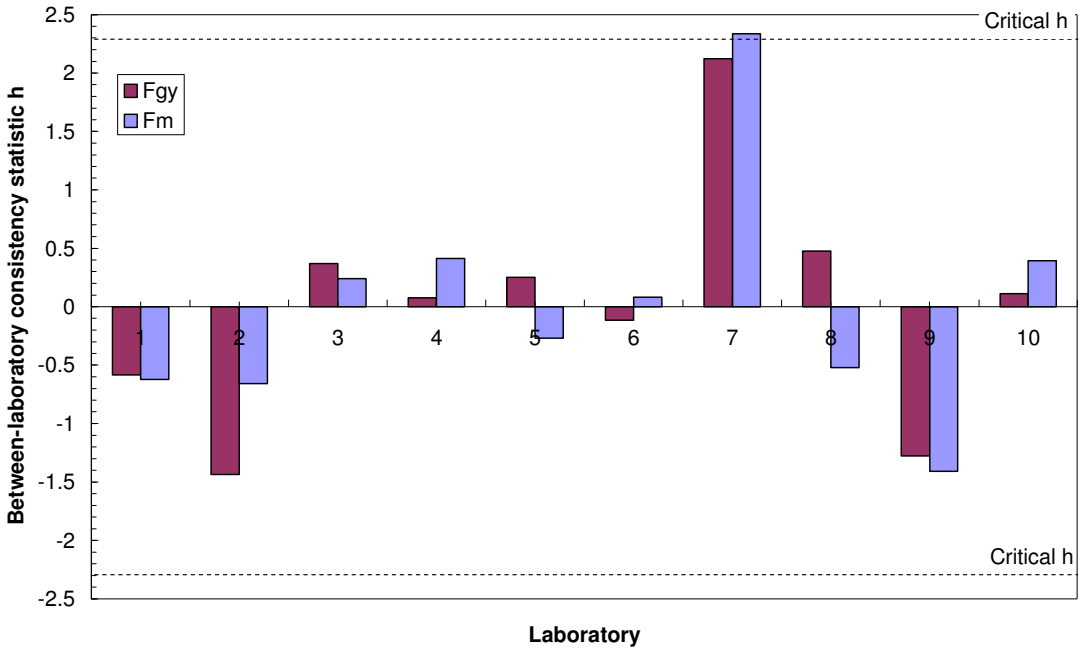

Figure B-24. Between-laboratory consistency statistic *h* for the original ILC data.

From Figures B-23 and B-24, we remark that no lab exceeds the critical *k* value for F_{gy}, or F_m, while lab 7 is very close to the upper *h* limit for F_{gy} and even exceeds it for F_m, thus confirming the anomaly recorded in the analyses of the RRE results. This circumstance is confirmed by Figure B-25, where instrumented Charpy curves from ILC tests are compared between labs 2, 5 and 7.

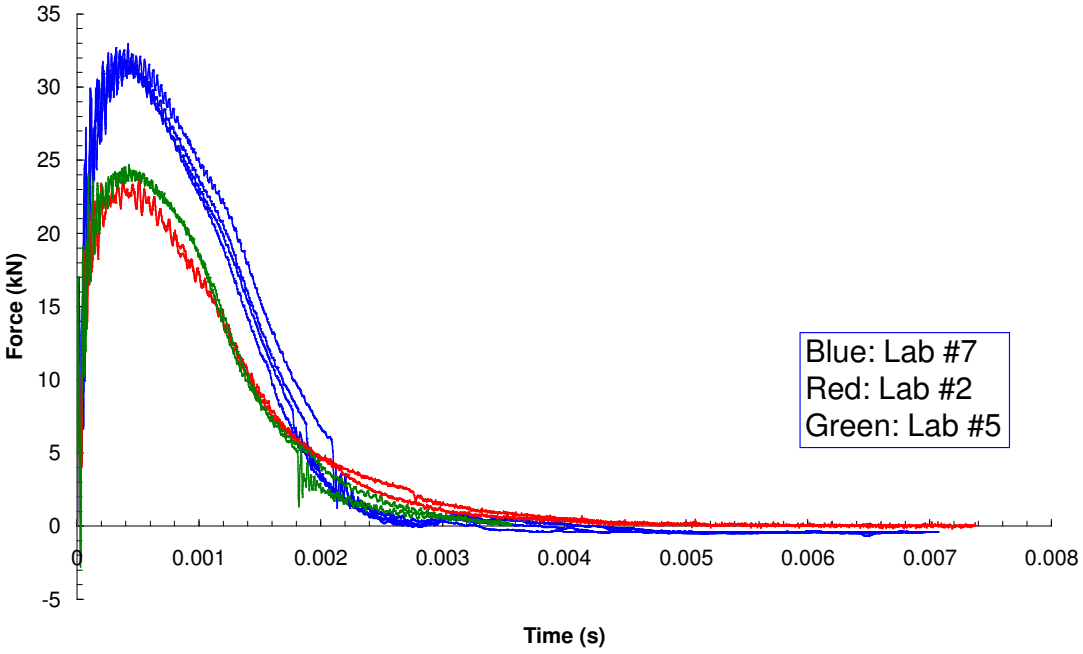

Figure B-25. Instrumented Charpy curves provided by labs 2, 5 and 7.

The effect of the dynamic force adjustment on the within-laboratory and between-laboratory consistency statistics can be appreciated in Figures B-26 (*k*) and B-27 (*h*).

We observe that the within-laboratory consistency (Figure B-26) remains quite acceptable, whereas the between-laboratory consistency (Figure B-27) is somewhat improved, particularly in the case of lab 7.

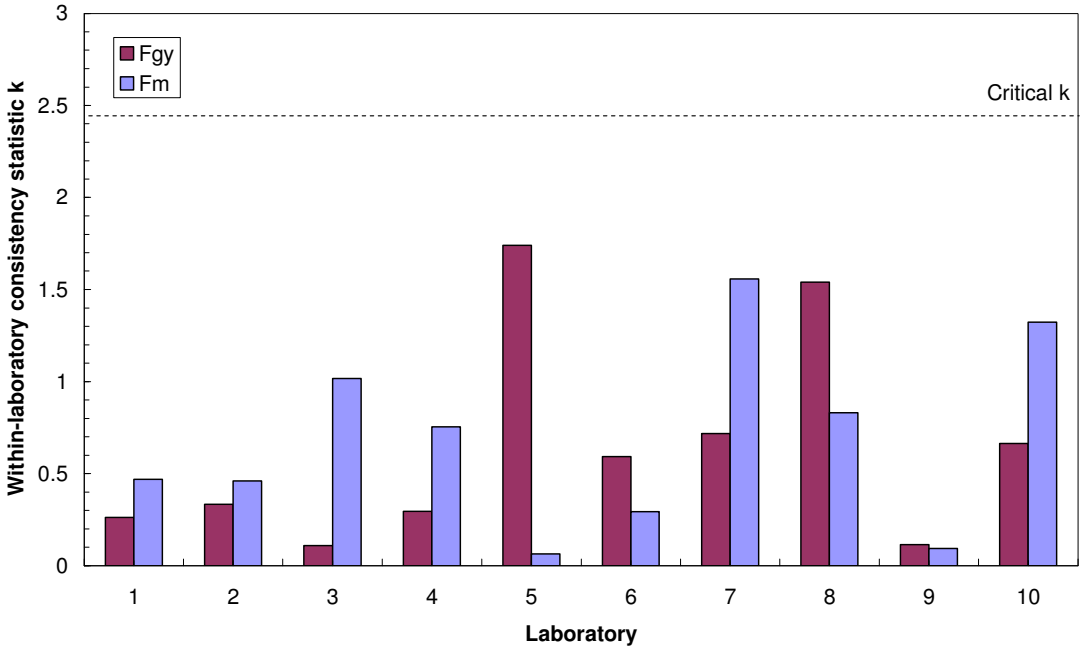

Figure B-26. Within-laboratory consistency statistic after dynamic force adjustment.

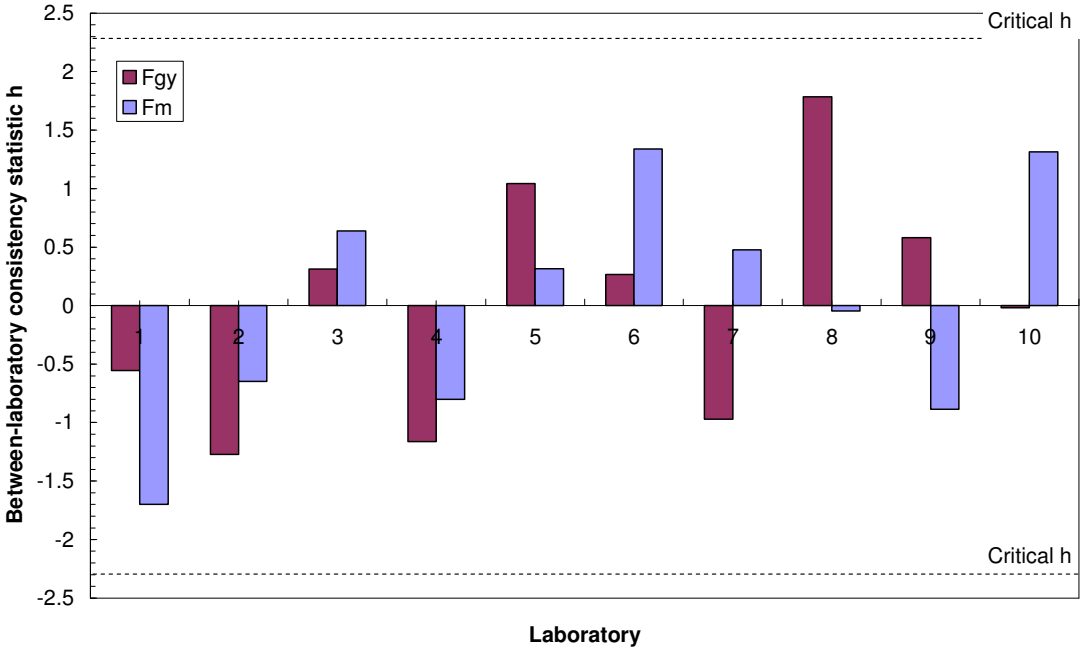

Figure B-27. Between-laboratory consistency statistic after dynamic force adjustment.

B.7.2 Influence of striker radius on general yield and maximum forces

A possible influence of the instrumented striker radius (2 mm vs 8 mm) on the ILC results was also investigated, although only four ILC participants (labs 3, 6, 8 and 10) used an 8 mm striker.

Figure B-28 shows for the original ILC results a slight increase of instrumented force values with increasing striker radius.

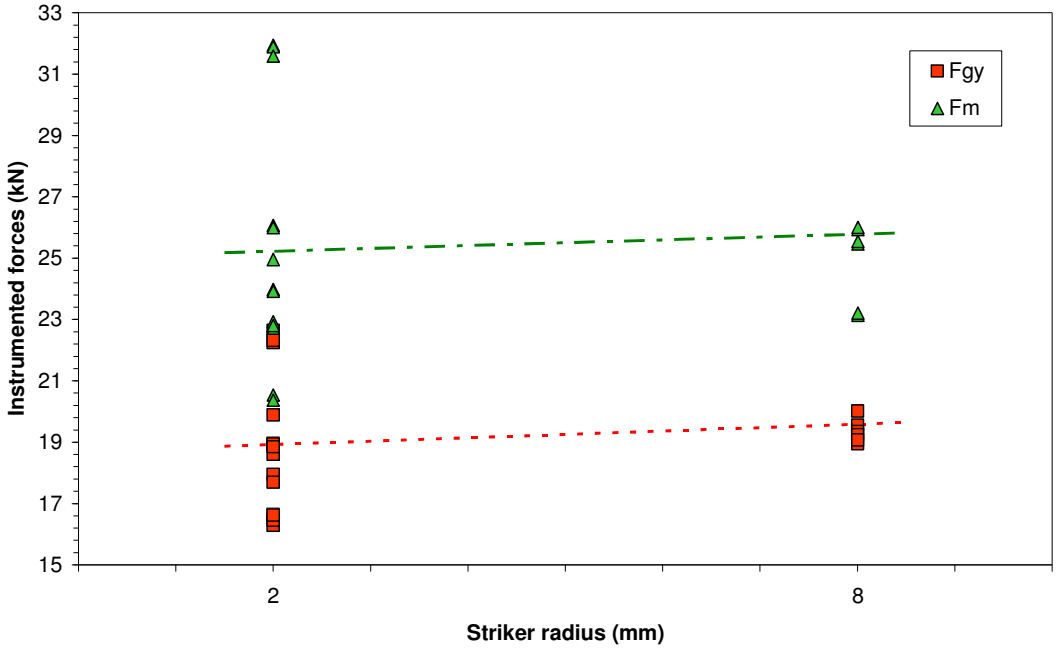

Figure B-28. Effect of striker radius on the original ILC results.

The trend remains unchanged after applying the dynamic force adjustment, as shown Figure B-29.

The possible influence of striker radius would anyhow need confirmation by a larger number of tests conducted using an 8 mm striker.

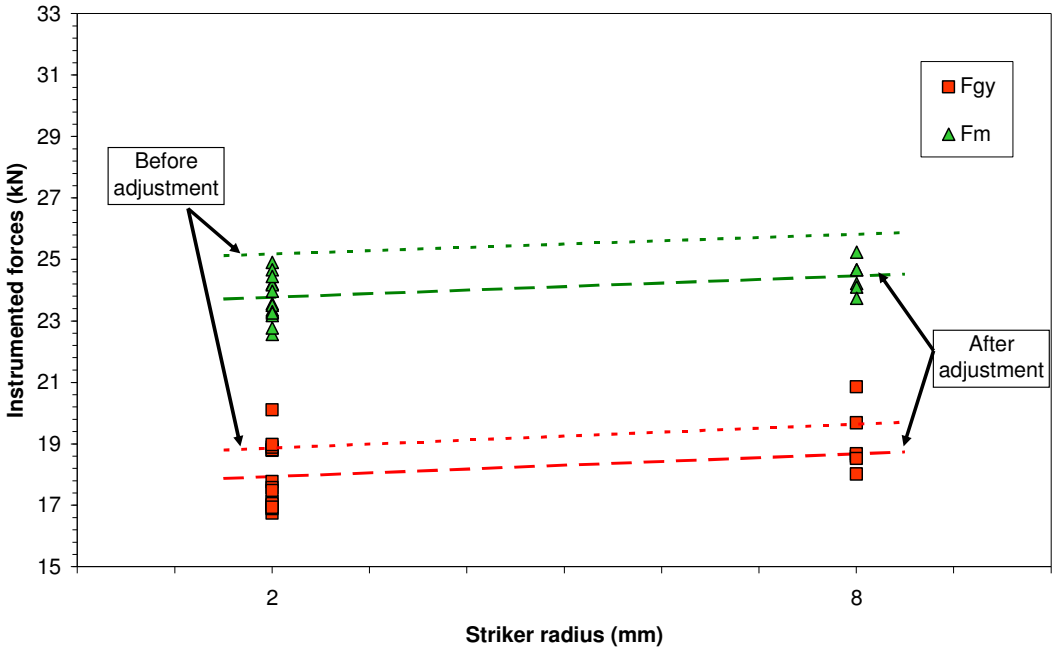

Figure B-29. Effect of striker radius on the dynamically adjusted ILC results.

B.8 Relationship between crack arrest forces from instrumented Charpy tests and NDT from Pellini tests

Licensing rules related to safety against brittle fracture of nuclear reactor pressure vessels (RPV) are based on the nil ductility transition temperature (NDT), which is measured by drop-weight (Pellini) tests in accordance with ASTM E208-06 [B-14]. The reference temperature RT_{NDT}, which is used for indexing both the initiation (K_{Ic}) and arrest (K_{Ia}) fracture toughness lower bound curves for the vessel in accordance with ASME Section III [B-15], is obtained by combining Pellini and Charpy test information for the unirradiated condition. The increase ΔRT_{NDT} caused by irradiation is assumed to be equal to the shift of the Charpy energy curve at the 41 J (30 ft-lb) level.

The use of crack arrest forces F_a from instrumented Charpy tests to correlate NDT was first proposed by GKSS [B-16]; more recently, Wallin [B-17], Iskander [B-18] and Fabry [B-19] have used Charpy F_a forces to describe the crack arrest behaviour of RPV steels.

In [B-19], A. Fabry proposed a "crack arrest master curve" formulation for the temperature dependence of arrest forces, based on the following equation:

$$F_a(T) = 3 \cdot \exp\left(\lambda T - NDT\right) \tag{B.14}$$

where $\lambda = 0.020$ for $T < NDT$ and $\lambda = 0.026$ for $T > NDT$ and the nil ductility temperature NDT corresponds to a median crack arrest force indexing level of 3 kN. This indexing level provides an accuracy of ±15 °C in NDT determination at the 95% confidence level, based on the investigation of 26 RPV steels [B-19] (Figure B-30). Other force values have been proposed for the determination of NDT, such as 4 kN in [B-17] and 2.45 kN in [B-18], leading to accuracies of ±10 °C and ±11 °C respectively but based on a more limited database (7 and 8 materials).

The excellent correlation between NDT values measured from Pellini drop-weight tests and median 3 kN crack arrest force temperature from Charpy tests is shown in Figure B-31, which is based on data given in Table B-10.

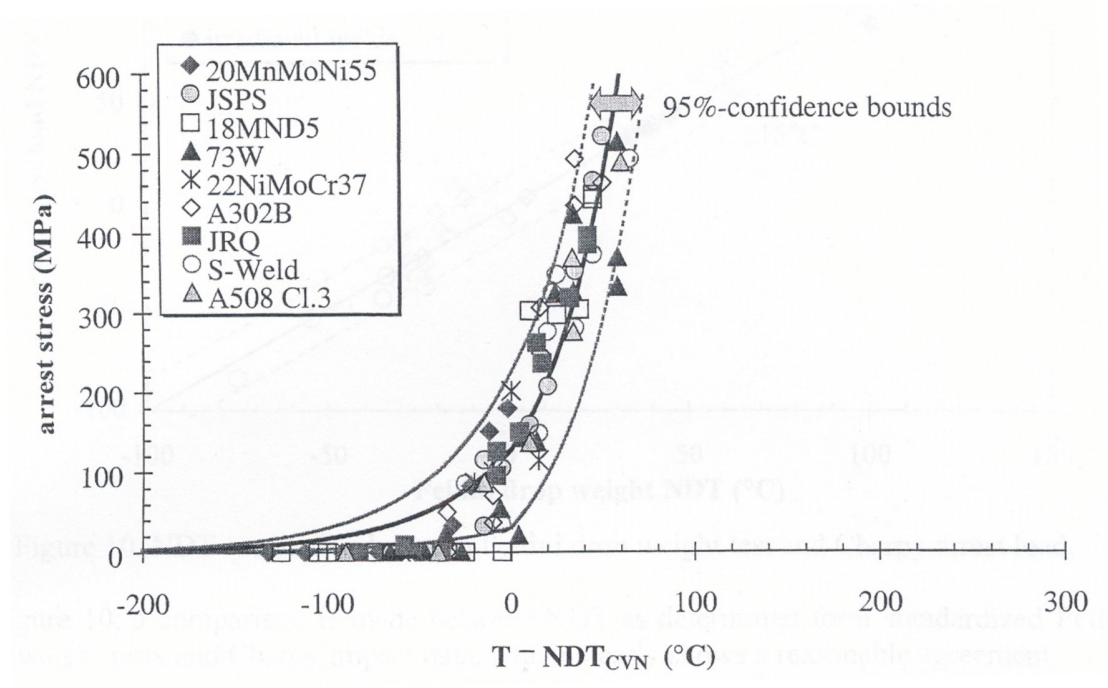

Figure B-30. "Master curve" regression of arrest stress values from instrumented Charpy tests [B-19].

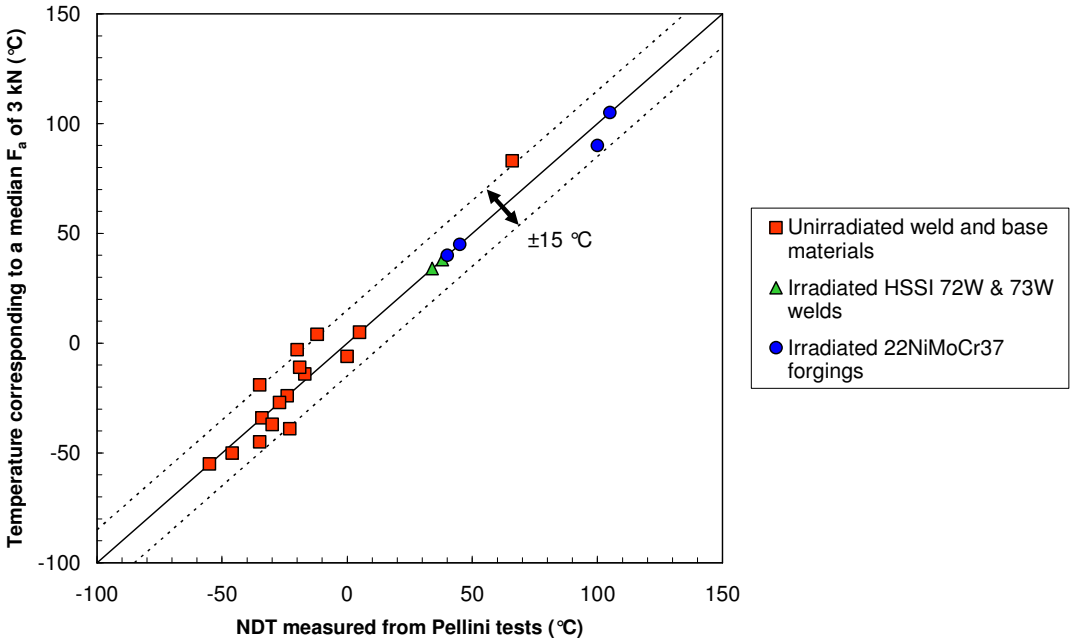

Figure B-31. Correlation between NDT and temperature corresponding to a Charpy median crack arrest force of 3 kN [B-19].

Table B-10 - Data used for Figure B-31 [B-19].

Steel	Condition	NDT Pellini (°C)	3 kN median F_a (°C)
A302B	Unirradiated	-17	-14
HSST-02		-19	-11
HSST-03		-12	4
KS-01 22NiMoCr37		5	5
KS-02 22NiMoCr37		0	-6
A508 Cl.2 (PTSE-1)		66	83
Belgian surv. forging 1		-24	-24
Belgian surv. forging 2		-35	-19
22NiMoCr37 surv. forging		-20	-3
HSSI 72W		-27	-27
HSSI 73W		-34	-34
Linde-80 weld		-23	-39
Quad Cities-2 surv. weld		-46	-50
Belgian surv. weld		-30	-37
22NiMoCr37 surv. weld		-35	-45
Midland vessel weld		-55	-55
KS-01 (2E19 n/cm²)	Irradiated	45	45
KS-01 (7E19 n/cm²)		100	90
KS-02 (2E19 n/cm²)		40	40
KS-02 (8E19 n/cm²)		105	105
HSSI 72W (1.5-2E19 n/cm²)		34	34
HSSI 73W (1.5-2E19 n/cm²)		38	38

As part of Fabry's work [B-19], it was also shown that the temperature T_A at which the median arrest fracture toughness K_{Ia} is equal to 100 MPa√m (arrest reference temperature) corresponds to a Charpy arrest force indexing level of 5.05 kN (Figure B-32); it was also shown that:

$$T_A = NDT + 20\ °C \tag{B.15}$$

with an uncertainty of ±12 °C at the 95% confidence level (2σ). This compares favourably with results from Wallin [B-20], who proposed:

$$T_{Fa4} = T_A - 10\ °C \tag{B.16}$$

(2σ = ±27 °C) where T_{Fa4} is the temperature at which the median crack arrest force is 4 kN. Based on eq.(B.14), this transforms in:

$$T_A = NDT + 21\ °C \tag{B.17}$$

which is very similar to eq.(B.15).

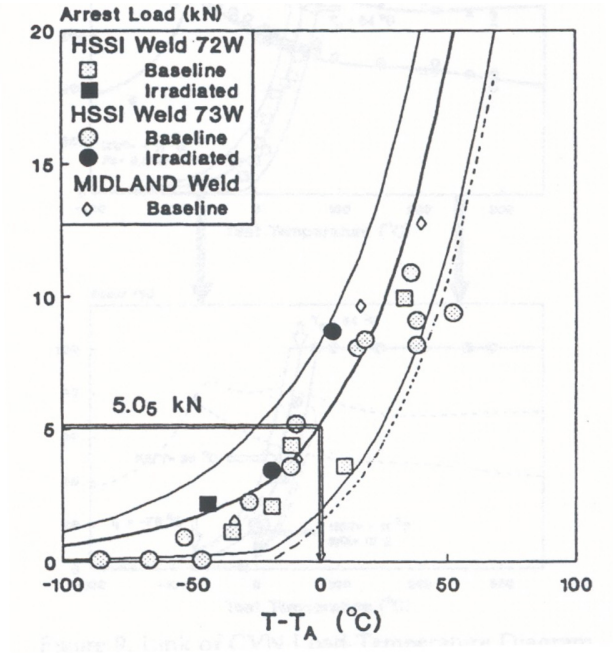

Figure B-32. Measuring crack arrest toughness from instrumented Charpy tests [B-19].

B.9 Correlation between T_o and T_{41J}

Using data included in the databases of FZD and SCK•CEN, empirical correlations have been established between measured values of T_{41J} (from Charpy tests) and T_o (from fracture toughness tests analyzed using the Master Curve approach), considering both base and weld materials, in the unirradiated and irradiated conditions.

The relationship obtained considering only base materials and imposing unity for the slope of the linear fit, is:

$$T_o = T_{41J} - 56 \ \ °C \tag{B.18}$$

with a standard deviation of 30 °C (Figure B-33).

If weld metal data are included, the experimental scatter is significantly increased and the correlation becomes

$$T_o = T_{41J} - 53 \ \ °C \tag{B.19}$$

with a very similar intercept but a clearly higher standard deviation (50 °C, Figure B-34).

Both relationships are considerably different from the one proposed by Sokolov and Nanstad [B-21] and presently included in §8.4 of ASTM E1921-05 (*Test Temperature Selection*):

$$T_o = T_{41J} - 24 \ \ °C \tag{B.19}$$

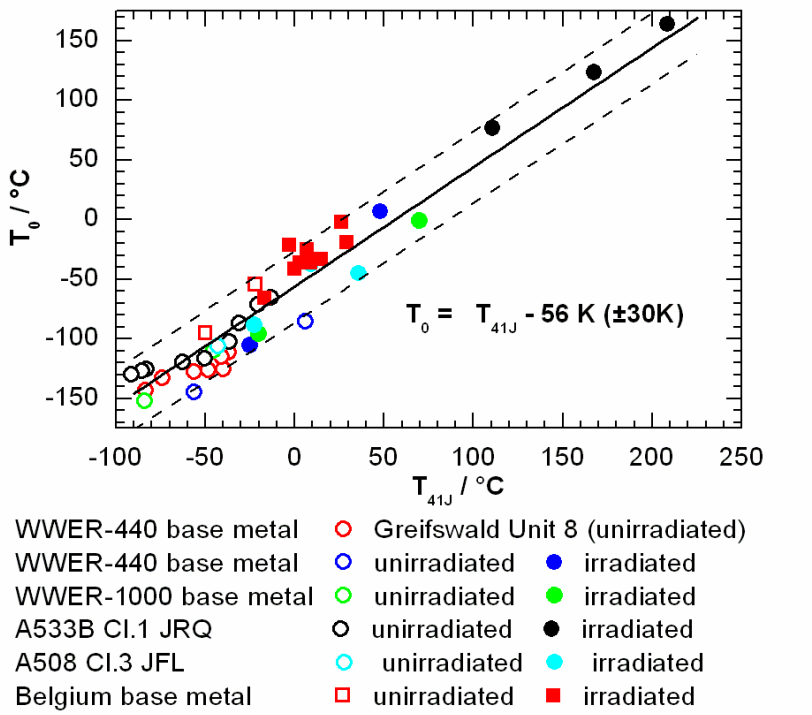

Figure B-33. Relationship between T_o and T_{41J} for base materials.

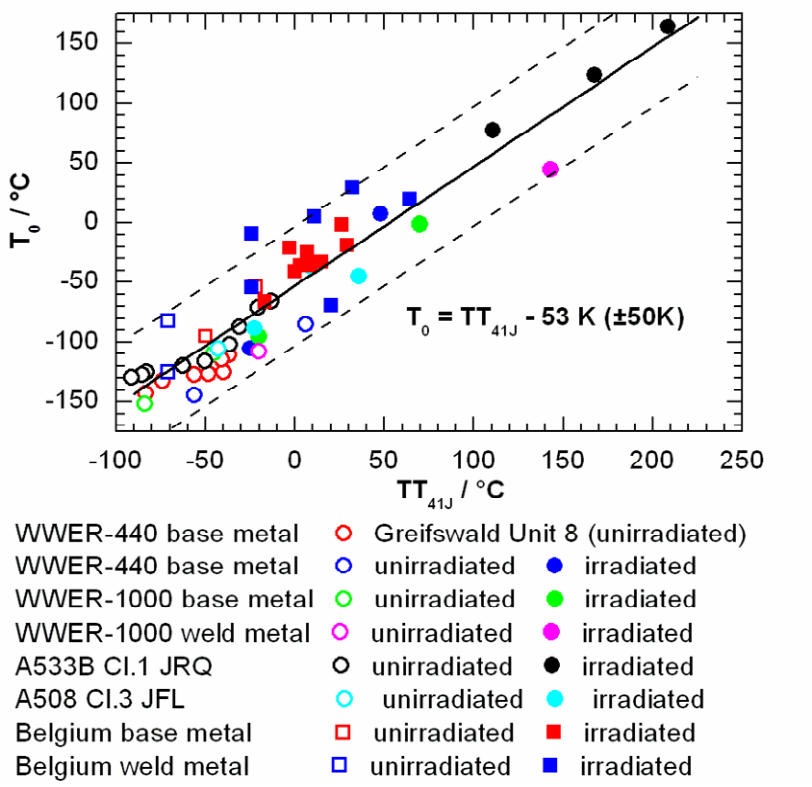

Figure B-34. Relationship between T_o and T_{41J} for base and weld materials.

References

[B-1] Lucon, E., Scibetta, M., Chaouadi, R., van Walle, E. and Gérard, R. (2007). Improved Safety Margins for Belgian Nuclear Power Plants by the Application of the Master Curve Approach to RPV Surveillance Materials. International Journal of Pressure Vessels and Piping, Volume 84, Issue 9, pp. 536-544.

[B-2] Wallin, K. (1997). Effect of Strain Rate on the Fracture Toughness Reference Temperature T_o for Ferritic Steels. *Recent Advances in Fracture*, The Minerals, Metals & Materials Society.

[B-3] Bennett, P.E. and Sinclair, G.M. (1966). Trans. ASME, J. Basic Eng., **88**, 518.

[B-4] Wallin, K., Nevasmaa, P., Laukkanen, A. and Planman, T. (2004). Master Curve Analysis of Inhomogeneous Ferritic Steels. Engineering Fracture Mechanics 71 (16-17), pp.2329-2346.

[B-5] Ireland, D.R. (1974). Procedures and Problems Associated with Reliable Control of the Instrumented Impact Test. ASTM STP 563, pp. 3-29.

[B-6] Ireland, D.R. (1976). Critical Review of Instrumented Impact Testing. Dynamic Fracture Toughness International Conference, London 1976, The Welding Institute of American Society for Metals, Effects Technology, Inc., Technical Report No. 79-55.

[B-7] McConnell, P. and Server, W. (1981). EPRI Instrumented Impact Test Procedures. In Proceedings C.S.N.I. Specialists Meeting on Instrumented Precracked Charpy Testing. EPRI NP-2102-LD, Prepared by Electric Power Research Institute, Ed. by R. A. Wullaert, Palo Alto, USA, pp. 1-1 to 1-22.

[B-8] ASTM E 24.03.03 (1980). Proposed Standard Method of Test for Instrumented Impact Testing of Precracked Charpy Specimens of Metallic Materials. Draft 2c, ASTM, Philadelphia.

[B-9] Böhme, W. (1990). Dynamic Key Curves for Brittle Fracture Impact Tests and Establishment of a Transition Time. ASTM STP 1074, Eds.: J. P. Gudas, J. A. Joyce, and E. M. Hackett, ASTM, Philadelphia, pp. 144-156.

[B-10] Kalthoff, J. F., Winkler, S., and Böhme, W. (1985). A Novel Procedure for Measuring the Impact Fracture Toughness KId with Pre-cracked Charpy Specimens. Journal de Physique, Coll. C5, Suppl. No. 8, Tome 46, pp.179 -186.

[B-11] Kalthoff, J. F. (1986). Fracture Behaviour under High Rates of Loading. Engineering Fracture Mechanics, 23, No.1, pp. 289-298.

[B-12] MacGillivray, H. J. and Cannon, D. F. (1992). The Development of Standard Methods for Determining the Dynamic Fracture Toughness of Metallic Materials. ASTM STP 1130, R. Chona and W. R. Corwin, eds., ASTM, pp. 161-179.

[B-13] ASTM E691-05. Standard Practice for Conducting an Interlaboratory Study to Determine the Precision of a Test Method. Annual Book of Standards, Volume 14.02.

[B-14] ASTM E208-06. Standard Test Method for Conducting Drop-Weight Test to Determine Nil-Ductility Transition Temperature of Ferritic Steels. Annual Book of Standards, Volume 03.01.

[B-15] American Society of Mechanical Engineers (2002). "Rules for Construction of Nuclear Power Plants, ASME Boiler and Pressure Vessel Code". Section III, ASME, New York.

[B-16] Ahlf J., Bellmann D., Föhl J., Hebenbrock H.D., Schmitt F.J. and Spalthoff W. (1986). Irradiation Behavior of Reactor Pressure Vessel Steels from the Research Program on the Integrity of Components. ASTM STP 909, pp. 34-51.

[B-17] Wallin, K. (1996). Descriptive characteristic of Charpy-V fracture arrest parameter with respect to crack arrest K_{Ia}. "Evaluating Material Properties by Dynamic Testing", ESIS Publication 20, pp. 165-176.

[B-18] Iskander S.K., Nanstad R.K., Sokolov M.A., McCabe D.E., Hutton J.T. and Thomas D.L. (1999). Use of Forces from Instrumented Charpy V-Notch Testing to Determine Crack-Arrest Toughness. ASTM STP 1325, pp. 204-222.

[B-19] Fabry, A. (1997). Nuclear Reactor Pressure Vessel Integrity Insurance by Crack Arrestability Evaluation Using Loads from Instrumented CVN Tests. SCK•CEN Open Report BLG-750.

[B-20] Wallin, K., Planman, T. and Rintamaa, R. (1995). Proceedings of the TWI-TSE Seminar on "Crack Arrest Concepts for Failure Prevention and Life Extension", Cambridge (UK).

[B-21] Sokolov, M.A. and Nanstad, R.K. (1999). Comparison of Irradiation-Induced Shifts of K and Charpy Impact Toughness for Reactor Pressure Vessel Steels. ASTM STP 1325, pp. 167-190.